



Investigation of the influence of fuselage door surrounding structure's geometric parameters on the weight and mechanical response of the fuselage

Ana Maria Carrasquinho de Macedo

Thesis to obtain the Master of Science Degree in

Aerospace Engineering

Supervisors: Prof. José Arnaldo Pereira Leite Miranda Guedes

Eng. Florian Dexl

Examination Committee

Chairperson: Prof. Fernando José Parracho Lau

Supervisor: Prof. José Arnaldo Pereira Leite Miranda Guedes

Member of the Committee: Prof. João Orlando Marques Gameiro Folgado

June 2018

Dedication

I dedicate this thesis to Luís Filipe Cardoso, a true engineer, scientist, artist and most of all, a good person, who dedicated his short life to science and left a good mark on everyone that crossed his way. For Luís, perfection did not matter, the most important was what the team would learn. He would love to see me get my degree, though I believe he will feel it.

Acknowledgements

I thank in the first place to my parents, the most important persons in my life and the ones that provided all that I am and have, including the possibility to study and be graduated.

To Prof. José Miranda Guedes for all the help in orienting this thesis. To Prof. Matos Neves for his precious help on ANSYS features and other aspects.

To Dipl.-Ing. Florian Dexl of Technical University of Dresden (TUD), for having coordinated my work in TUD, always showing willing to help and patience, and to Dipl.-Ing. Andreas Hauffe, Prof. Dr.-Ing. Klaus Wolf and Prof. Fernando Lau for accepting my application to start working for the thesis in TUD and making the experience of studying abroad possible.

To all others who in some way took a positive part in my life during these years, mainly:

- Professors that taught me and believed in my capacities along these years at IST;
- Colleagues of S3A and AEROTÉC with whom I worked;
- Co-members of Olisipo Team, that participated in Air Cargo Challenge 2015 in Stuttgart, Germany, for the experience and good times.

my meaningful thanks.

Furthermore, I want to thank my beloved Luís Cardoso for all the counselling, patience and support even in his most difficult times. To my friends Odelma Teixeira and Sara Afonso for having supported me during these years and given me so much strength in these final times. I additionally thank them for having revised this Thesis and corresponding Extended Abstract in such detail.

Finally, I give special thanks to my university godfathers, Paulo Ferreira in first two years and David Melo the following ones, for all the help and counselling they gave me. Without them I would have felt lost at some time. Also to Rita Wahl from GATU for giving me strength to deliver this thesis.

Abstract

Cut-outs are an inevitable part of a fuselage structure. There are cut-outs for windows, passenger doors, cargo doors, fuel tanks, etc. Some of them are big enough to break the load path in the fuselage's skin and develop high concentration of stresses, causing a significant redistribution of loads in the structure, mainly in the cut-outs' surrounding.

A great challenge in aeronautic industry is to construct lightweight structures, which can be done by studying the available materials and also the design. Despite the increased use of composite materials due to their lightweight and mechanical properties, there is still research going on structural behaviour in some situations. The properties of metallic materials are better known due to their isotropy and applications.

A structural analysis of the fuselage is generally done computationally, with the Finite Element Method (FEM). For this purpose, a half-section of a generic metallic fuselage with a door cut-out is created as a parameterized model using the commercial FEM program ANSYS. After analysing the initial model for static behaviour and stability, some parameters – the Design Space – are varied and their effects in the overall section's weight are studied, through a developed routine in MATLAB.

This process is called a Sensitivity Analysis (SA), which can provide data for an optimisation. A SA will serve to identify what parameters most influence the fuselage's structural behaviour. Having a quantitative information of that influence, an optimum solution can be more easily reached, hence making the design process more efficient.

Keywords: door surrounding structure, Sensitivity Analysis, ANSYS, metallic fuselage

Resumo

Os recortes na estrutura aeronáutica são uma parte inevitável. Existem recortes para as janelas, portas de passageiros, porão, tanques de combustível, entre outros. Alguns são grandes o suficiente para interromper o fluxo de cargas na casca da fuselagem e criar grandes concentrações de tensão, causando uma redistribuição das cargas na estrutura em torno dos recortes.

Um grande desafio na indústria aeronáutica é encontrar estruturas leves, o que pode ser conseguido fazendo um estudo de materiais e um projecto estrutural. Apesar do crescente uso de Materiais Compósitos em estruturas aeroespaciais, devido à relação propriedades mecânicas-peso, há ainda muita investigação a ser feita sobre o comportamento estrutural em algumas situações. As propriedades dos materiais metálicos são mais bem conhecidas, atendendo à sua isotropia e aplicação em diversos tipos de estruturas.

A análise estrutural de uma fuselagem é geralmente feita numericamente, através do Método dos Elementos Finitos (MEF). É criado um modelo parametrizado de meia-seção de uma fuselagem metálica genérica com um recorte para porta de passageiros, usando o programa comercial ANSYS. Depois de analisar o modelo inicial, alguns parâmetros geométricos são variados e o seu efeito no peso da estrutura é estudado, através de uma rotina criada no MATLAB.

Este processo é chamado Análise de Sensibilidade (AS), que pode fornecer dados para uma optimização. Uma AS servirá para identificar os parâmetros que influenciam mais o comportamento estrutural da fuselagem. Tendo-se uma informação quantitativa dessa influência, uma solução óptima pode mais facilmente ser atingida, tornando o processo de projecto aeronáutico mais eficiente.

Palavras-chave: estrutura envolvente das portas, Análise de Sensibilidade, ANSYS, fuselagem metálica

Contents

- Dedication..... iii
- Acknowledgements iv
- Abstract.....v
- Resumo vi
- List of Figures ix
- List of Tables xii
- Symbols and Nomenclature xiii
- 1. Introduction..... 1
 - 1.1 Background 1
 - 1.2 State of the Art..... 3
 - 1.3 Thesis Objectives 5
 - 1.4 Structure of the Thesis 5
- 2. Fundamentals..... 7
 - 2.1 Fuselage Structures 7
 - 2.1.2 Metallic Fuselage..... 7
 - 2.1.3 Fuselage Structural Members 9
 - 2.2 Door cut-out and surrounding structure..... 10
 - 2.3.2 Airworthiness and Regulations 12
 - 2.3 Review on Mechanics of Aircraft Structures..... 12
 - 2.3.1 Stresses and Strains 12
 - 2.3.2 Elastic Energy..... 13
 - 2.3.3 Natural Frequency 13
 - 2.3.4 Instability of Structures 13
 - 2.3.5 Plates..... 13
 - 2.3.6 Beams..... 14
 - 2.3.7 Shear webs..... 14
 - 2.3.8 Structural idealisation of aircraft structures 15
 - 2.4 Fuselage Loads 17
 - 2.4.1 Cabin Pressurisation 17
 - 2.4.2 Other loads 19
 - 2.6 Sensitivity Analysis..... 21
 - 2.5.1 Relationship between Sensitivity Analysis and Optimisation 22
- 3. Methodology and Implementation 23
 - 3.1 Introduction..... 23
 - 3.2 Interface ANSYS-MATLAB..... 24
 - 3.3 Construction of the model..... 24

3.3.1 General Considerations.....	25
3.3.2 Coordinate systems.....	26
3.3.4 Finite Element types.....	26
3.3.5 Material.....	27
3.3.6 Modelling the components.....	28
3.3.7 Mirror and mesh.....	30
3.4 Application of Loads.....	32
3.5 Application of Boundary Conditions.....	36
3.5.1 Symmetry.....	36
3.5.2 Rigid body motion.....	37
3.6 Calculation of the weight.....	38
4. Analyses.....	39
4.1 Static Analysis.....	39
4.2 Stability Analysis.....	40
4.3 Convergence Analysis based on mesh refinement.....	42
5. Sensitivity Analysis.....	49
5.1 Parametric Study.....	49
5.1.1 Case 1: Internal pressure.....	49
5.1.2 Case 2: Internal Pressure + Shear Load.....	62
5.1.3 Case 3: Internal Pressure + Bending Moment.....	67
5.2 Finite Differences.....	74
6. Conclusions and Further Work.....	77
References.....	79
Appendix.....	81
A.1 mv2s.mac.....	81
A.2 B_variation.m.....	95

List of Figures

- Figure 1 - Passenger door on a transport aircraft [1]. 2
- Figure 2 - The ideal configuration of each Engineering Group, according to C.W.Miller [3]. 3
- Figure 3 - picture of DeHavilland Comet 1A, showing the squared windows [12]. 7
- Figure 4 - Weight fractions of each material in A320 structure (adapted from [13]) 9
- Figure 5 - fuselage structure type: a) Monocoque b) Semi-monocoque [14]..... 10
- Figure 6 – A320 fuselage members [13] 10
- Figure 7 - Generic fuselage structure with a cut-out [1]. 11
- Figure 8 – Diagonal Tension in a shear web (adapted from [15]). 15
- Figure 9 – Shear flow developed around a cut-out in a circular shell [2]. 17
- Figure 10 - The airplane cabin modelled as a Pressure Vessel, with the resulting internal loads in the edge frames and the shear flow distribution around a door cut-out [2]..... 18
- Figure 11 - The resultant force caused by pressure on the door FDS and its components..... 19
- Figure 12 – loading in the fuselage (adapted from [5]) 20
- Figure 13 - coordinate systems: a) CSYS,0 b) CSYS,1 [24]..... 26
- Figure 14 – Used elements: Left – SHELL181; Right – BEAM188 [11]...... 27
- Figure 15 - Dimensions of model (versions 1 and 2). 28
- Figure 16 - Resolution of problems with the mesh after the mirror. 31
- Figure 17 - Reference structure meshed showing different types of element through colours..... 32
- Figure 18 - Internal pressure applied in the skin. 33
- Figure 19 – MPC Beam vs MPC Link (x is the horizontal component in the 2D plate)..... 34
- Figure 20 - Axial force due to bulkheads applied using MPC184. 35
- Figure 21 - Pressure on the door transmitted to the door-stops using RBE3 elements..... 35
- Figure 22 – Left: Meshed part before mirror; Right: Full cylinder with cut-outs. 37
- Figure 23 – Left: With simple support at $y = \pm 90^\circ$; Right: With clamping at $z = bs$ 38
- Figure 24 – Sum of displacements in versions 1 (mv1.mac) and 2 (mv2.mac) with group 1 of BCs.... 40
- Figure 25 - Local instability with internal pressure: Left - $UY=0$ in upper line; Right - $UY=0$ at extremity $z = bs$ (mv2.mac)..... 41
- Figure 26 - Local instability in load case 2: Left - $UY=0$ in upper line; Right - $UY=0$ at end $z = bs$ (mv2.mac)..... 41
- Figure 27 - Local instability for the third load case and $UY=0$ at $z = bs$ ($Bf=-0,386E-01$) (mv2.mac)... 41
- Figure 28 – Convergence Study of Version 1 of model (mv1.mac). 43
- Figure 29 - Convergence Study of Version 2 of model (mv2.mac). 43
- Figure 30 - Stress distribution in Version 2 (mv2.mac). 44
- Figure 31 - Stress distribution in version 2 without the singularities at the cut-out corners (mv2s.mac) 45
- Figure 32 - Convergence obtained by variation of number of elements in the model without the nodes in the corners (mv1s.mac). 45

Figure 33 - Convergence obtained by variation of number of elements in the model without the nodes in the corners (mv2s.mac).....	46
Figure 34 – Variation in model 1 with the cut-out’s width, B (mv1s.mac).	50
Figure 35 – Variation in model 1 with the cut-out’s height (mv1s.mac).	51
Figure 36 - Variation with width after changes are done in the geometry of Version 1 (mv1o.mac). ...	52
Figure 37 - Stress distribution in the chosen configuration (mv1o.mac).....	53
Figure 38 - Variation with height after changes are done in the geometry of Version 1 (mv1o.mac)...	54
Figure 39 – Variation in model 2 with the cut-out’s width (mv2s.mac).....	55
Figure 40 – Variation in model 2 with the cut-out’s height (mv2s.mac).	56
Figure 41 – Distribution of stress in configurations H=1800 mm, H=1805 mm and H=1810 mm (mv2s.mac).....	57
Figure 42 - Maximum stress in regions 1, 2 and 3 for version 2 for height variation (mv2s.mac).	58
Figure 43 – Stress distribution in altered version 2 (mv2o.mac).....	59
Figure 44 - Variation with width after changes are done in the geometry of Version 2 (mv2o.mac). ...	60
Figure 45 - Variation with height after changes are done in the geometry of Version 2 (mv2o.mac)...	61
Figure 46 – Displacements caused by load case 2.....	62
Figure 47 – convergence analysis for reference model with load case 2 (mv2sf.mac).	62
Figure 48 – Variation in Version 2 with the cut-out’s width (mv2sf.mac).	63
Figure 49 – Variation in model 2 with the cut-out’s height (mv2sf.mac).	63
Figure 50 - Stress distribution in reference structure (version 2) subject to case load 2 (mv2sf.mac). ...	65
Figure 51 - Weight vs door width for comparison with improved model (mv2sf.mac).....	65
Figure 52 - Variation with width of altered model 2 (mv2of.mac).....	66
Figure 53 – Distribution of stresses in load case 3. Left: group 1 of constraints. Right: group 2.....	67
Figure 54 – Displacements caused by load case 3. Left: group 1 of constraints. Right: group 2.	67
Figure 55 – Convergence of Stress in reference structure (Version 2) subject to case load 2.....	68
Figure 56 - Contour plot of the model subject to case load 2 showing the deleted nodes and also the regions where maximum stresses will be taken. Note: the image is previews to the change in internal pressure value (mv2sm.mac).	68
Figure 57 - Convergence of Stress in reference structure subject to case load 2 in defined zones.	68
Figure 58 – Variation in model 2 with the cut-out’s width (mv2sm.mac).....	69
Figure 59 - Maximum stress (mv2sm.mac). Left: B=760mm (Smax= 479,79 MPa); Right: B=780mm (Smax= 480,34 MPa).	69
Figure 60 - Plots of Stresses in zones 1 and 2 vs door width (mv2sm.mac).	69
Figure 61 – Variation in model 2 with the cut-out’s height (mv2sm.mac).	70
Figure 62 - Variation of B for version 2 (mv2om.mac).	71
Figure 63 - Variation of H for version 2 (mv2om.mac).	72
Figure 64 - Stress plot of the altered version of the model (version 2, mv2om.mac).....	73
Figure 65 – Sensitivity of the maximum stress to the width, for each configuration	74
Figure 66 – Sensitivity of the maximum stress to the height, for each configuration	74
Figure 67 – Sensitivity of the weight to the width, for each configuration	75

Figure 68 – Sensitivity of the weight to the height, for each configuration 75
Figure 69 – variation of the weight with both variables (mv2s.mac). 76
Figure 70 – variation of the maximum stress with both variables (mv2s.mac). 76

List of Tables

Table 1 - Metallic materials used in aerospace industry [1]. 8

Table 2 - Characteristics of Aluminium Alloy Al 2024-T3 [25]. 27

Table 3 – Geometric Parameters of the initial model. 29

Table 4 - Summary of analyses performed in chapter 4 and 5. 39

Table 5 - Design variables, initial inputs and bonds. 49

Table 6 - Design Constraints. 49

Table 7 - Chosen configuration in terms of stress for H=1850 mm (mv1o.mac). 53

Table 8 - Chosen configuration in terms of displacements for B=810 mm (mv1o.mac). 54

Table 9 - Chosen configuration for a structure subject to pressurisation for H=1850 mm (mv2o.mac).60

Table 10 - Chosen configuration for a structure subject to pressurisation for B=810 mm (mv2o.mac).61

Table 11 - Chosen configuration for a structure subject to pressurisation and shear load 66

Table 12 - Chosen configuration for a structure subject to pressurisation and bending moment. 73

Symbols and Nomenclature

A_{door}	area of the door
b_c	cut-out width
b_d	doublers Width
b_{fra}	frame base width
B_r	boom area
b_s	fuselage section's width
b_{si}	sill width (°)
b_{str}	stringer base width
E	Young's Modulus
{f}	vector of loads
F	force load
f_j	interest function
F_{DS}	force load on door-stops
g	equality constraint function
h	inequality constraint function
h	altitude
h_c	cut-out height
h_d	doublers height
h_{fra}	frame web height
h_l	intercostal height
h_{si}	sill height (°)
h_{str}	stringer web height
I_{xx}	second moment of area about x-axis
I_{xy}	product of inertia
I_{yy}	second moment of area about y-axis

$[K]$	stiffness matrix
l_e	effective column length
lb	lower bound of design variable
m	mass
M	moment load
N_{fra}	number of normal frames on each side
N_{str}	number of stringers below cut-out
O	truncation error
p	pressure
P_{cr}	critical load
p_e	atmospheric pressure
p_i	internal pressure
q	shear flow
q_b	shear flow in the open section for a closed section beam
q_s	total shear flow of the closed section beam
$q_{s,0}$	shear flow of the cut part in a closed section beam
r	radius of gyration
R	radius of a generic pressure vessel
r_s	fuselage radius
S_x	shear load in x-direction
S_y	shear load in y-direction
s_{fra}	spacing between frames
s_{str}	spacing between stringers
t_d	doublers thickness
t_{fra}	frame web and flange thickness
t_i	intercostal thickness

t_s	skin's thickness
t_{str}	stringer web and flange thickness
{u}	vector of degrees of freedom
U	displacements
U	Elastic Energy of Deformation
ub	upper bound of design variable
x_i	design variable i
x_r	x-coordinate of the rth boom
y_r	y-coordinate of the rth boom

Greek letters

α	cut-out's height from XZ-plane
β	cut-out's height from the bottom of airplane (door sill height)
γ	cut-out total height in degrees
δ	maximum deflexion of a plate
ε	strain
φ	angle from fuselage's upper line to cut-out's sill
λ_{ij}	design coefficient
ν	Poisson's coefficient
ρ	density
σ	normal stress
σ_{eqv}	von Mises stress
σ_L	longitudinal stress
σ_{yeld}	yeld stress
σ_θ	hoop stress
τ	shear stress

Acronyms

AIAA	American Institute of Aeronautics and Astronautics
ALCAS	Advanced Low Cost Aircraft Structure
APDL	Automatic Parametric Design Language
CAD	Computer Aided Design
CAE	Computer Aided Engineering
CP	Coupling nodes
CUFUS	CUt-out FUSelage
DOF	Degrees-of-Freedom
DSS	Door Surrounding Structure
EASA	European Aviation Safety Agency
FAA	Federal Aviation Administration
FAR	Federal Aviation Regulations
FEM	Finite Element Method
FEA	Finite Element Analysis
IST	Instituto Superior Técnico
MPC	Multipoint Constraint
TUD	Technische Universität Dresden
TU Delft	Technische Universiteit Delft
SA	Sensitivity Analysis

1. Introduction

1.1 Background

The airframe of a generic aircraft consists in the fuselage, wings, tail, landing gear and control surfaces. Beyond having specific functions, they include important parts such as electronic and hydraulic systems, fuel tanks, and others. Furthermore, in all parts there must be openings. An opening in an aircraft structure is called a cut-out.

Cut-outs in aircraft fuselages are undesirable because they break the load path of the skin and stiffeners and induce high concentrated stresses in the region around it [1]. The increase of the stress in some parts demands for reinforcement on the region, which by itself increases the weight and cost of the aircraft. However, like almost every component in an aircraft, cut-outs are inevitable. Important examples of these are:

- Lightning holes in webs;
- Passages for wires;
- Cargo compartment doors;
- Passenger doors;
- Emergency exits;
- Windows;
- Access to fuel tanks and other systems;
- Access to components for maintenance purposes.

Not all cut-outs in an airframe have significant effects in the load bearing of the structure. The lightning holes in webs for example save structural weight when required minimum gage thicknesses. Passages for wires are so small that the only reinforcement consists in a thicker plate riveted to the skin around the cut-out whose mass is generally equal to the amount of removed material. Passenger, Cargo and fuselage nose and rear loading and unloading doors' cut-outs are the most hazardous [2].

There are four passenger doors, the two at the forebody and the two at the rear of the aircraft. Other cut-outs are outside the scope of this thesis. A generic fuselage passenger door is shown in Figure 1.

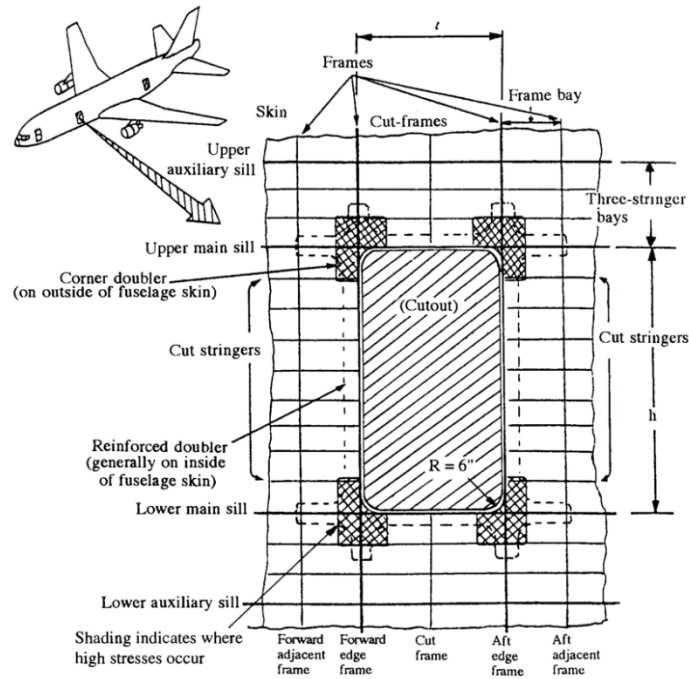


Figure 1 - Passenger door on a transport aircraft [1].

Based on past experience, there are now several aspects to account for when designing and sizing aircraft structures, being the most important the weight savings. In commercial flight, a lower cost of the airplane is more important than having less weight. The contrary happens for military airplanes. The ease and cost of manufacture is also important for the sizing of airframe parts. However, many aspects enter in the conceptual design and all of them “want” to make the airplane in a different direction (Figure 2), and there must be a compromise between them.

With the minimization of weight as one of the main objectives, investigation is done on what would make a commercial aircraft lighter and, being the stress level on the structure one of the factors for the increase of material, there must be a lot of study on the parts where they are biggest, such as around the cut-outs. The goal of the Sensitivity Analysis is to know what happens to the structure’s behaviour when some part of its geometry is changed and what structural changes can be done there to decrease the amount of material.

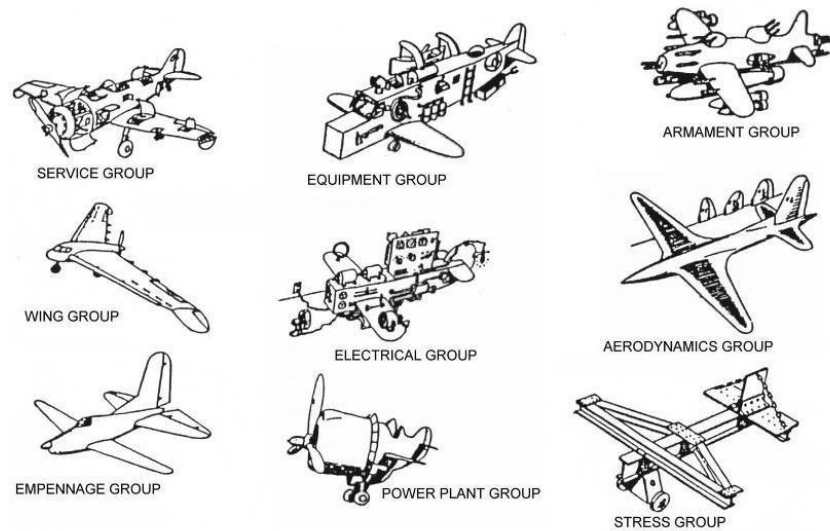


Figure 2 - The ideal configuration of each Engineering Group, according to C.W. Miller [3].

The study of the structural response of a fuselage in which parameters are varied a big number of times is only possible if a parameterised model is used. For this reason, a Finite Element Model is created with sufficient detail to perform such analysis.

The obtained Sensitivity Data gives information for some types of Optimisation algorithms. Some examples of these are the Direct method, the Adjoint method, etc. These use the derivatives of the function in each point to know which direction in the function to search for the minimum, taking in consideration the constraints of the problem. The difficulty of the study depends on the number of design variables and of objective functions.

1.2 State of the Art

In this subchapter a review of the important research done about cut-outs and Sensitivity analysis methods is done. There is more recent research in composite-made fuselage structures, which is explained by the rapid acknowledgement of carbon-fibre composite as an efficient material for aerospace industry, but little information on their influence in the behaviour of the airframe. In the following paragraphs a brief description is presented of what some authors that have focused on this theme have done and the conclusions they reached.

M. E. Heerschap [4] developed in 1997 an interactive design tool, called CUFUS (CUt-out in a FUSelage), using the FEA software MSc Nastran. The algorithm consists in a model generator, with possibilities of editing the geometry and properties interactively and provides the post-processing options of a Design Sensitivity Analysis and Optimisation, features of Nastran. Using symmetry, only a quarter of a cut-out surrounding structure was modelled.

Having developed a Design Engineering Engine (DEE), Van Tooren [5] performed a Multidisciplinary Design Optimisation (MDO) of a fuselage structure based on A320, in the subjects structural, thermal and acoustic. Of concern is the Sensitivity coefficients that were reached in the study. The load cases in this thesis were taken from the study of van Tooren.

Seeger and Wolf [6] worked in Multi-objective Design (MDO) of an existing composite (Carbon Fibre Reinforced Plastic – CFRP) fuselage structure. The used approach for optimisation is based on Evolutionary Algorithms, a type of method that do not require information of the derivatives of the objective functions. An optimisation tool called GEOPs², developed in Technische Universität Dresden, is used. They test Evolutionary Algorithms and the Pareto Front to optimise a parameterised fuselage model with cut-outs based on the ALCAS (Advanced Low Cost Aircraft Structure) project, a structure developed by Airbus. The same model is later used by Dextl [7] to study the parameters that most influence the static behaviour of this model. One limitation of this model is the difficulty in varying the stringer spacing.

Bruyneel [8] uses finite Differences for the Sensitivity Analysis of a fuselage model with the aim of minimising the weight for the variation of number of stringers, using the software NASTRAN. Other tool used is the STIFFOPT (Stiffened Panel Optimisation). An optimisation of the number of stringers, the stringer profile and cross sectional area, and thicknesses of stringers and skin is done using various approaches.

A group of students of Fachhochschule München, supervised by Prof. Dr.-Ing. E. Sperling [9], developed a study on a fuselage airframe, using FEM. Having investigated a rectangular shear-panel-box with cut-out, one of their conclusions was that the skin “vis-à-vis” of the cut-out carries almost no loads. Only the top and bottom shear-panels act as “bending-beams” with one end fixed and the other remaining parallel to the former.

In what relates to Design Sensitivity methods, Sobieszczanski-Sobieski [10] makes a review of different Sensitivity Analysis methods for aircraft design, namely those that provide tools for multilevel and multidisciplinary optimisation, like the Implicit-Function Theorem, improving Hierarchical Decomposition (example of a transport aircraft wing optimisation for improved fuel economy), that is already able to treat a thousand design variables. If all design variables were computed simultaneously the problem would be very broad and its solution impractical. According to the research, the Sensitivity derivatives indicate by their relative magnitude which design variables are the most influential ones and whether their influence is positive or negative, which is very useful for deciding how to modify the design.

Akgün [11] studies the sensitivity of von Mises stress and local buckling constraints to demonstrate the efficiency of the Adjoint method over the Direct Method, under multiple load cases using three examples with increasing complexity. These are very used methods in structural optimisation. The advantage of the Adjoint Method increases with problem size. Though, for a single load case, it requires substantially more time than the Direct Method.

1.3 Thesis Objectives

Having understood the context of the theme, what is proposed in this thesis is to study the influence of changes in the dimensions of a cut-out in the weight of a generic fuselage's structure. The main objectives of this work are to:

- Investigate an approach that can help perform the intended study;
- Construct a parameterised Finite Element model of a fuselage with a door cut-out;
- Implement an algorithm for the Sensitivity Analysis;
- Propose designs in which the weight is reduced and still good strength is guaranteed or vice-versa.

1.4 Structure of the Thesis

In Chapter 1 the theme of this work was presented and the context explained, followed by the State of the Art, a review on what have been done related to the theme.

Chapter 2 starts by explaining the important terms and concepts for the understanding of this work, following a reference to loads that are applied in the fuselage. A brief explanation of the concept of Sensitivity Analysis and its difference from optimisation is also done.

In Chapter 3 the developed work and the methodology adapted is presented, along with the choices for the modelling and application of loads and constraints; it then presents the implementation of the chosen methodology: the generated models, the interface between the softwares MATLAB and Ansys and the type of analyses to get the desired results.

Chapter 4 describes the analysis that will be performed and shows the results for manual analysis of ANSYS. Being the FEM a numeric method, and thus approximated, it is possible that it does not converge, so a convergence study is first made for each of the models.

In Chapter 5, the Sensitivity Analysis is performed for the first load case and the results are then shown and interpreted.

Finally, In Chapter 6, after some concluding remarks, recommendations are given for a possible further and more detailed work on the theme.

2. Fundamentals

2.1 Fuselage Structures

Only after the considered first succeeded flight, by the Wright brothers, have serious structural studies and implementations been performed to construct more and more efficient flying structures. Their implementation was the wire-braced structure in which the struts were rectangular beams supported by wires in diagonal that prevented them from collapsing, and wood was the material used. The structure was resistant to bending and twisting. Biplanes like this were used until 1930's. In 1931, metal structure started being used and then in 1933 skin started being used as a way of transmitting stresses, along with vertical and longitudinal members, so that the airplane could accommodate not only one or two pilots. E.g. DC3.

The war had an important role in the advent of aviation, for military purposes. Some intelligence was then used to construct machines also for commercial purposes (E.g. Boeing 314). It was in World War II that took place a huge development in aerospace field. Spitfire was the most efficient airplane, due to its elliptical wings, but at a too high cost, due to its difficult manufacture.

Aircraft started being pressurised in 1920, which made the commercial transport of people possible. Though many were the accidents that took place at that time and they were mostly caused by wrongly dimensioned structures. The first commercial Jet airliner was called de Havilland Comet 1, which, at the service of British Overseas Airways suffered an explosion in 1954, caused by a depressurisation on the cabin (Figure 3).



Figure 3 - picture of DeHavilland Comet 1A, showing the squared windows [12].

2.1.2 Metallic Fuselage

The structure of the fuselage started being constructed in fabric and wood. Only in the mid 1930s did the structure began to be metallic. Today, the majority of airplanes in service have metallic fuselage, but there are others that already have composite laminates in a substantial area of its airframe. E.g. A380 and B787 have 80% of Carbon Fibre Reinforced Panel (CFRP) and other composites in less percentage. Investigation is also being done on the use of other types of Composite Laminates, Sandwich Structures and Fibre Metallic Laminate (FML), e.g. GLARE ("glass reinforced aluminium", a fibre metal laminate (FML), which is a type of composite material).

Although there is an increasing use in composite materials for their excellent properties and weight, there are still some research going on, so these can't be used integrally in primary structures of the aircraft. There are two biggest disadvantages of composites:

- The still unpredicted behaviour under conditions of fatigue, as an initial crack in the structure is not easy to identify. The time from the appearance of a micro-fracture to the rupture is very low, so it is of extreme importance to identify the crack as soon as possible, which is easier in aluminium.
- The other disadvantage has to do with environmental concerns. After their fabrication, composites cannot be recycled. There should also be an intention to reduce the waste produced by the industry. Composites cannot be used even in other applications, but metals can be recycled and are still used in the majority of aircraft components, beside not being as efficient as composites regarding weight-strength ratio.

The used metals in aircraft structures are in Table 1.

Table 1 - Metallic materials used in aerospace industry [1].

Alloy Type	Advantages	Disadvantages
Aluminium, Al	<ul style="list-style-type: none"> • high strength-weight ratio; • low density; • easy to work on; • available in many forms. 	<ul style="list-style-type: none"> • needs protective finish from corrosion; • some alloys have limited strength at high T.
Titanium, Ti	<ul style="list-style-type: none"> • high resistance to corrosion; • higher melting point; • lower thermal expansion. 	<ul style="list-style-type: none"> • more expensive than Al; • difficult to machine.
Steel	<ul style="list-style-type: none"> • cheap; • high strength; • high corrosion resistance (stainless steel). 	<ul style="list-style-type: none"> • low strength-weight ratio; • high density.

The most used material, for example in the fuselage skin and stiffeners, is the aluminium, which is actually used in the form of aluminium alloys (AA). An example of a common AA is the 2024-T3, which is one of the group 2000, characterised by having Copper as the major element in the alloy and being “primarily used in tension applications where fatigue and damage tolerant design is critical, e.g. (...) pressurised fuselage skin.” [2] and the T means that it is heat treated.

In fact, “all aluminium alloys used in primary airframe applications are the heat treated tempers” [1] and AA 2024-T3 makes the majority of Airbus airplanes fuselage skin, so this is the material used in the developed model. Alloys with copper have good fatigue life and fracture toughness. The weight fractions of each material and type of structure in A320 structure is shown in Figure 4.

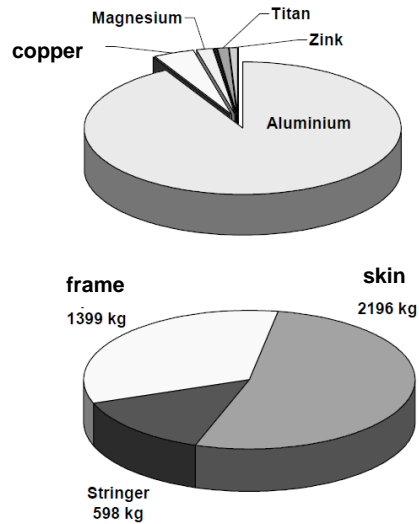


Figure 4 - Weight fractions of each material in A320 structure (adapted from [13])

2.1.3 Fuselage Structural Members

An airplane's fuselage has essentially a structure of one of two types: Monocoque, which means single shell (from the Greek word "mono" - one, and the French word "coque" - shell) and Semi-Monocoque Structure (Figure 5).

- **Monocoque Structure:** consists in a structure made of formers and bulkheads at the ends of the body, that dictate its shape; these are covered with a skin of the same material or another. One disadvantage of this is the inability to support bending loads. The bending causes tension in one part and compression on the other side of the same section. That compression often leads to buckling;
- **Semi-Monocoque Structure:** the configuration skin+circumferential stiffeners will also have longitudinal stiffeners, called longerons and stringers, so that the compression loads are supported and the skin is protected, as well as the fuselage's shape. This is called a stiffened panel and is the typical configuration nowadays. The general constituents and their functions are (Figure 6):
 - **Skin:** it consists on a panel, designed to withstand tensile loads caused by pressurisation (hoop stress), by bending (tension and compression) and also shear loads because of the torsion that lateral loads on the fin (like gust) cause in the fuselage [9].
 - **Frame:** circumferential member that keep fuselage shape and transfer axial loads; they are axially loaded due to hoop stress from cabin pressurisation [4];
 - **Stringer:** axial stiffeners that support the skin in compressive loads due to bending;
 - **Longeron:** axial stiffeners whose cross-sectional is bigger than the stringers' one, designed to help in compressive forces transmission.

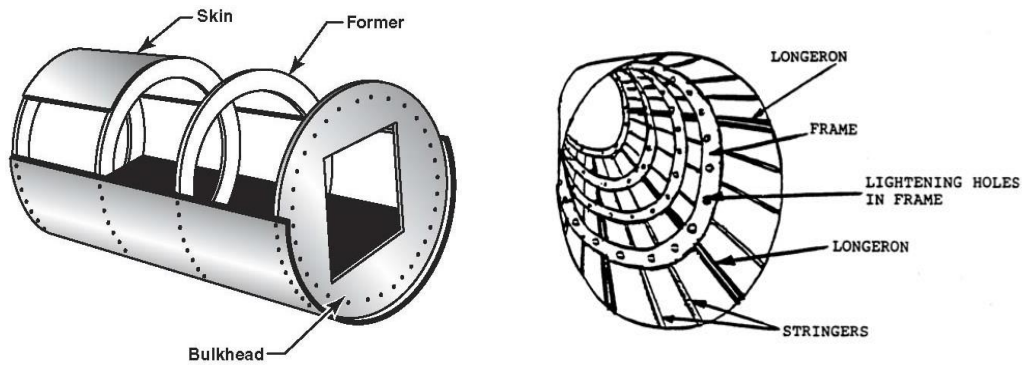


Figure 5 - fuselage structure type: a) Monocoque b) Semi-monocoque [14]

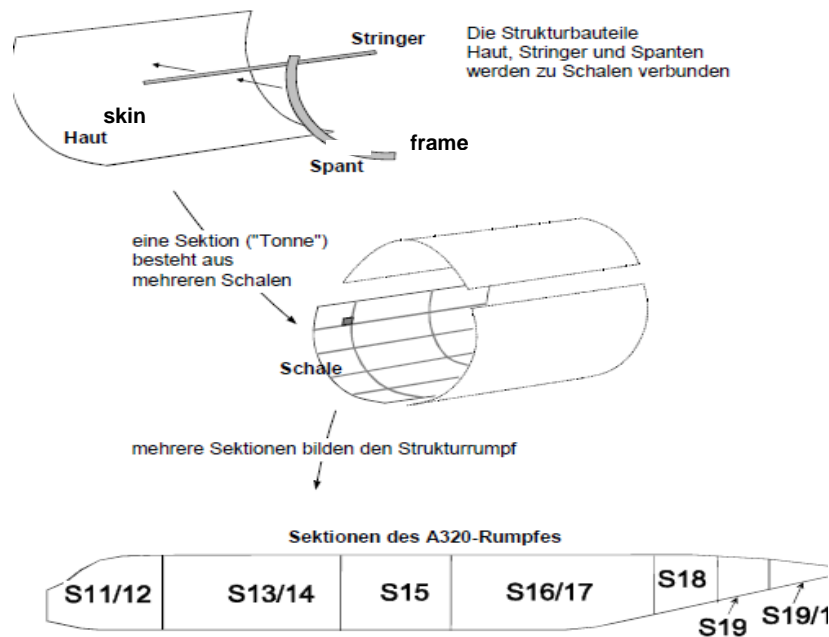


Figure 6 – A320 fuselage members [13]

Further elements to have in consideration regarding the structure of a fuselage are the bulkheads. These are “walls” inside the hull of the fuselage, which are positioned in different sections. The most important are the ones in the extremities of the cabin, one at the tail and the other between the cockpit and the nose.

2.2 Door cut-out and surrounding structure

The fuselage of an aircraft is already a very efficient structure for the purpose of flying with safety [9]. However, it cannot be a continuous structure and must have cut-outs for entrance doors, for the fuel, the cargo and emergency exits, and also for the inclusion of windows. Entries for fuel tanks do not influence the load paths as much as the cuts for passenger entrance and for cargo, which are bigger.

The aspect ratio of the cut-out is defined as the ratio width-to-height, b/h . In Niu [1] the preliminary sizing of a plug-type door is based on an aspect ratio of 0,6. Cut-outs are main contributors to failure of fuselage shells, which lead to airplane crash, because they create high local stresses [15]. Therefore, the structure around these holes must be reinforced. The following members are commonly used for the structure around doors (Figure 7):

- **Sill:** a longitudinal stiffener usually thicker than the stringer, that limits the cut-out above and below; it can have a varying cross-sectional area so that twisting loads are more easily borne; sometimes two sills are considered – a main sill and an auxiliary sill – at each part of the cut-out [1].
- **Intercostal:** a short beam that makes a bridge between a main frame and the edge frame at the laterals of the cut-out [9];
- **Doubler:** an outside reinforcement around the cut-out, most commonly used for the corners of rectangular cut-outs;
- **Door-stop:** fixed structural members of the door and doorframe that limit the directions of the door's movement [16]; these distribute the force caused on the door by the internal pressure to the two edge frames at the right and left of the door [9].
- **Edge frame:** like the main frames, are axially loaded due to hoop stress, but are additionally subjected to bending due to the presence of the door and to point loads from the door-stops that are attached to it (Figure 7); usually there exist an auxiliary frame, which carries the same bending load as the edge frame, but with less magnitude; there are also cut-frames, which are located between the two edge-frames and above and below the cut-out; these have the same job as the main frames [4].

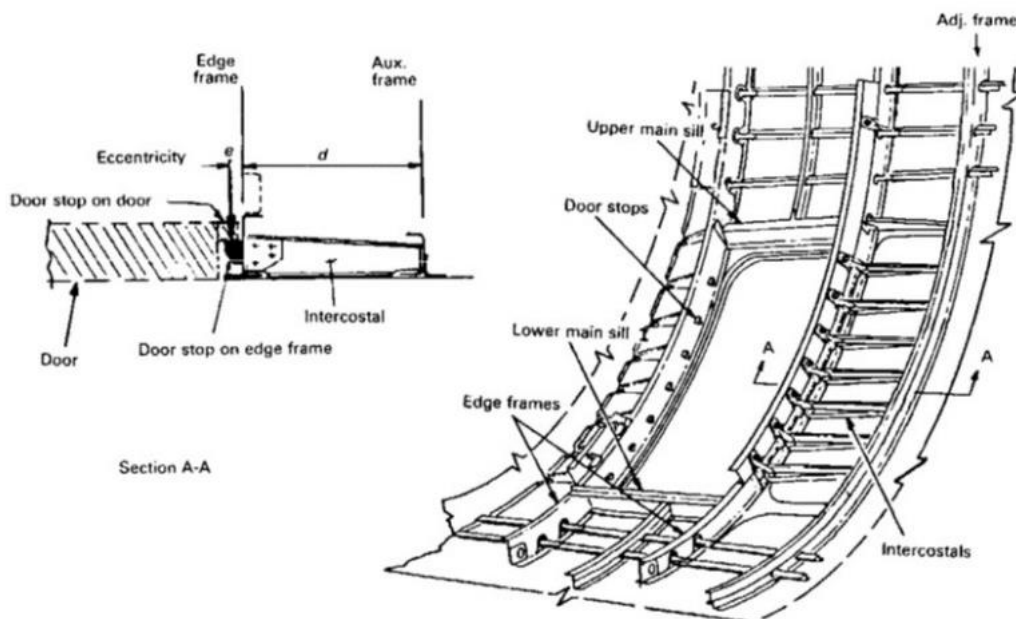


Figure 7 - Generic fuselage structure with a cut-out [1].

2.3.2 Airworthiness and Regulations

According to FAA Airworthiness Standards, “strength requirements are specified in terms of limit loads (the maximum loads to be expected in service), and ultimate loads (limit loads multiplied by prescribed factors of safety)” [17]. The factor of safety in use is of 1.5. An aircraft in Europe must also be certified by EASA CS-25 – Large Airplanes, subpart C [18]. The door cut-out in the current study is of type II of these regulations. The important information for this work is related not only to the loads the structure may be able to stand, like “The structure must be able to support limit loads without detrimental permanent deformation”, but also to its characteristics. E.g.: “Each door must have means to safeguard against opening in flight as a result of mechanical failure, or failure of any single structural element.” [18]

2.3 Review on Mechanics of Aircraft Structures

2.3.1 Stresses and Strains

Stresses are of two types [15]:

- Normal (axial) stresses: are in the direction normal to the plane in consideration (e.g. the cross-section of a beam or along the thickness of a shell) and that can be of tension (+) or compression (-); represented by the Greek letter σ .
- Shear (tangential) stresses: are represented by the Greek letter τ .

The airframe is, for the stress engineer, a combination of beams, plates and shells. Both the wing and the fuselage are considered beams, which in turn are made of a plate, stiffened by transversal and/or longitudinal beams. This configuration is called a stiffened panel.

In a complex structure like in an aircraft, it is difficult to calculate the stresses and then verify if the strength of the material is enough to carry them. Finite Elements Method is therefore a powerful tool for calculating the stresses and other phenomena in the overall structure. A common indicator of the static behaviour of the structure is the von Mises Stress, defined by:

$$\sigma_{eqv} = \sqrt{\frac{1}{2}[(\sigma_1 - \sigma_2)^2 + (\sigma_2 - \sigma_3)^2 + (\sigma_3 - \sigma_1)^2]} \quad (1)$$

Where σ_1 , σ_2 and σ_3 are the principal stresses of the loading on the structure. If its value is above the strength of the material, the structure will fail.

To be able to analyse the behaviour of the system with the presence of forces and constraints applied in a specific region of the body as surface loads, the Saint-Venant Principle is considered: the method of application of forces and their distribution in extremities is irrelevant when considering a section far away. So with a good approximation is always possible to substitute a loading with another statically equivalent loading (i.e. that has the same effects) that is more convenient.

2.3.2 Elastic Energy

Another important quantity is the Elastic Energy of deformation, U , a measure of the stiffness of the material. It is defined by :

$$U = \frac{1}{2} \{\sigma\}^T \{\varepsilon\} \quad (2)$$

A high elastic energy means that the material deforms more under the same load, a characteristic of elastic materials. The more it deforms, the less is its stiffness, which measures the rigidity of the material.

2.3.3 Natural Frequency

Furthermore, another quantity of interest in this study will be the natural frequency of the structure. It is the frequency at which the system tends to oscillate when a perturbation is made and then taken away. Knowing the natural frequency of a structure is important, although in the present work this value will be retrieved only to observe how it changes with the geometry. The whole structure would have to be modelled in order to obtain a real value.

2.3.4 Instability of Structures

The members that form a fuselage can fail under loads that are below the strength of the material from which they are made. It depends on the type of loading and structure. For a column, if a member is compressed axially and a transversal load is suddenly applied:

- If $P < P_{cr} = \frac{\pi^2 EI}{l_e^2}$, the column will restore its initial position after removing the transversal load;
- If $P = P_{cr}$, the column becomes unstable and may lead to the column failure.

l_e is the effective length of the column, i.e. the length of a pin-ended column that would have the same critical load as the column of length l . A high critical load means that the structure supports a high compressive load without buckling. There are many ways of buckling, depending on the constraints. Two types of instability can occur in these structures, the primary, called the global instability, and the secondary, or crippling, which occurs locally. Whether it is one or the other, or both, usually depends on the slenderness ratio, l_e/r , of the member components.

2.3.5 Plates

A structure is called a plate if it is plane and one of its dimensions is much less than the other two. The proportion of the maximum deflexion the plate suffers, δ , to its thickness, t , defines its type [2]. It is capable not only of resisting bending but also membrane forces, and is the type of structure that forms the skin of a wing and of a fuselage. The most accepted theory is the Mindlin-Reissner, or first-order shear-deformation theory.

2.3.6 Beams

A beam is a structural member that transmits bending moments and transverse loads. In analysis of structures, the parts of a beam are commonly called the web and the flange. The web supports transverse loads, while the flange generally supports normal loads and bending moments. The geometry and orientation of the beam affects its stiffness. The most famous theories of beams are the following [19]:

- Classic Theory (Euler-Bernoulli): when a moment applies to an initially straight beam, it is bent with a radius of curvature and the sections that were normal to its longitudinal axis will remain plane and perpendicular to the axis; the strain along the neutral axis is zero;
- Timoshenko Theory: in this theory the sections remain plane, but may not be perpendicular to the axis after deformation, and accounts for transverse shear stresses;

In airframes there are many members formed by tapered beams, i.e., their height changes along its length, although the cross-section has always the same geometry. If the beam is constant in height the shear flow is constant throughout the web where a constant shear force is applied. In the case of a tapered beam, the flange can take axial load only and the web is ineffective in bending;

2.3.7 Shear webs

As said earlier, a plate fails more easily if the ratio width-to-thickness, b/t , is high. For this reason, a fuselage shell behaves in a better way if stiffened by longitudinal members, which give support to “new and narrower plates”. If the shell is further stiffened by transversal members, the length of the column is reduced and the structure can be said to fail as a whole because, in terms of stability, the critical load will be nearly the same everywhere.

For example, the spars that constitute aircraft wings have the shape of Figure 8. When applied a transversal point load at the free end of the structure, compressive stresses are developed in direction diagonal to the axis of the structure. As a consequence, it can fail by buckling on the web regions, in the “Direction of buckle”, being developed tensile stresses in the perpendicular direction (“Diagonal Tension”).

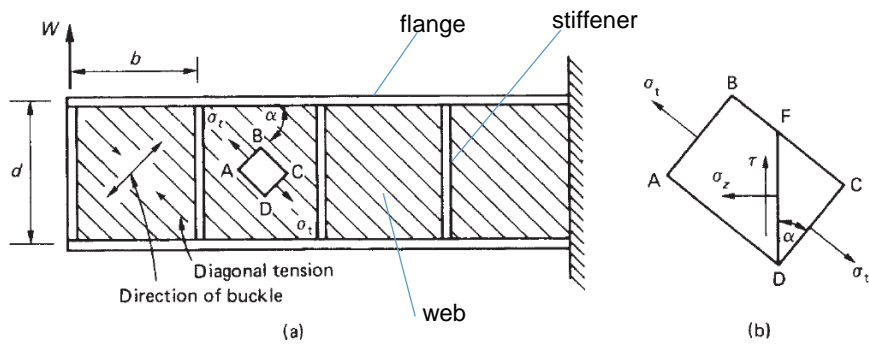


Figure 8 – Diagonal Tension in a shear web (adapted from [15]).

The flanges and stiffeners carry axial forces, while the shear is carried in the web. The forces in the flanges are from a combination of the diagonal stress in the web and the axial stresses in the stiffener. With this in mind, it is unthinkable to have transverse loads applied on an unstiffened web. Without stringers and frames, the skin of a fuselage would buckle under many load cases [9].

The assumptions generally made for beams are:

- Thin-walled beams;
- Classic theory (or Euler-Bernoulli);
- The booms have constant cross section area along their length;
- The loads are applied in the shear or torsion centre.

For a beam with an open section if the shear load is applied at a distance from its shear centre, torsion of the structure will occur. The stiffeners are ineffective to torsional loads.

Admitting that the wall of the beam is so small that the variation of the stresses in the direction of the thickness can be neglected and the section can be represented by a line. If we define a distance along this line as s and make its origin at a fixed point, the shear flow, q , is the flux of shear stress along this distance:

$$q = \tau t \quad (3)$$

2.3.8 Structural idealisation of aircraft structures

For the analysis of structures it is important to determine the neutral line position, the location of the centroid and the moment of inertia of the section. Of interest is also the location of the shear centre.

Structural Idealisation consists in modelling a structure made of skin and stiffeners as a thin plate, that resists shear loads, and “booms”, that resist normal loads [15]. The latter have contribution of the adjacent panels and the spar flanges in their boom area, which is proportional to their distance to the

axis of symmetry. This changes the approach, as we only have to calculate the area of the booms and their distance from the axis.

Fuselages resist to in-plane tensile stresses and shear stresses, but may buckle for low compressive loads in the same plane. For that reason, the concept of shear web is used and the skin is reinforced by frames and stringers. These are able to carry compressive stresses and transverse compressive point loads.

An aircraft is basically an assembly of stiffened shells, considered as beams in terms of behaviour, which are subject to axial loads, bending, shear and torsion. The fuselage is regarded as a single cell closed section beam, stiffened by thin-walled open-section beams. For a closed section beam, the shear flow is calculated as [15]:

$$q_s = - \left(\frac{S_x I_{xx} - S_y I_{xy}}{I_{xx} I_{yy} - I_{xy}^2} \right) \sum_{r=1}^n B_r x_r - \left(\frac{S_y I_{yy} - S_x I_{xy}}{I_{xx} I_{yy} - I_{xy}^2} \right) \sum_{r=1}^n B_r y_r + q_{s,0} \quad (4)$$

Where S_x and S_y are the shear loads in x and y directions respectively, B_r is the mass of the r -th boom, I_{ii} is the 2nd moment of area, I_{xy} the product of inertia and the pair (x_r, y_r) the r -th boom position in the section. If the section has at least one axis of symmetry, $I_{xy} = 0$. Additionally, if a shear load is only being applied in one direction, then the expression reduces to:

$$q_s = - \frac{S_y}{I_{xx}} \sum_{r=1}^n B_r y_r + q_{s,0} \quad (5)$$

The first portion of the sum, $-\frac{S_y}{I_{xx}} \sum_{r=1}^n B_r y_r$, is the shear flow in the open section, q_b , i.e., if a cut is made in the section between two booms. This shear flow is constant between booms and symmetric relatively to the axis of symmetry. The second term is the shear flow of the cut part, found by calculating moments about the shear centre. $q_{s,0}$ is added to q_b for the final solution.

Figure 9 shows a sketch of a round shell with a cut-out and the developed shear flow around the cut-out. The shear flows needed to be calculated are the ones above and below the cut-out, q_1 , in laterals, q_2 , and in the corners, q_3 . Far from the cut-out surrounding, the shear flow has the same value as if no cut-out existed in the area [1].

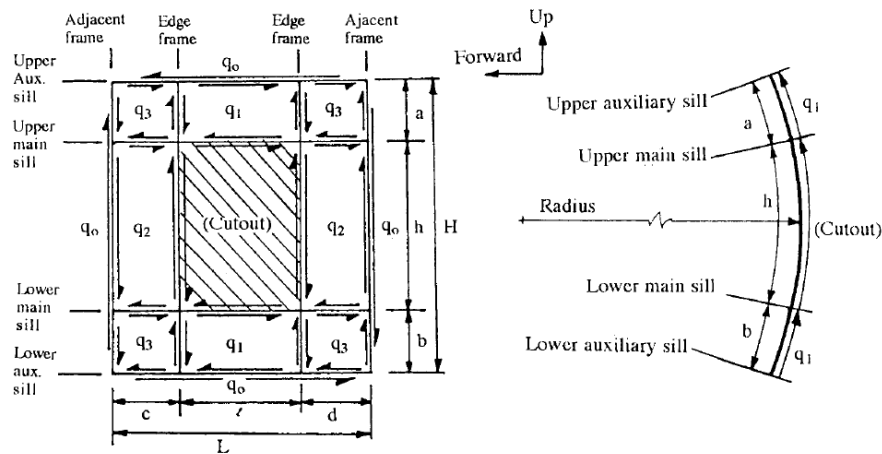


Figure 9 – Shear flow developed around a cut-out in a circular shell [2].

We are now in conditions to understand what happens to the members around a cut-out. Due to the eccentricity of the loads from the door-stops to the shear centre of the frame, there is going to exist a twisting moment on the latter. The frame generally has an open-section and its torsional stiffness is reduced. The job of balancing the torsion they may suffer is of the intercostals, which are perpendicular to the frames and, having high bending stiffness, can carry the load [4],[9].

The skin around the cut-out has tension in two directions due to pressurisation and carries large shear loads due to redistribution of loads caused by the cut-out. It is locally subject to high bending stresses also due to the cut-out [4]. Near the corners of the cut-out, it is commonly thickened, forming the doubler.

The sills and the skin-stringer-panel form the upper and lower "bending-beams", that are essential to carry the fuselage torsion in the surrounding of the cut-out and to act as tension and compression members in fuselage bending. Also the cut-frames create tensile loads that result in additional bending of the sills [19].

2.4 Fuselage Loads

2.4.1 Cabin Pressurisation

A fuselage is made of compartments. The cabin is the compartment where the passengers and crew are, that stands between two bulkheads and is the only compartment to be pressurised. The effects of cabin pressurisation in the fuselage structure increase as the airplane goes up because of the decreasing air pressure. The human can't stand a value of pressure below a certain level for a long time, so above some altitude inside the cabin the pressure has a value greater than on the outside.

The pressure difference is maximum at the maximum operating altitude of the aircraft. In the case of a large bi-motor airplane, like A320, it is considered a ceiling of $h = 40\,000\text{ ft} = 12\,192\text{ m}$, giving a

pressure outside of $p_{ext} = 18\,754\text{ N/m}^2$. According to EASA CS-25 regulations [18], the cabin altitude must be $h = 1\,800\text{ m}$, although Airbus considers an altitude of 2400 m . Using a value of $h = 6300\text{ ft} = 1920\text{ m}$, the internal pressure will be maintained at $p_{int} = 80\,285\text{ N/m}^2$

The difference of pressures is then:

$$\Delta p = p_{int} - p_{ext} \approx 61\,500\text{ N/m}^2 \quad (6)$$

This differential causes an expansion of the fuselage panels, similarly to what happens inside a cylindrical Pressure Vessel (Figure 10). According to the latter regulations [18], "The aeroplane structure must be strong enough to withstand the pressure differential loads corresponding to the maximum relief valve setting multiplied by a factor of 1,33." With this in mind, without further loads applied, the internal pressure will be multiplied by that number.

The stresses caused in the fuselage by internal pressurisation can therefore be found by the vessel equations [20]:

- Longitudinal stress: normal stress applied in the walls along the axis of the cylinder.

$$\sigma_L = pR/2t \quad (7)$$

- Hoop stress: normal stress in circumferential direction of the cylinder. This is double of the longitudinal stress

$$\sigma_\theta = pR/t \quad (8)$$

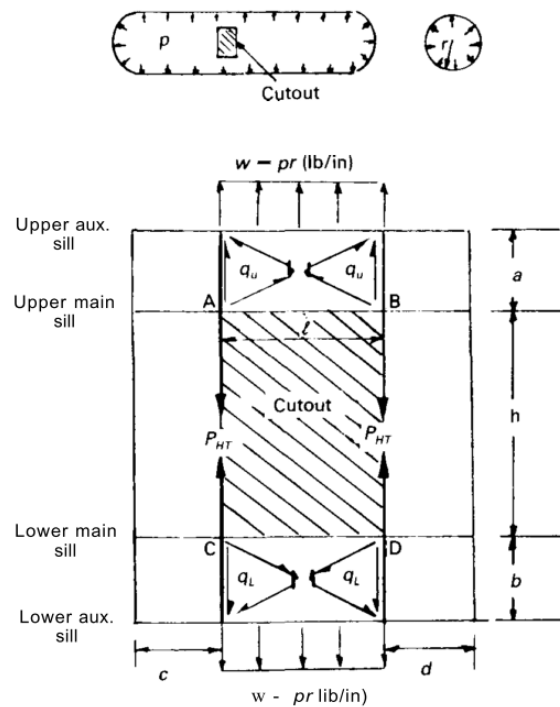


Figure 10 - The airplane cabin modelled as a Pressure Vessel, with the resulting internal loads in the edge frames and the shear flow distribution around a door cut-out [2]

Determined the stresses in the fuselage's skin and stiffeners, there is also a component to take into account because there is a cut-out where there should be material. The pressure applied in the door is transmitted to the surrounding structure through door-stops, that are attached to the structure [1]. It is calculated from the internal pressure as (Figure 11):

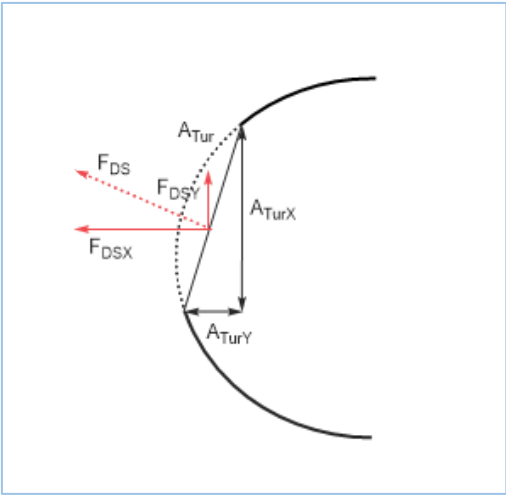


Figure 11 - The resultant force caused by pressure on the door F_{DS} and its components.

$$F_{DS} = \Delta p \cdot A_{door} \tag{9}$$

Additionally, a force is applied in each bulkhead, that makes them go apart and exert a longitudinal tension in the cylinder. This force must be taken into account as the bulkheads are not modelled and is calculated as:

$$F_z = \frac{1}{2} \cdot \pi \cdot \Delta p \cdot r_s^2 \tag{10}$$

As already stated, the stresses caused in the structure by this load are different in each member. The skin will expand and develop a hoop and longitudinal stress. These are transmitted to the stiffening members. The frames are in the circumferential direction, so they carry the hoop stress. The axial stress is carried by the stringers. Near the cut-out, the frames are also subjected to a redistribution of loads from the presence of the cut-out and two more components due to the pressure on the door in flight: bending and torsion. The stringers in the upper part of the fuselage will experience tension, while in the lower part experience compression and probably buckle.

2.4.2 Other loads

On a commercial transport jet, the number of investigated airframe load conditions are nearly over 10 000 and the actual critical design conditions are about 300 to 500, meaning almost every type of

manoeuvre required by FAR. Furthermore, critical internal loads may occur at 20 000 locations on an average wide-body size jet transport [2]. Examples of loads in the fuselage are the dynamic landing, braked roll, vertical and fin lateral gust, rudder and elevator deflections, etc. The skin is subject to cabin pressure and shear loads, and at the doors besides the pressurisation also wind and hand loads are present.

For this study the applied external loads were taken from the study of van Tooren [5] and assumed as typical loads in the A320. They are a vertical shear load, F_y , and a bending moment about the lateral axis, M_x (Figure 12).

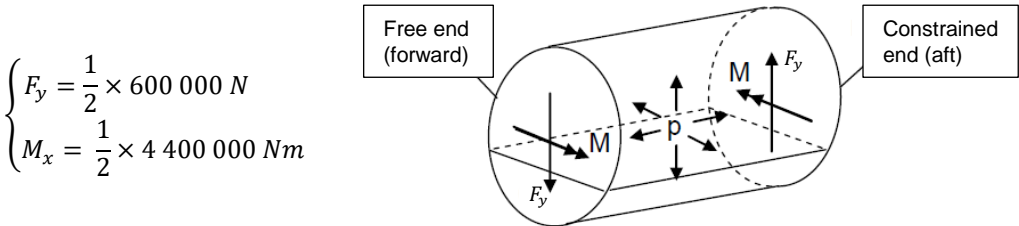


Figure 12 – loading in the fuselage (adapted from [5])

These two loads refer to half of the fuselage, reason why they are multiplied by $\frac{1}{2}$. Additionally, when applying these loads, the internal pressure is $\Delta p = p_{int} - p_{ext} = 61\,500\text{ N/m}^2$, due to the rule [18]:

“The aeroplane structure must be strong enough to withstand the flight loads combined with pressure differential loads from zero up to the maximum relief valve setting”

There are different contributions to the calculation of the loads in each part of the fuselage. For the present study more importance is given to observing the behaviour of the structure to variations in its geometry and not in the way it is loaded, so it is relatively irrelevant that the values are accurate. For the values to be the exact ones, it means a loads analysis should be done, which is outside the scope of this thesis.

2.5 Finite Element Method

The Finite Element Method, henceforth designated by FEM, is a numerical method widely used in aerospace industry and others. It is an approximated method so, contrarily to analytical methods, it does not give exact solutions. Hence, it is only used for situations when it is not possible to reach the exact solution by analytical methods [21].

Before analysing a complex system, a model must be created, phase known as pre-processing, which includes the definition of the domain, the properties of the material, the type of analysis and finite element, the boundary conditions and the applied loads. The method consists in discretising the domain in minor pieces – the finite elements – and solve a system of equations for the constraints and properties of the model (the processing) The results of this method are then shown in a variety of formats, like

graphics or tables, and reflect the solution of the system of equations in nodes or elements (post-processing). Briefly, the basic steps of the method are:

1. Discretisation of the domain. The FE can be uni-dimensional, bi-dimensional or tri-dimensional. Furthermore, they can also be linear or quadratic. The type of finite element depends on the problem to be solved;
2. Determination of Element matrices and vectors: the stiffness matrix, $[K^e]$, that contains the geometric characteristics and properties of the element, the vector of displacements $\{u^e\}$, whose entries are the nodal displacements and/or rotations (the degrees-of-freedom), and the vector of loads, $\{f^e\}$;
3. Assembly of each type of matrix in one for the overall structure, according to the position and connectivity of the elements in the mesh;
4. Reduction of the system of equations $[K]\{u\} = \{f\}$, by introducing the boundary conditions; the resulting system has many equations to solve as number of unknown degrees-of-freedom.
5. Resolution of the system of equations, calculating the nodal displacements and interpolating the solution to other points in the elements;
6. Determination of deformations and stresses from the displacement field (both in nodes or elements).

The error decreases if more equations are solved per analysis, with the disadvantage that the time of computing will increase. The amount of CPU time depends on the level of discretisation and on the complexity of the problem. A finer mesh implies more nodes and therefore more equations. For geometries with some curvature, there is the possibility of using finite elements of higher order, which may result in a more exact solution but increase the amount of equations to solve. The complexity of the analysis also depends on the linearity or non-linearity of the problem.

2.6 Sensitivity Analysis

The definition of Sensitivity Analysis depends on the field of study. A Sensitivity Analysis, in the context of structural mechanics, consists in calculating the rates of change of a function of interest – the structural response of a system – with respect to changes in its design parameters [22]. The important concepts are [19]:

- Design variables: are quantities, x_i , $i=1, \dots, n$, that are changeable and independent of each other. In structural mechanics, these can be geometric changes, like the shell thickness or the dimensions of members, or can also be material properties;
- Structural Response: a function, f_j , which can be both a linear or a non-linear combination of the design variables;

- Sensitivity Coefficients: are the partial derivatives of the function defining the structure's response in order to the design variables, $\lambda_{ij} = \frac{df_j}{dx_i}$.
- Design Constraints: are the functions which limit the variation of the interest function; these constraints tell either if the configuration inside the range of each design variable can exist in physical terms or for the purpose to which it will serve.

Usually the SA is based on the computation of derivatives of the function(s) with respect to its design variables or state variables. The derivatives are important not only for the optimisation of the system, but themselves represent trends to help the designer make estimates [23].

The most simple method of Sensitivity Analysis is by using Finite Differences, whose cost of calculation increases with the number of design variables. One of the methods in Finite Difference Method is the Forward Differences Scheme, of first order:

$$\frac{df}{dx} = \frac{f(x+\Delta x) - f(x)}{\Delta x} + O(\Delta x) \quad (11)$$

where $O(\Delta x)$ is the truncation error, that-measures the order of approximation of the scheme to the derivative and depends on the number of considered terms of the Taylor series. If the step-size Δx is chosen to be small, the truncation error is minimised, although care should be taken regarding the round-off error of the computations. The choice of method also depends on the number of loads (E.g., [11])

2.5.1 Relationship between Sensitivity Analysis and Optimisation

A Structural Optimisation is the process of finding the optimum design of a system, by minimising or maximising an interest function, satisfying various performance requirements [22]. Constrained optimisation consists in almost every situation and can be formulated as:

$$\max_x f(x), x \in \mathbb{R}^n$$

subject to the constraints

$$g(x) \geq 0$$

$$h(x) = 0$$

$$lb \leq x \leq ub$$

The constraints can be either equalities, h , or inequalities, g . The type of optimisation depends on the problem. There are situations in which a gradient-based optimisation is the most suitable and others whose process of finding the optimal design is more efficient with non-gradient based methods. A Sensitivity Analysis is part of a gradient-based optimisation framework. It improves the efficiency of the search method.

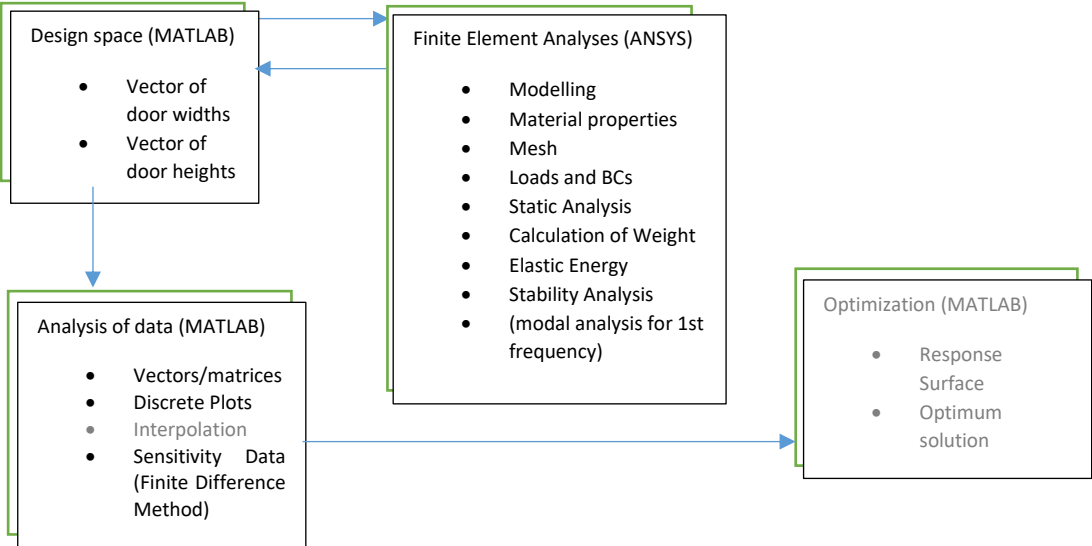
3. Methodology and Implementation

3.1 Introduction

This chapter presents the chosen and implemented methods for the development of the work. Two softwares were used:

- ANSYS – where the parameterisation of the model and Finite Element Analysis (FEA) is done. ANSYS Mechanical APDL (Ansys Parametric Design Language) is commonly used not only in academic environment but also in the industry; it was chosen to make the task of parameterising the model easier and have the possibility to change its geometry or properties, which allows for a better control of the model; the files with the APDL scripts is in the directory where Ansys is launched, where it is ran and all the output files are written.
- MATLAB – creates the interface with Ansys and processes the parametric studies and Sensitivity data. A MATLAB file was created for each type of analysis.

The purposed algorithm is schematised in the following diagram. In the present work, only the items in black are accomplished, although not fully, the rest being left to a further work on this theme.



3.2 Interface ANSYS-MATLAB

The algorithm in MATLAB creates input files and processes the analyses in Ansys. After each analysis, MATLAB reads the output and performs the Sensitivity Analysis.

1. The design space is created, by generating the vectors for the Design Variables width, B and height, H, followed by the load case and the analysis type;
2. The vectors are then travelled in a two-index for-loop, which for every pair (B,H) writes the values of B and H and the load case in a file called *param_file.txt* and calls ANSYS;
3. The calling of Ansys is done using the DOS command, that consists in running a specified command from the command line; The inputs in this case are the path for ANSYS APDL executable in batch mode, the input file (*param_file.txt*), the working directory, which will replace the defined one in the launcher in case it is different, and the output file.
4. Once in Ansys, the input file is read by the function *PARRES*, a command for reading parameters from an external file, and the assignment of the variables is automatically saved in Ansys parameters list. Having the configuration, the load case and the type of analysis, the APDL script includes the necessary parameters, routines and commands to generate the model.
5. The output file of the analysis, sent to the same folder of the MATLAB's file, is called *Results.txt* and has 10 lines:
 - the weight;
 - the maximum deformation;
 - the maximum equivalent stress (von Mises Stress);
 - the total elastic energy;
 - the buckling factor;
 - the first natural frequency;
 - x, y and z locations of the maximum stress in the model.

MATLAB reads the data using the command *fscanf* and saves the values in variables inside the program.

6. In the For-structure, data is written in Excel sheets for a posterior visualisation and plottage of the variations of each quantity with each design variable.

3.3 Construction of the model

The modelling of the fuselage structure was done with the objective of making it versatile, easy to change, without need for inputs from the user and possible to handle the analyses for any configuration. Ideally by changing one parameter all the others would change accordingly. However, to control all the dimensions in the model would take some time and the goal was to make the dimensions of the cut-out variable. Thus, only the elements that depended on it – the stringer spacing/number and the frame

spacing/number – would change. The dimensions of the stiffeners' cross section could also be variables, but it was outside the scope of the thesis.

Parameters like the position of a fictitious floor (where the cut-out lower sill is positioned), or the dimension of the doubler around the cut-out are fixed, although the APDL script can be changed by who reads it. These changes require that the user tests if the final geometry makes sense.

Two versions of the model were developed and studied so the number of results and analyses could be increased.

- Version 1 (mv1.mac): this model was the first to be fully working for the purpose of this thesis. The structure is divided in parts: above and below the cut-out, and at the lateral another division; the number of stringers changes with the height of the cut-out. The spacing is calculated from the number of stringers below the cut-out, $s_{str} = \beta/n_{str}$, as the floor height is fixed, and can always be changed in the APDL script. This approach wasn't the most versatile for calculus of Sensitivity Coefficients, so a method for accomplishing a smooth variation was once again tried;
- Version 2 (mv2.mac): both the number of stringers and frames are fixed, their spacing changing with the part of the section – below ($s_{str} = \beta/n_{str}$), above ($s_{strU} = \varphi/n_{strU}$) and lateral to the cut-out ($s_{strC} = \gamma/n_{str}$). The number of stringers below and at the lateral were chosen to be the same, as the doors' height wouldn't differ much from the floor height. Above the cut-out the number of stringers should be such that the spacing didn't differ much from the other two. Contrarily to mv1.mac, the distance between stringers and sills (members attached to cut-out) are the stringer spacing in the corresponding part.

A 3rd version was also attempted, in which the corners of the cut-out were round. This would avoid very high stresses in the corners, called singularities, which have no physical meaning, and there would be concentrations of stress instead. However, a regular mesh around the cut-out was not easy to program.

3.3.1 General Considerations

The Finite Element Method gives only an approximated solution for a problem. The used software sometimes is not able to solve a problem with too much complexity. On the other hand, to get realistic results, the structure should not be too simple. So, the model had to consider several aspects:

- The aircraft is a conventional transport aircraft – a narrow body type;
- The portion of the aircraft under consideration is the forebody, whose diameter doesn't change significantly along the length;
- Only half of a fuselage section is modelled, due to symmetry about the aircraft axis;
- Although a floor was not modelled to provide support to the structure, its location is fixed (and so it is the door sill height relatively to the ground);
- The number of frames is fixed.

3.3.2 Coordinate systems

The coordinate system in use is cylindrical, defined by an axial component Z , a radial, R and an angular component, θ . In Ansys this system is referred by using the command `CSYS,1`, after which the X-component of the default direct cartesian system (`CSYS,0`) stands for R-direction, the Y-component for the angular direction, and the Z-component remains the axial direction. The cartesian and cylindrical coordinate systems are shown in Figure 13. Further systems were defined in order to ease the creation of entities in the model and perform other tasks.

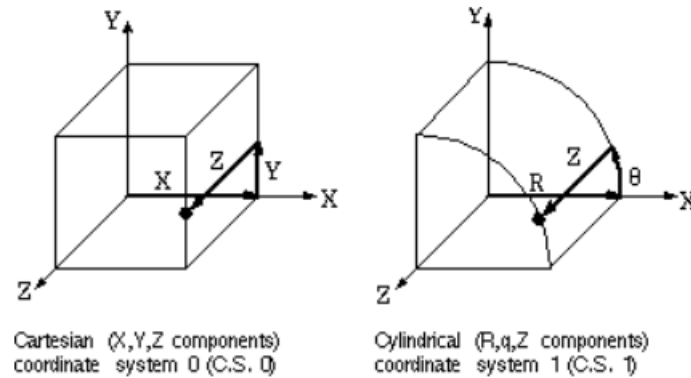


Figure 13 - coordinate systems: a) `CSYS,0` b) `CSYS,1` [24]

3.3.4 Finite Element types

The types of the elements used in the analysis are shell and beam elements. Shell elements are used to model thin 3D structures, i.e. when one dimension is much smaller than the other two, like the skin of a fuselage. Beam elements are used for the stiffeners (both transversal and longitudinal); it was possible to make use of shell type finite elements for the modelling of stiffeners, as the beam is made of thin plates and the solution would actually be more accurate, but the construction of geometry for every type of stiffener and the control over their position for each configuration would be too difficult and hence unpractical.

The used elements and their main characteristics are the following (Figure 14) [19]:

- **SHELL181**: Plane shell type with 4 nodes and 6 degrees of freedom in each node (3 displacements and 3 rotations). It is suitable for thin-to-moderately-thick structures analysis in which we wish to calculate transverse shear stresses due to bending (Reissner-Mindlin shell formulation);
- **BEAM188**: 3D beam element with 2 nodes and 6 degrees of freedom at each node (3 displacements and 3 rotations); it is formulated by the Timoshenko theory of beams, that includes shear-deformation. The classic theory, Euler-Bernoulli accounts for axial stresses due to bending, but neglects the developed shear stresses, which are of interest in this work.

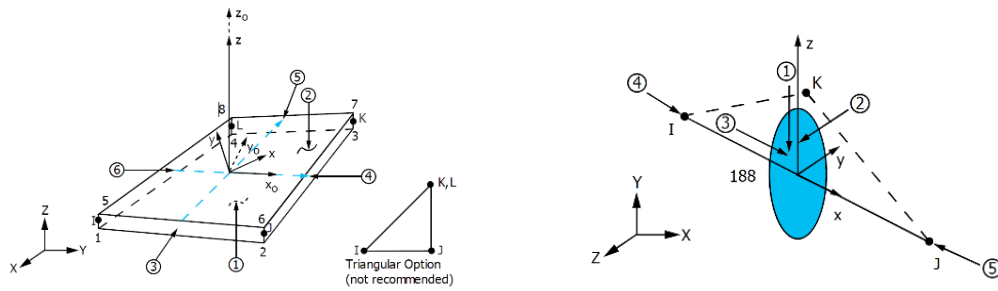


Figure 14 – Used elements: Left – SHELL181; Right – BEAM188 [11].

Only the beam types support sections. The input for shells is the thickness, t_s , and the offset from the nodal coordinate system. Z-profiles are chosen for every stiffener, with exception of the edge frames and the upper and bottom sills, which have C-profiles. Each type of element has its fixed dimensions and the offsets are also dependent on the position of the member in the shell. For example, the first stringer from the bottom is positioned upwards, so it does not go out of the shell.

3.3.5 Material

Only a material was assigned to both the fuselage skin and the stiffeners – Al 2024-T3. The reason for its use was expressed in Chapter 2. In ANSYS the introduction of the material is done by writing its properties for an isotropic metallic material (Table 2).

Table 2 - Characteristics of Aluminium Alloy Al 2024-T3 [25].

Material Property	Symbol	Value
Young's Modulus	E	73,1 GPa
Density	ρ	2,780 g/cm^3
Poisson's Coefficient	ν	0,33
Tensile Strength	σ_{yeldT}	290 MPa
Compressive Strength	σ_{yeldC}	290 MPa

3.3.6 Modelling the components

Only half of a fuselage section was modelled to take advantage of its symmetry. At the other side of the door there is an emergency door. The model consists on the skin and stiffeners: doublers, stringers, frames, cut-stringers, intercostals, edge frames, sills and cut-frames (Figure 15). The dimensions chosen for the reference model were taken from an Airbus technical document [26]. Dimensions not found there were taken from a study done with A320 parametric model [27].

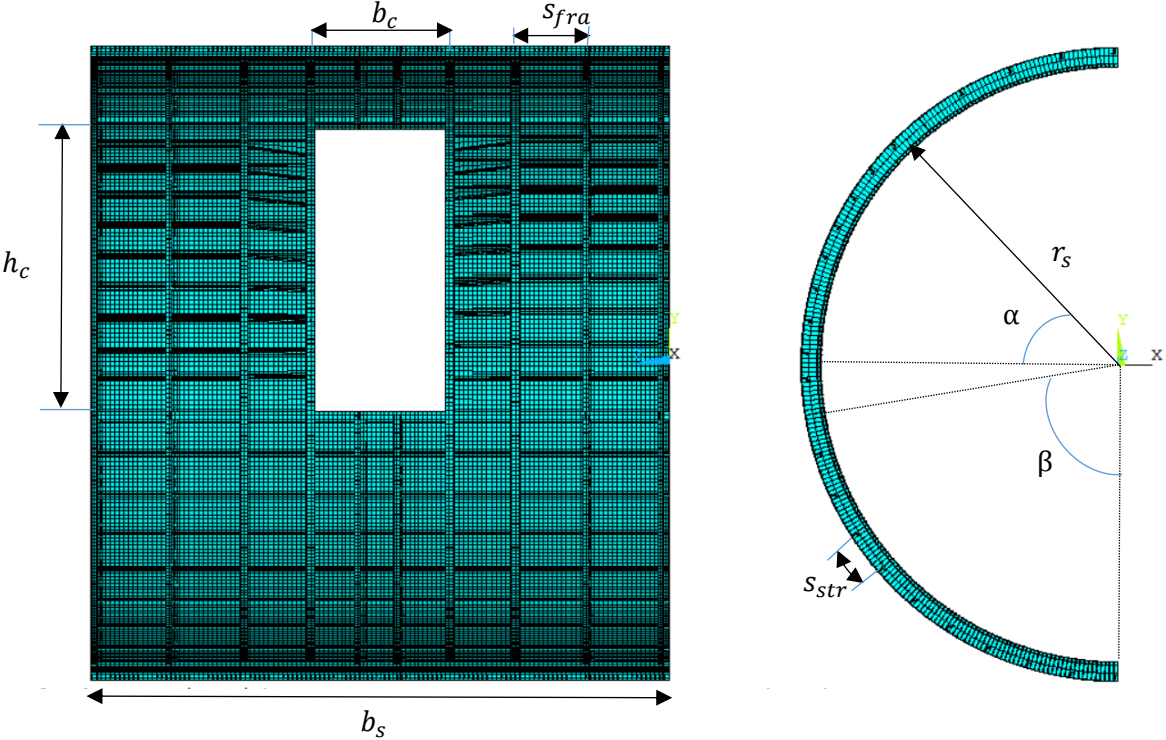


Figure 15 - Dimensions of model (versions 1 and 2).

Table 3 – Geometric Parameters of the initial model.

Parameter	Symbol	Ansys parameter	Reference Model
Fuselage Width	b_s	b_s	3600 mm
Fuselage Radius	r_s	r_s	1975 mm
Skin's Thickness	t_s	t_s	1 mm
Cutout Width	b_c	b_c	810 mm
Cutout Height	h_c	h_c	1850 mm
Cutout height in °	γ	gama	$\cong 60,18^\circ$
Cut-outs angular position from centre	α	alpha	$\cong 51^\circ$
Cut-outs angular position from bottom	β	beta	$\cong 80,8^\circ$
Number of stringers	n_{str}	n_str	600 mm
Stringer base width	b_{str}	b_str	20 mm
Stringer web height	h_{str}	h_str	35 mm
Stringer web and flange thickness	t_{str}	t_str	1 mm
Stringer pitch (version 1, version 2 - bottom)	s_{str}	s_str	v1: $8,08^\circ$
Stringer pitch (upper, version 2)	s_{strU}	s_stru	$9,75^\circ$
Stringer pitch (lateral, version 2)	s_{strC}	s_strc	$6,02^\circ$
Number of normal frames (each side)	n_{fra}	n_fra	2
Total number of frames	-	-	4 frames + 4 main fr. + 2 cut-fr.
Frame base width	b_{fra}	b_fra	35 mm
Frame web height	h_{fra}	h_fra	100 mm
Frame web and flange thickness	t_{fra}	t_fra	1,2 mm
Frames pitch	s_{fra}	s_fra	464,2 mm
Doubler's width	b_d	b_d	172 mm
Doubler's height	h_{dDeg}	h_d_deg	5°
Doubler's thickness	t_d	t_d	3 mm
Sill width	b_{si}	b_si	50 mm
Sill height	h_{si}	h_si	100 mm
Sill thickness	t_{si}	t_si	1,5 mm
Intercostal width	b_l	b_l	1 mm
Intercostal thickness	t_l	t_l	1 mm
Edge frame height	b_{ef}	b_ef	120 mm
Edge frame width	h_{ef}	h_ef	50 mm
Edge frame thickness	t_{ef}	t_ef	1,2 mm

The way of modelling consisted in dividing the fuselage half shell in some parts defined by the cylindrical coordinate θ . At the beginning the model should consist in a cylindrical area with a hole at a certain position, with parameterised dimensions, but some features of Ansys were only available for planar surfaces, so the structure had to be done in a different way, starting by keypoints and lines, so that the position of all the elements could be parameterised. Areas were created with their lines representing the stiffeners. One advantage of having done the model like this is that there is no need for creating contact surfaces between the different elements because the software already recognises they are stucked to each other. The modelling of the different elements is described next:

Skin: it is divided in many little shell areas, limited by the stiffeners' lines. Each area is made after each group of lines that constitute a stringer, by using the command *AROTAT*, and within it also the frames are created. Only the thickness, t_s , is assigned to this element.

Doublers: many ways of doing this were tried, from making new areas and attach them to the existing skin using contact pairs, like in real situation, to assigning a different thickness (and eventually material) to areas around the cut-out. The second was the chosen method, as it would be easier to implement and control. A new line had to be attached to the group of horizontal lines before using the command to create the areas. The attributes of this element are its thickness, t_d , the horizontal length in the lateral panels, b_d , and the vertical angular distance of the panels above and below the cut-out, h_{dDeg} .

Stringers and cut-stringers: as already described, the stringers are represented by horizontal lines with a BEAM188 section attached. The stringer section has the thickness (equal in all parts), t_{str} , the height (length of the web), h_{str} , and the width of the flanges, b_{str} as parameters. The cut-stringers are located between the floor position and the door's height and are connected to intercostals at the intersection with the main adjacent frame

Frames and Cut-Frames: created with the areas, there is a fixed number of these in the model (3 main frames + 1 adjacent frame at each side of the cut-out, and 1 cut-frame above and below the cut-out). As the cut-out width is changed, the spacing between the frames also changes, but not the number of frames. Like the stringers, they are assigned BEAM188 sections, with the parameters thickness, t_{fra} , height of the web, h_{fra} , and width of the flanges, b_{fra} .

Intercostals: these are the extent of the cut-stringers, as tapered beams (BEAM188), starting at the line of the adjacent frame (smaller height, h_{fra}), and ending at the line of the edge frame (bigger height, h_{ef}). As happens with the cut-stringers, the number of intercostals depend on the height of the cut-out.

Edge-Frames: the section of these have different values for the same attributes of the main frames, for making part of the doorframe.

Sills: one above the cut-out and the other below, they are basically stringers with different mesh attributes. It was also thought to be designed with varying cross-area, like the intercostals, being a stringer from the adjacent frame to the end of the stiffened panel. But it would mean more work and a simple structure was intended here, so it is left to a further work.

3.3.7 Mirror and mesh

A mirror of the modelled structure is done using the plane at $z = b_s/2$. Because it also affects the element attributes, after this feature further attributes had to be assigned to the new entities. The command *LREVERSE* was sometimes needed so that the orientation of the section fitted the one in the other parts. For example the left frames were positioned with the same orientation of the right ones, otherwise they would have a symmetric orientation and offset, and would also fall out of the left-ended skin. As well, the stringers below the z-axis have the right orientation relative to global coordinated

system, but the ones above it have to see their x-axis reverted so the section will have the same orientation of the ones below. However, it was not an easy task to find the way of entering the right orientation in the commands. Even after experimenting all the possible combinations, because it would not be worthwhile, one of the intercostals stayed different from the others (Figure 16).

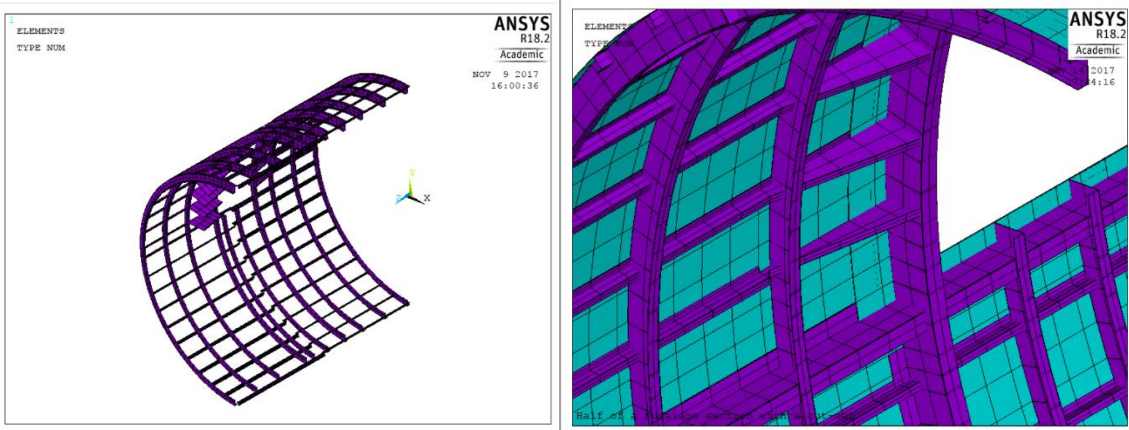


Figure 16 - Resolution of problems with the mesh after the mirror.

The meshing of all the model is done at the same time, using the attributes of each part – material, type of element, section properties and orientation keypoint. The last item is an extra KP, created for elements whose orientation in space must be defined, such as the beams. For example, the assignment of mesh attributes to the frames depended on their position. The orientation keypoints are at the centre of the fuselage, along the z-axis and in front of each frame. One keypoint at the origin wouldn't be enough for all of them, hence the assignment of attributes could not be done in one step, otherwise they would be rotated relatively to y-axis. An image of the meshed model with the types of element in different colour is shown in Figure 17.

Each stiffener has an offset in radial direction defined in order to make it interior to the fuselage skin. In the case of the doubler there is no offset, because the created area has the thickness of the skin+doubler, t_d , having nonetheless the part correspondent to the doubler on the inside. The angular/longitudinal offset of each member depends on its location in the cylindrical panel, to avoid having a stiffener outside the skin. Twelve types of sections were then defined for the beam types.

The mesh size is an input, so the number of elements created is in accordance with this. It is then expected that when varying the element size, the number of elements not always will change. An element is only created if its line's length reaches the value of the input, *size*.

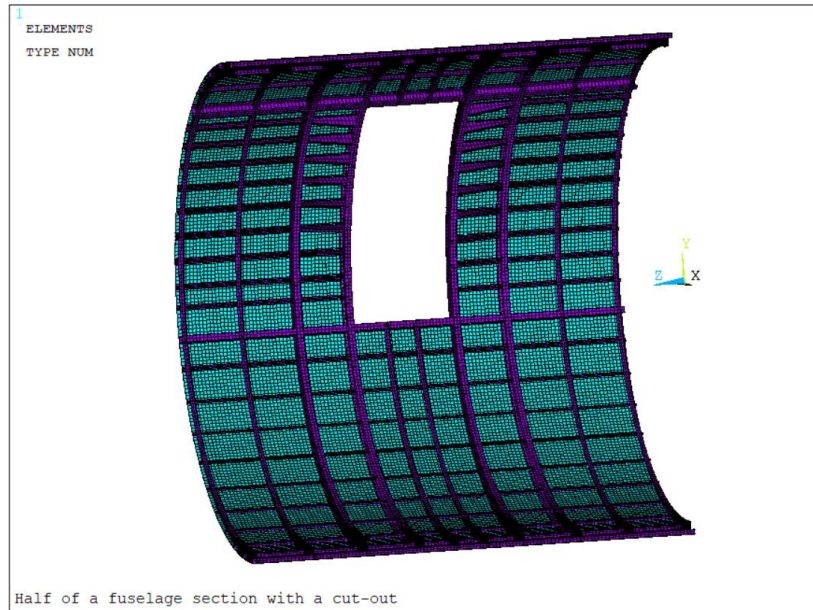


Figure 17 - Reference structure meshed showing different types of element through colours.

The solution will be more precise with a higher number of elements. Common practice in a FEM analysis is to refine the mesh in places where high gradients of the quantities are expected. However, a refinement of the mesh implies that the modelling be done so that the lines at those locations are subdivided in more stretches. Furthermore, in this model the places where the biggest gradients would occur are at the cut-out corners and points of application of forces, which are discontinuities of geometry and of loading, respectively. Those places are likely to be points of singularities, meaning that the increase in the number of elements would result in non-converged (increasingly higher) values of the stress. A way to avoid these singularities is to take some nodes off the corners at the post-processing. Another solution, following the actual construction of panels with cut-outs, singularities can be avoided by modelling fillets in the cut-out corners. To have a good mesh in that case requires a good knowledge of how to model the structure accordingly, so it is left to a further work.

3.4 Application of Loads

Three load cases were implemented to observe the behaviour of the structure to different loadings.

- Case 1: Internal Pressure only
- Case 2: Internal Pressure + Shear Load
- Case 3: Internal Pressure + Bending Moment

The internal pressure is applied directly in the skin (Figure 18), having been noticed in advance to which direction the shell normals were pointed and then checked the deformation (it should expand) to decide if a positive or negative value should be entered (positive value). The axial force F_z due to forward

bulkhead force and the door-stops force F_{DS} are also applied. Both values were already calculated in Chapter 3 of this thesis.

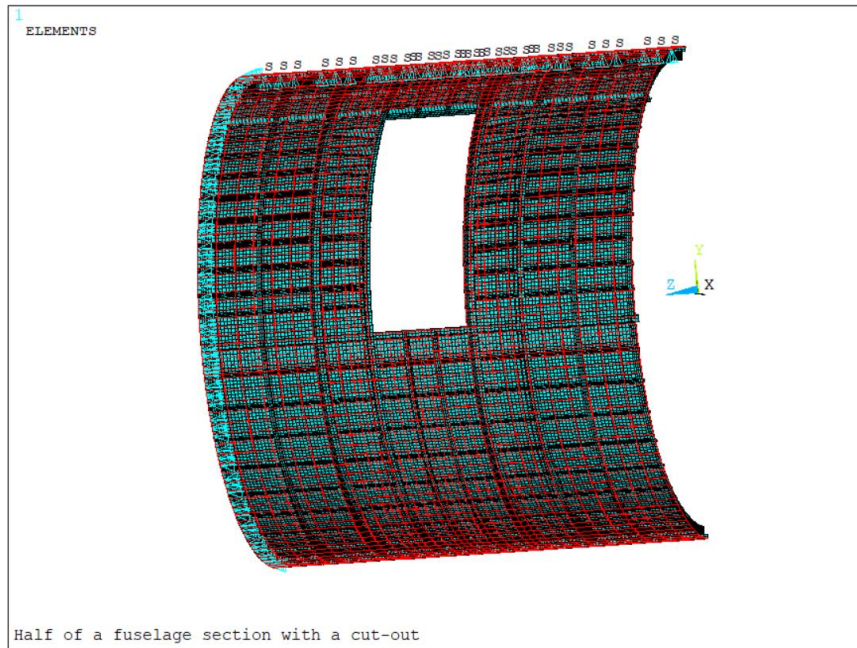


Figure 18 - Internal pressure applied in the skin.

The application of forces and moments can be done by using Multipoint Constraint (MPC) elements, through a method which is common in FEA (sometimes called a spider web) [28]. In this method a node is created at some point – the master or independent node –, connecting it to nodes that belong to the structure and then applying the load in the masternode. A code from PADT, inc. [29] was used and saved with the name *mpc_gen.mac*. It receives the nodes where to operate and creates the elements with them. The element created by this routine is the MPC184, a rigid element that creates a constraint between two deformable regions and transfers loads between them (forces in Link behaviour and additionally moments in Beam behaviour [19], [30]).

Some tests were first done to different structures in order to make the best choices for commands using this technology – MPC184 vs CERIG vs RBE3, and MPC Link vs MPC Beam.

MPC184 is suited for non-linear problems, reason why a warning appears in every analysis, stating that if finite rotation and large deflection effects are to be considered, the command *NLGEOM,ON* must be used. In the present work only the linear behaviour is considered, so the warning is not important. The element uses by default the Direct Elimination Method, that create MPC equations, where the DOFs of a dependent node are eliminated in favour of the master node [30].

CERIG, or the element RBE2, generates Constraint Equations (CE) that define a rigid region, so the elements which are created between the nodes transmit different loads to the nodes they are connected to [31]. The difference between using this command and using MPC184 elements was not fully

understood, as the results obtained with both from the experiences were the same. The most easily implemented method was the one used.

When using RBE3, the forces or displacements applied to the masternode are distributed to the other nodes through shape functions that make each transferred load an average. The difference between MPC beam and RBE3 is that while one transfers forces, the other transfers deformations.

To choose between an MPC rigid link or an MPC rigid beam it is important to know that the link can transmit only axial forces between the extremities and the beam can also transmit moments on them [30]. As both are rigid elements, they will not deform, so the load applied to the masternode will only depend on the displacement of the elements. The difference between the beam behaviour and the link behaviour is evidenced in Figure 19, which shows the x-displacement plot of a plane shell subjected to the same axial load using the two approaches.

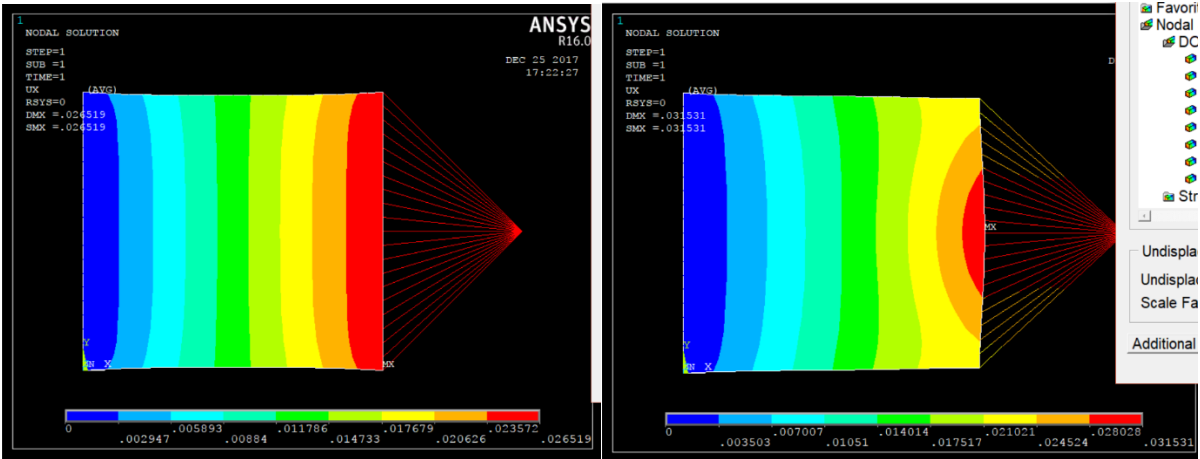


Figure 19 – MPC Beam vs MPC Link (x is the horizontal component in the 2D plate).

In the case of the longitudinal and shear forces, MPC184 were created at the right end of the model between a masternode at the origin of axes and the nodes of the shell at the same z-location (Figure 20). In the masternode, all force and moment loads to be transmitted to the overall structure were applied. For the longitudinal force it did not matter the location in axial direction, the force would be the same.

For the load F_{DS} the same method was used, but using the RBE3 element. This special element asks for a masternode with some mass. The most common is to mesh a KP with the type MASS21, a unit mass that provides also rotational inertia. The method CERIG was tried as well, but it was intended that the cut-out surrounding deformed under the loading, which did not happen if this was used. A masternode was created at the exact centre of the cut-out and linked to the nodes at the end of the intercostals, which simulate the door-stops (Figure 21). Then the contribution of the pressure at the door to the force was applied at the masternode in the respective components.

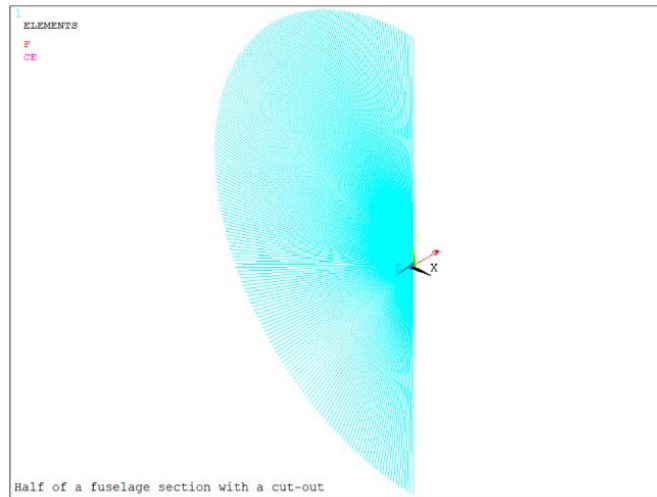


Figure 20 - Axial force due to bulkheads applied using MPC184.

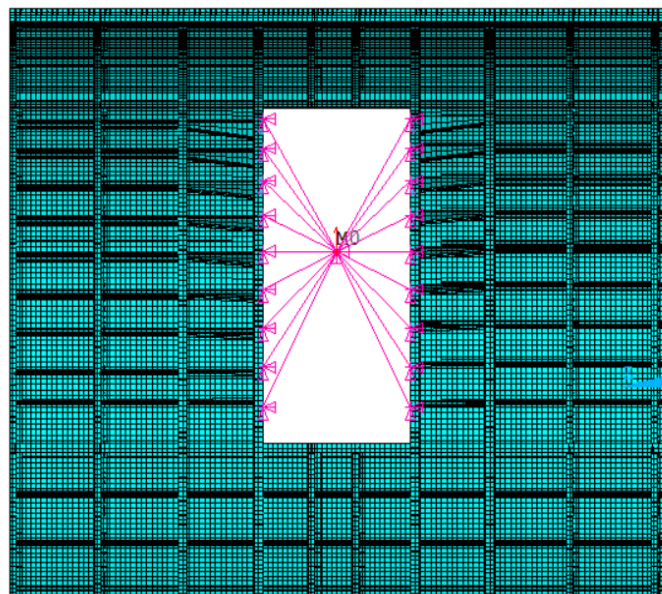


Figure 21 - Pressure on the door transmitted to the door-stops using RBE3 elements.

For the case of the shear load, F_y , if the upper line is constrained in UY, neither of the nodes on that line will move downward. As the MPC Beam elements are rigid, an applied force in the direction along the elements will not be transmitted. If the master node is at a distance from the structure, there will exist a non-zero moment at the end of the section, although it is very small. If the left end has also the nodes constrained in UY direction, there is the possibility of applying the force in y direction without having to apply it at a distance from the structure.

The bending moment, M_x , was also applied using MPC Beam.

3.5 Application of Boundary Conditions

3.5.1 Symmetry

Three conditions of symmetry occur in the fuselage section, which deserve special attention, because the results will depend on the way they are defined:

1. Symmetry about an XY plane passing through the centre of the cut-out.
2. “Infinite” fuselage
3. Symmetry about the longitudinal plane

The first existing symmetry could be modelled by using the ANSYS command *DL*, with the option *SYMM*, which eliminates the DOFs that make the nodes go outside of the XY plane (so $UZ=0$, $ROTX=0$ and $ROTY=0$) (Figure 22, Left). Other motivation for trying this was the wrong orientation of the left intercostals of Version 1. The commands initially used were *DSYMM* and *D*, whose results (for a pressure applied on skin) were different from the complete half-fuselage with both extremities fixed, so the idea was dropped and the mirror was performed with the necessary changes.

The second type is not exactly a symmetry condition, as there is only a door along that fuselage part, so the condition here is only a constraint in axial direction in one of the edges, in this case the left one ($z = b_s$). The other extremity of the half cylinder is subjected to the loading.

The third type refers to the fact that there is a door at the other side of the section (considering an emergency exit with the same dimensions). A method used in the studies of the ALCAS model is called Coupling Nodes (CP), which consist in coupling the same degrees of freedom of a pair of nodes, so they have the same value. Instead of being the solver, it is the user that says that certain nodes have the same displacements. An attempt to model the full cylinder was made (Figure 22, Right), but the results were not similar to those obtained with the CP method. The method was tested for different couplings on the same pairs of nodes, but the results were not conclusive and the CP method was not understood. This way, the chosen method for the symmetry about the plane normal to X-axis, was the traditional, i.e., applying the command *DL* in the upper and lower lines ($y = \pm 90^\circ$), option *SYMM*, in which the displacement *UX* and rotations *ROTZ* and *ROTY* are made zero automatically. Due to lack of time, this command was not used for the first type of symmetry, and actually the orientation of the intercostal would not be significant for the results.

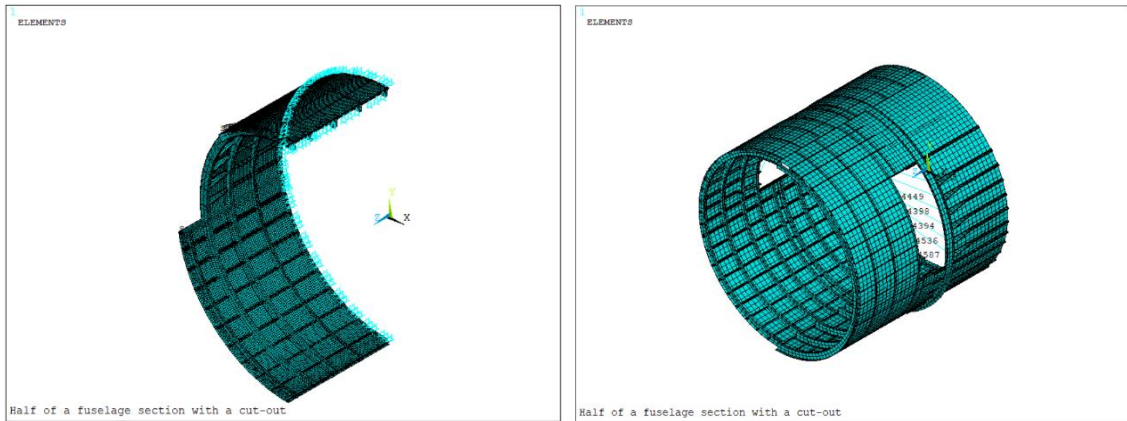


Figure 22 – Left: Meshed part before mirror; Right: Full cylinder with cut-outs.

3.5.2 Rigid body motion

In a Finite Element Analysis, the model must be fixed relatively to the global coordinate system in order not to allow for free body motion, or the Static Analysis won't work, because the system of equations to be solved will include a singular matrix, which can't be inverted. The other aspect is that when an internal pressure is applied on the area, the structure is expected to expand, so freedom must be given to the translations in radial direction. With these aspects in mind, two possible groups of constraints (in the cartesian system, but considering cylindrical coordinates when referring the part of the structure) are:

$$1: \begin{cases} z = b_s & \rightarrow U_z = 0 \\ y = \pm 90^\circ & \rightarrow U_x = 0, ROTZ = 0, ROTY = 0 \\ y = 90^\circ & \rightarrow U_y = 0 \end{cases}$$

$$2: \begin{cases} z = b_s & \rightarrow U_z = 0, U_y = 0 \\ y = \pm 90^\circ & \rightarrow U_x = 0, ROTZ = 0, ROTY = 0 \end{cases}$$

In the first group, the left edge of the fuselage section has only zero z-translation DOF. The top line of the fuselage has not only constrained DOFs in x-direction to simulate symmetry but also translation in the vertical direction, UY. In the second version, the top line of the fuselage only has the symmetry condition, as well as the bottom line. The left edge of the section is constrained in z and y directions. Figure 23 shows these boundary conditions.

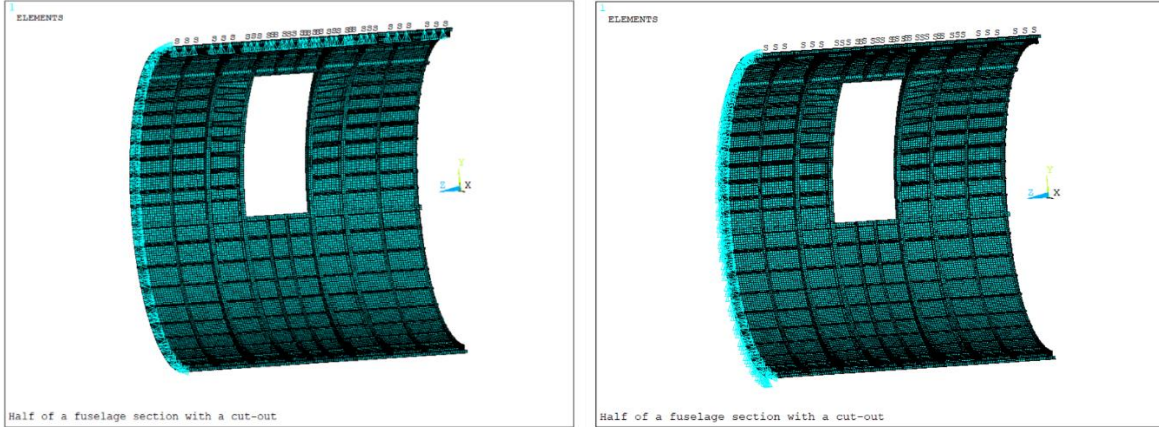


Figure 23 – Left: With simple support at $y = \pm 90^\circ$; Right: With clamping at $z = b_s$.

The constraints are applied to the lines, which allows a change in the mesh without affecting their distribution. The loads are then transmitted to the nodes, where the calculations are done. The boundary conditions, as well as any other motion dependent nodal operation, correspond to the nodal coordinate system, which is the global cartesian system (NCSYS=CSYS,0) by default [24].

3.6 Calculation of the weight

The weight of an imaginary door was accounted in the computation of the overall weight. With increasing door dimensions, its mass also increases. Supposing the door can be modelled as a circular shell of the same thickness of the structure's skin and no members are attached to it, the component (considering also the opposite door) is calculated as in equation 12.

$$\text{Door's mass:} \quad m_2 = 2 \cdot A_{door} \cdot t_s \cdot \rho = 2 \cdot \left(\frac{\gamma\pi}{180} r_s \cdot b_c\right) t_s \cdot \rho \quad (12)$$

The weight of the model is calculated selecting all the elements of type shell and beam and using the command *ETABLE,VOLUME,VOLU*, followed by *SSUM*. Then the mass of the model (full cylinder) is calculated as in equation 13:

$$\text{Door surrounding structure's mass:} \quad m_1 = 2 \cdot Vol \cdot \rho \quad (13)$$

$$\text{Overall weight:} \quad W = (m_1 + m_2)g, \quad g = 9,81 \text{ m/s}^2 \quad (14)$$

4. Analyses

The type of analyses performed with the models are in Table 4. Changes in the model had to be done so different situations could be analysed. The legend of each model follows the table.

Table 4 - Summary of analyses performed in chapter 4 and 5.

Analysis	Model	Load case	Results
Convergence Analysis	mv1, mv2, mv1s, mv2s	Internal Pressure	Weight, Displacement, Stress, Buckling Factor, Natural Frequency, Elastic Energy
Parametric Study	mv1s mv2s	Internal Pressure All load cases	
Variation of the Structure	mv1s mv2s, mv2sf, mv2sm	Internal Pressure All load cases	
Varying both parameters at the same time	mv2s	Internal Pressure	Weight and Stress

- mv1.mac – version 1 of the model
- mv1s.mac – version 1 of the model without singularities
- mv1o.mac – modified version 1
- mv2.mac – version 2 of the model
- mv2s.mac – version 2 of the model without singularities
- mv2o.mac – modified version 2
- mv2sf.mac – version 2 of the model for case load 2
- mv2of.mac – modified version of mv2sf
- mv2sm.mac – version 2 of the model for case load 3
- mv2om.mac – modified version of mv2sm

4.1 Static Analysis

Through a static analysis, one can evaluate the strength of the structure and decide if it is able to carry the loads that are being applied. Static means that there isn't any motion in the structure and a force or pressure is applied. In post processing, the von Mises Stress is requested and its maximum value in the structure is written in the files, as well as the maximum displacement.

For every time the Static Analysis is done, the algorithm lists the nodal solution sorted from minimum values to the maximum (*Stresses.txt* and *Displacements.txt*). After this analysis the weight of the model is obtained by summing all the elements' volume and multiplying the result by the specific mass, ρ . Only

the elements of the structure are selected – SHELL and BEAM – ignoring all elements of other defined types. Furthermore, the *ETABLE* command is once again issued to get the elastic energy of each element. Then a summation over the entire model is done and the total elastic energy is also written in the results file.

Considering that the fuselage has a symmetric geometry, a symmetric stress distribution from a symmetric loading would be expected, independently of the boundary conditions. This is the case, as observed, with the exception from the fact that the frames are not symmetric at each side of the door. However, the difference does not have much influence on the solution.

Comparing both models, for the same groups of constraints, the values do not differ much (Figure 24).

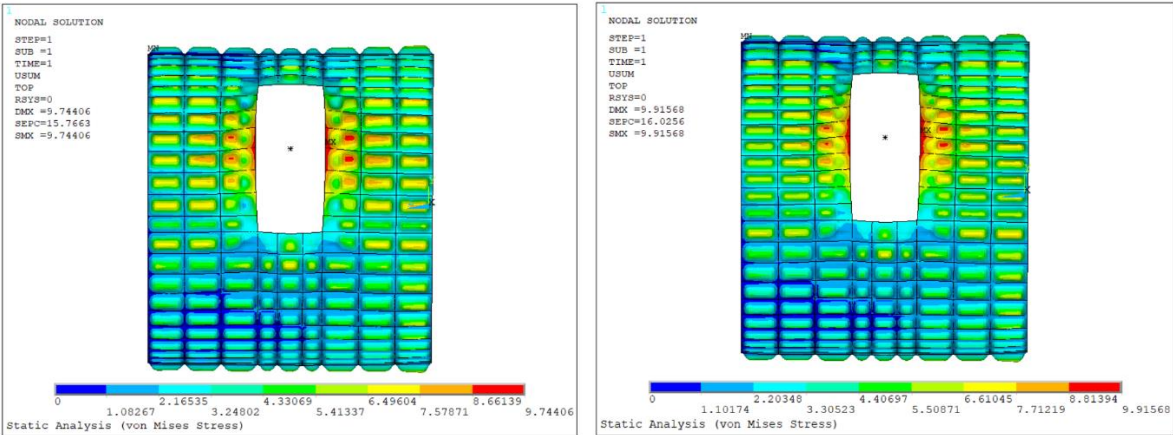


Figure 24 – Sum of displacements in versions 1 (mv1.mac) and 2 (mv2.mac) with group 1 of BCs.

4.2 Stability Analysis

Stability or Buckling analysis is crucial to successful structure design and simulation, especially when thin structures such as shells and beams are involved [15]. For this analysis to be performed, a static analysis with a pre-stress must be done before.

In the case of the first load case (internal pressure only), no compression of the fuselage members may occur. For this reason in the analyses where only this loading is presented, the stability data does not allow to take many conclusions.

The type of load has some influence on the buckling factor. The results of buckling analysis with different boundary condition and for the first load case in model 2 are in Figure 25.

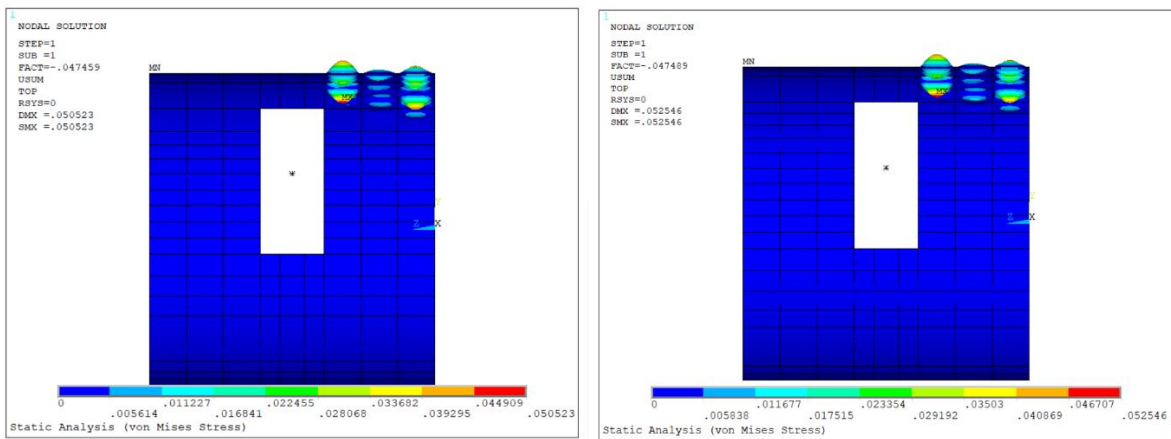


Figure 25 - Local instability with internal pressure: Left - UY=0 in upper line; Right - UY=0 at extremity $z = b_s$ (mv2.mac).

In Figures 26 and 27 are the plots obtained applying both the internal pressure and the moment (load case 2) in the second version of the model, for both groups of BCs, and applying both the internal pressure and the shear force (load case 3), for the 2nd group of BCs, respectively.

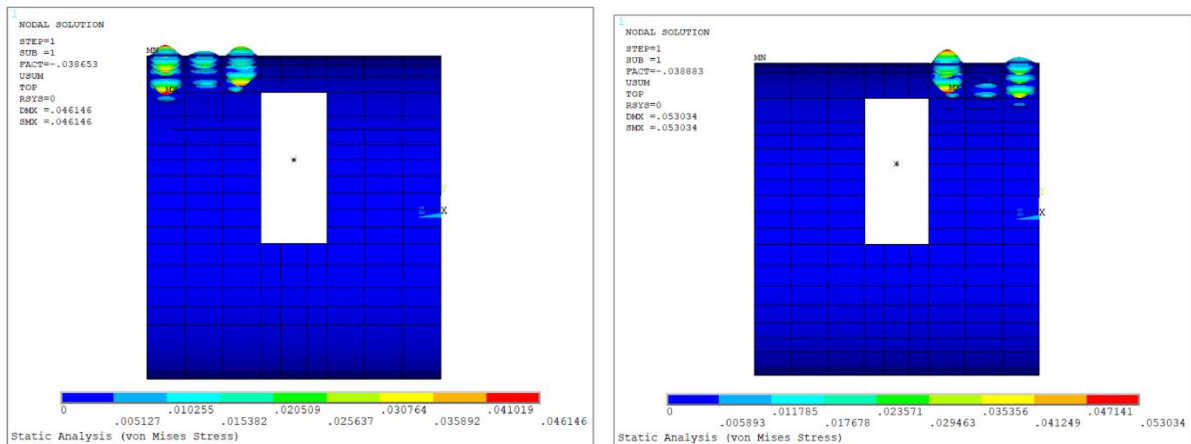


Figure 26 - Local instability in load case 2: Left - UY=0 in upper line; Right - UY=0 at end $z = b_s$ (mv2.mac)

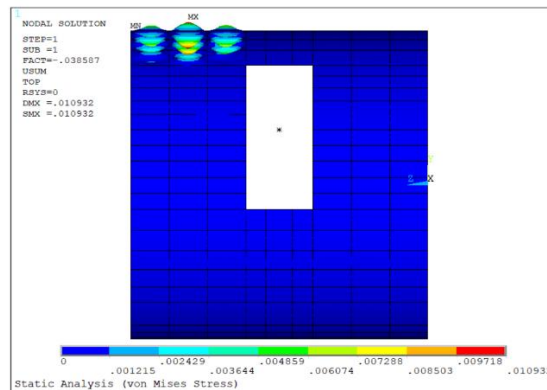


Figure 27 - Local instability for the third load case and UY=0 at $z = b_s$ ($B_f = -0,386E-01$) (mv2.mac).

All the existing modes reveal only local instability. The negative values of b_f mean that the sum of loads will not destabilize the whole structure. If the resultant of forces is multiplied by -1, the buckling factor will be positive. This type of instability, known as crippling, appears in the areas near the constrained edges or the application of forces. A way of minimising this effect is to insert additional members, which reduce the effective length of the area of the panel.

However, the fuselage's section is not sufficiently large in length, so the results of this analysis are not an evidence of the real structure's behaviour in terms of stability. Any study of this part will only reveal the way in which the buckling factor changes. The whole cylinder should be modelled to have accurate values of buckling factors and natural frequencies.

4.3 Convergence Analysis based on mesh refinement

The reference model, based in the commercial transport aircraft Airbus A320-200, is used to evaluate if the modelled structures converge. Some of its dimensions are not the official values, due to lack of information, but are taken from other sources [27] for the structure to be more realistic possible.

For a fixed configuration, when refining the mesh, i.e. increasing the number of elements of the mesh, the solution may or may not converge to a value (which in turn can also be a wrong value). Having fixed all parameters and changing only the number of divisions of each line of the model, a convergence study of different quantities was performed. The model that represents the reference geometry is subjected to only the internal pressure and the first type of constraints.

As said earlier in the subsection about the mesh, as the element line length increases, the number of elements is the same for some of the first variations (which makes sense once the elements are bigger and the variation in their length may not be enough to create another element in the same line), so the number of elements should be considered and not the number of divisions.

Figure 28 shows the plots of the Weight (N), the maximum displacement (mm), the maximum equivalent stress (MPa) and the total deformation energy (J) of the model, relatively to the number of elements, Nelem, for the Version 1 of the model. The plots of the same quantities obtained with the Version 2 of the model are in Figure 29.

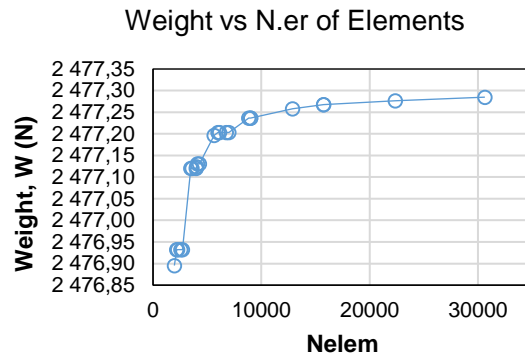
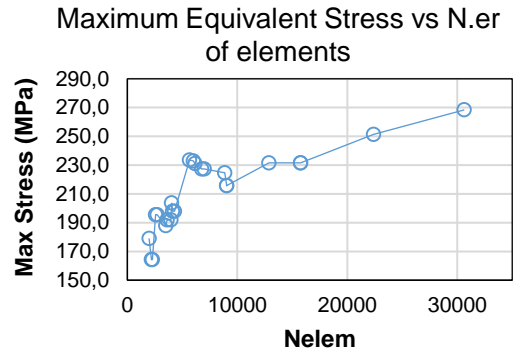
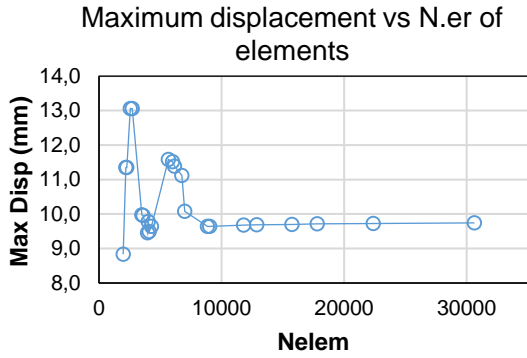


Figure 28 – Convergence Study of Version 1 of model (mv1.mac).

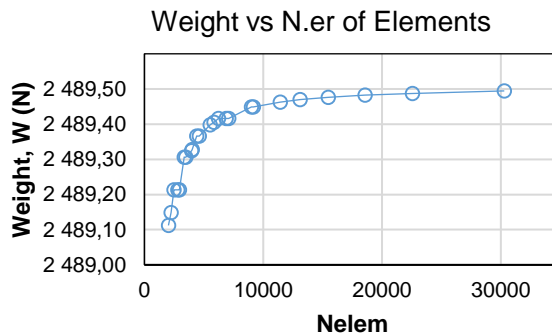
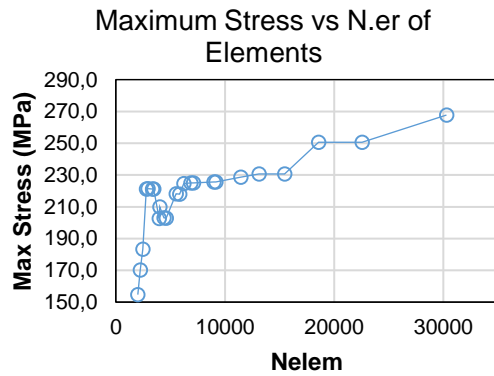
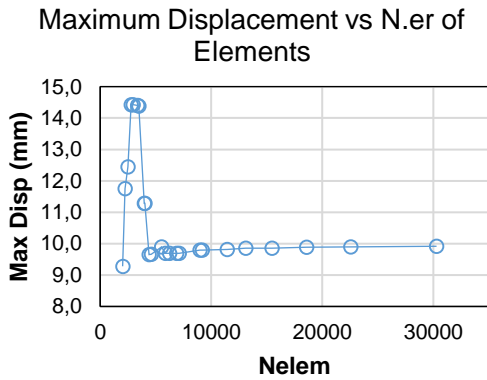


Figure 29 - Convergence Study of Version 2 of model (mv2.mac).

It is observed that the stress value increases with increasing number of elements, which suggests that there is at least one singularity at the solution. It was expected, as there are some areas in the FE model, like the corners of the cut-out, which are difficult to solve. If the mesh is further refined, the values in these places will tend to infinite, something physically impossible. Observing the distribution of equivalent stresses on the reference model for size = 30 mm (Figure 30), the points of maximum and minimum values are at the corners of the cut-out.

One way to solve this is taking the nodes in the vicinity of the corners from the solution, so that the post-processing will show the stress distribution in the model neglecting the solution at those nodes. This only needs to be done when writing the stress in the *Results.txt* file. All the other quantities are computed independently of the existence of singularities. The nodes at approximately 30mm from the corners were put into components and their selection was inverted, so the contour plot would not show the solution on these points. The new distribution of stresses is shown in Figure 31. Stresses are higher in the middle of the lateral panels and also above cut-out, near the stiffeners.

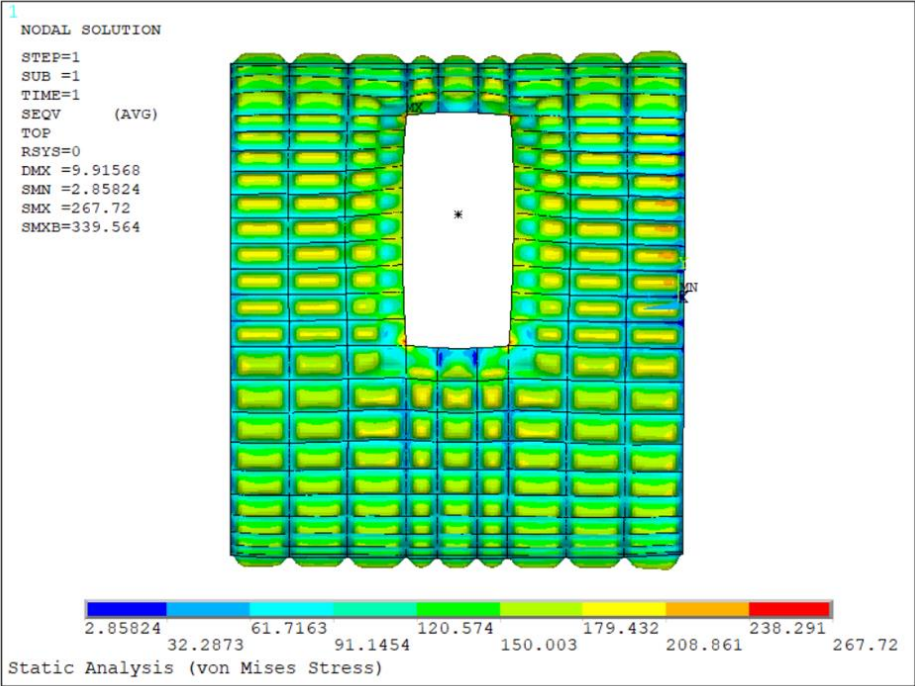


Figure 30 - Stress distribution in Version 2 (mv2.mac).

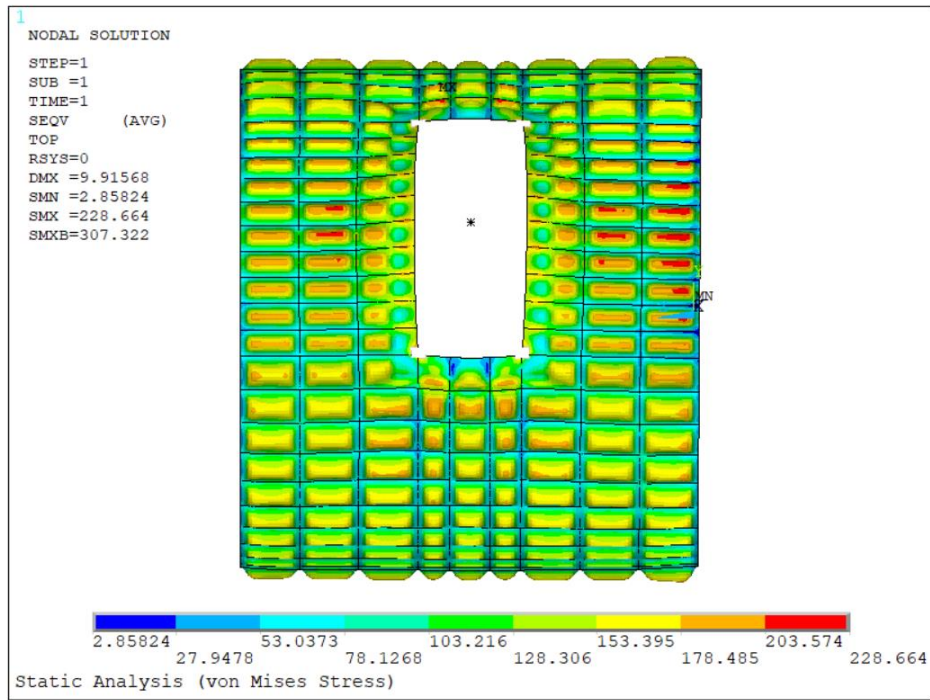


Figure 31 - Stress distribution in version 2 without the singularities at the cut-out corners (mv2s.mac)

The final results of the convergence study are plotted in Figures 32 and 32, respectively for versions 1 and 2. Stress singularities do not affect the displacement of the structure or the other quantities.

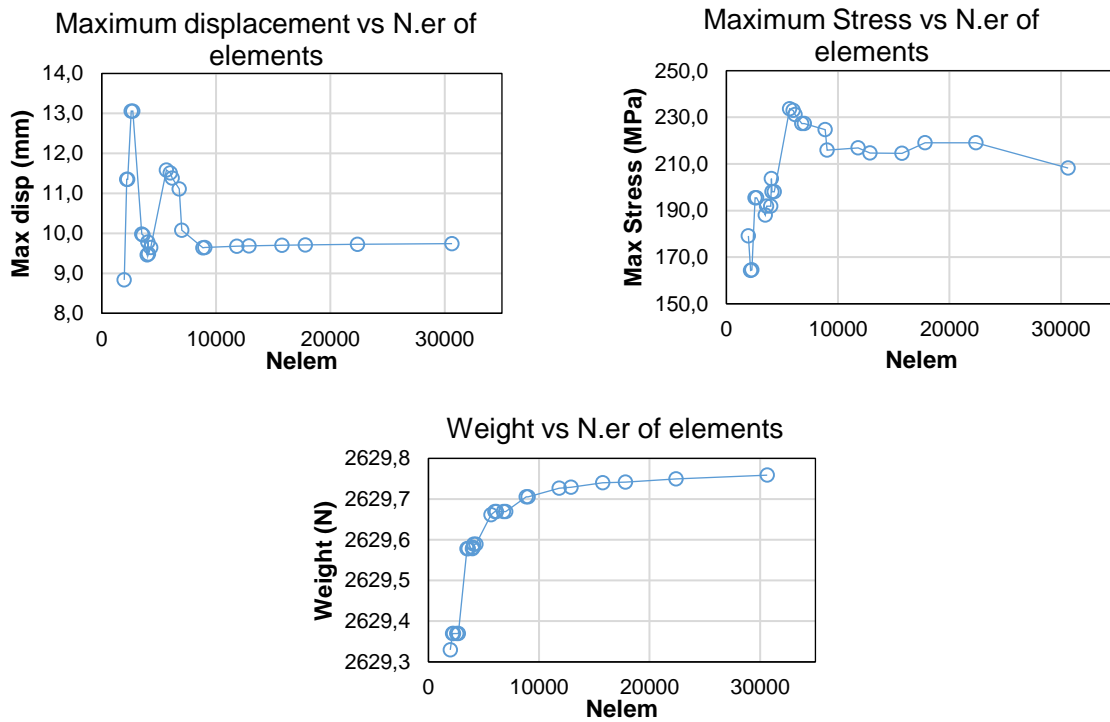


Figure 32 - Convergence obtained by variation of number of elements in the model without the nodes in the corners (mv1s.mac).

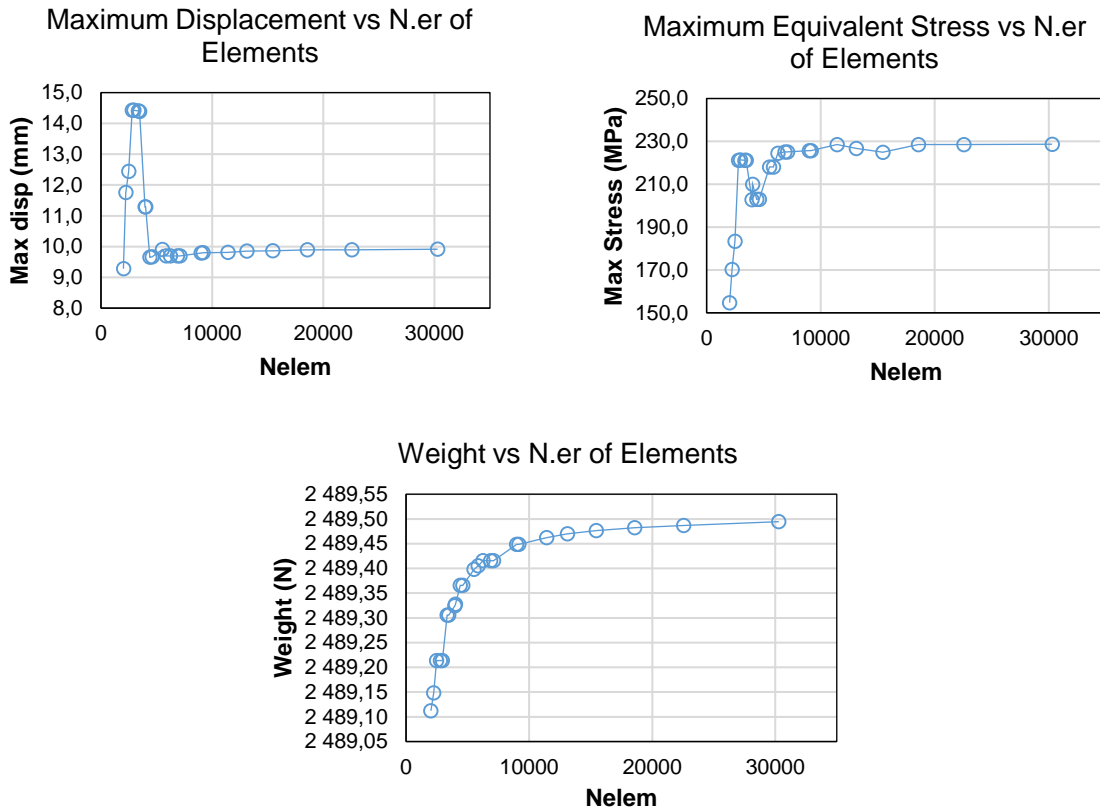


Figure 33 - Convergence obtained by variation of number of elements in the model without the nodes in the corners (mv2s.mac).

In version 2, unlike the situation in the overall model, the value of the maximum stress stabilizes in about 228 MPa, which suggests there are no more singularities in the model.

The buckling analysis was not performed in the convergence study of the second version because for some of the meshes ANSYS hung, i.e. the simulation stopped working in the middle of the analysis, due to some encountered error.

This study was done for the reference structure, so with fixed dimensions. If the geometry changes the values will differ and the singularities appear in other places, being more likely to occur around the cut-out corners and/or near other discontinuities. To save time, the convergence was not evaluated for every structure obtained by variation of the parameters. To ensure the values of the stress are real and not singularities, three regions where it is expected that the highest stresses in the model occur were defined and evaluated in ANSYS for the maximum stress within each area. They were picked after observing a pattern of high stresses in the convergence study of the full model. The areas are far from discontinuities like the cut-out edges and points of application of loads and constraints.

The weight of the model is increasing with the refinement of the mesh (Figure 28) because the used type of shell element is 2D (planar) so it does not exactly fit the curved areas. What happens with the refinement is that the dimension of each shell element decreases and in the limit the size of the element side approximates the perimeter of the arc. The model in the coarsest mesh is made of planar plates

that are away from the real structure, while in the finest mesh the accounted area tends to all the cylindrical area.

It is convenient to have the most reduced runtime of the analysis possible. The size of elements for the study was chosen to be 30 mm, not only because the Ansys version did not allow for more elements, but also because it was observed that the results stabilized for a much coarser mesh and the differences in the values obtained with a finer mesh would be insignificant. The time spent for each convergence study was no longer than 6 minutes.

5. Sensitivity Analysis

For this part, Ansys is called in MATLAB for different values of the cut-out width, B, and height, H,. The size of the mesh is 30 mm. This was performed for each loading condition, and all the analysis types were performed in each, despite the option of only running one in the MATLAB script, because the structure IF-THEN-ELSE structure was not included in the APDL file. The same happens with the load type, which is changed manually in that file. Tables 5 and 6 show data related to the design variables and to the design constraints, respectively.

Table 5 - Design variables, initial inputs and bonds.

Design Variable	Symbol	Initial input (mm)	Lower bond (mm)	Upper bond (mm)	Increment (mm)
Door width	B	810	700	1100	20
Door height	H	1850	1700	2200	20

Table 6 - Design Constraints.

Design Constraint	Symbol	Value
Strength	σ_{yeld}	290 MPa
Displacement	U_{max}	18 mm

5.1 Parametric Study

The design variables B and H were varied one at each time to perform this parametric study, making MATLAB travel each vector, save the results from Ansys in vector form and send it to a different sheet (one for B variation and another for H variation) of a same excel document.

After each parametric study, instead of an automatic optimisation, a “what-if” study is done in some cases, which is understood as a hand driven optimisation [4]. The user prescribes a change in one variable and observes the changes in the values and plots due to that change.

5.1.1 Case 1: Internal pressure

The width of the cut-out was varied between 700 and 1100 mm with increments of 20 mm, fixing its height at 1850 mm. When varying the height, the cut-out width was maintained at 810 mm. The plots of

each quantity taken with MATLAB are shown in Figures 34 and 35 for Version 1 of the model, and in Figures 39 and 40 for Version 2.

- **Version 1, load case 1: variation of door cut-out's width (height = 1850 mm)**

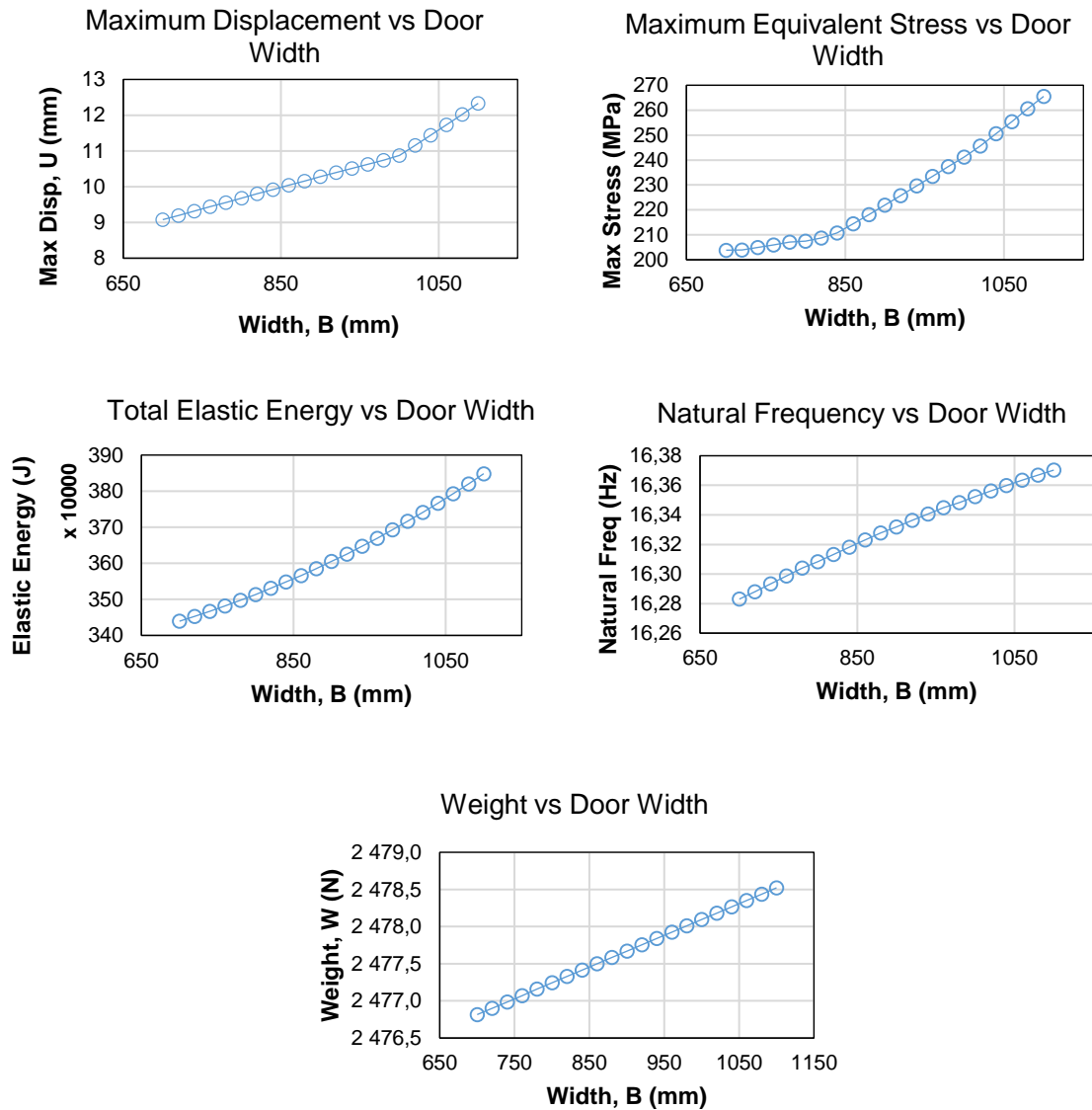


Figure 34 – Variation in model 1 with the cut-out's width, B (mv1s.mac).

- **Version 1, load case 1: variation of door cut-out's height (width=810 mm)**

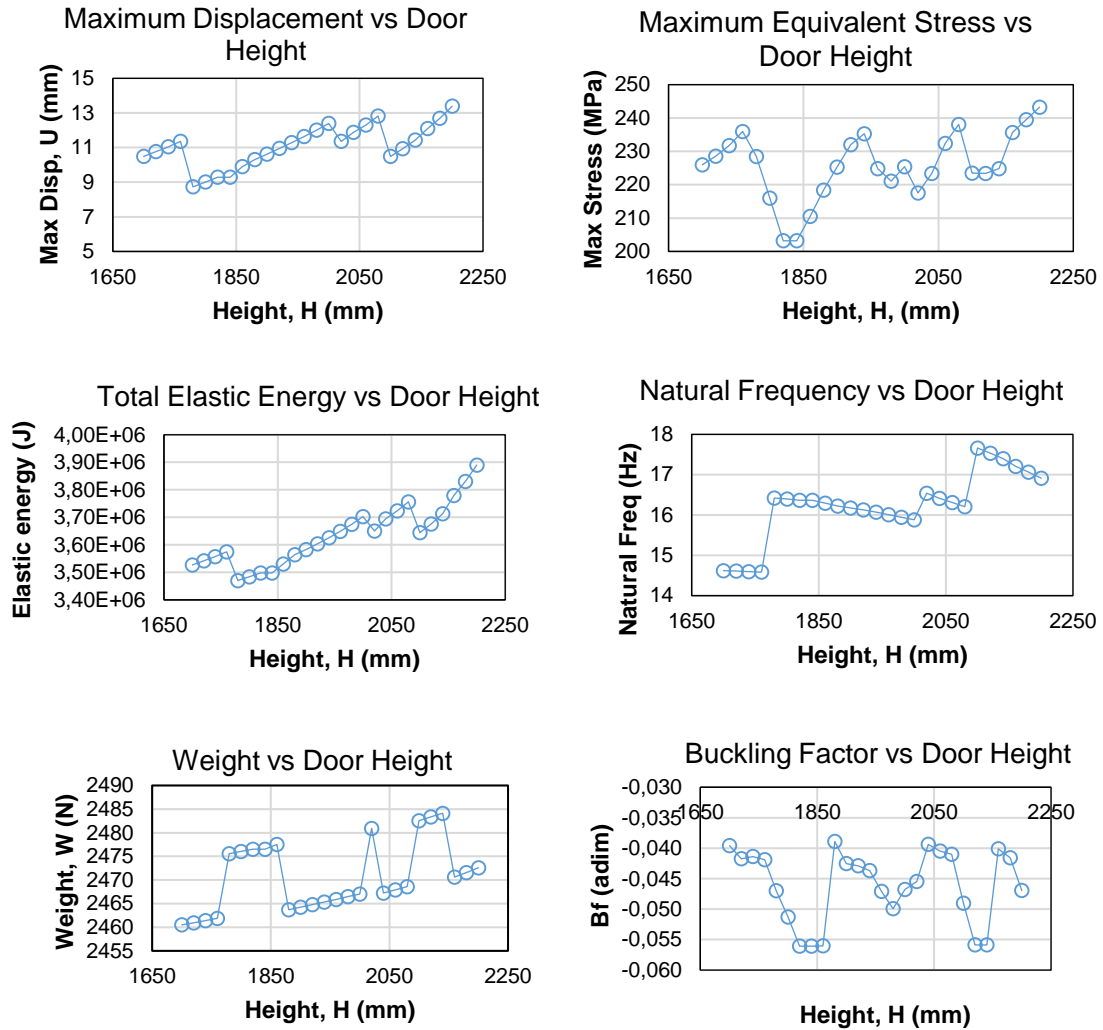


Figure 35 – Variation in model 1 with the cut-out's height (mv1s.mac).

As observed, the weight is unexpectedly increasing as the door cut-out enlarges. There is a decrease in the spacing between frames, hence a decrease in the area. However, the doors' mass is also being accounted, so the calculation may not be in conformity with the model, or the weight would actually be constant. As expected, the maximum stress increases, not reaching the material's admissible stress. The variations are approximately linear, also with elastic energy and natural frequency increasing as well and the buckling factor increasing in absolute value.

Relatively to the variation of the door height it is interesting to note the discontinuities in the plots. As the height increases, there is a sudden jump to a lower value of the quantities and above some height another jump to a higher value, although with the same slope. This happens respectively because a stringer is added to the model (a cut-stringer) and another stringer (above the cut-out) is deleted from the model. The same does not happen in the variation of the width, due to fixed number of frames at

each side of the door. Here the solution is only dependent on the spacing between frames and the number of elements the mesher will be able to create in the model for the element size input.

- Parametric Study of Model 1 based on the Stress

Some parameters of the model were changed in order to elevate the levels of stress. The changes done were the following:

- the frame web height decreased to 50 mm;
- the same dimension of edge frame decreased to 100 mm;
- the frame flange width decreased to 20 mm;
- the thickness of each sill decreased to 1,2 mm.

A convergence study was performed only to see if the levels of stress would increase and converge to a value. The latter was inconclusive, but the levels also were not that high. A further change was done:

- the number of stringers below the cut-out went from 10 to 5.

The new plots of the variation of the quantities to the variation in cut-out's width are in Figure 36.

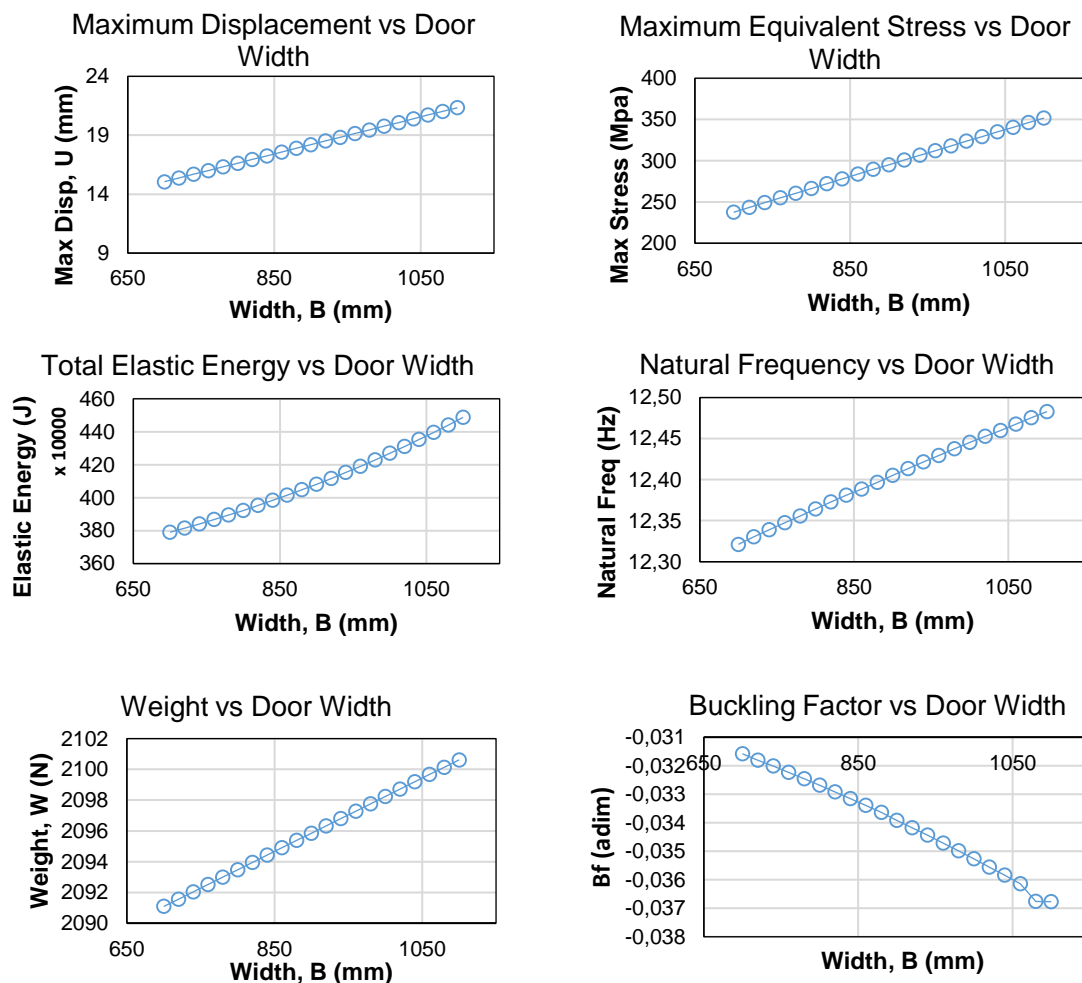


Figure 36 - Variation with width after changes are done in the geometry of Version 1 (mv1o.mac).

The von Mises Stress is above the strength of the material for a cut-out width of 900 mm. Below this point, the weight is decreasing, so it seems that for this range of stresses we can have even less material. As the weight increases with the width, the configuration will be chosen based on the minimum weight (Table 7). The meshed model of this configuration and its stress distribution is shown in Figure 37.

Table 7 - Chosen configuration in terms of stress for H=1850 mm (mv1o.mac).

Variable	Value
Width, B	700 mm
Height, H	1850 mm
Weight, W	2091,09 N
Maximum Stress	237,53 MPa
Maximum displacement	15,06 mm
Total elastic energy	3790,16 KJ
Natural frequency	12,32 Hz

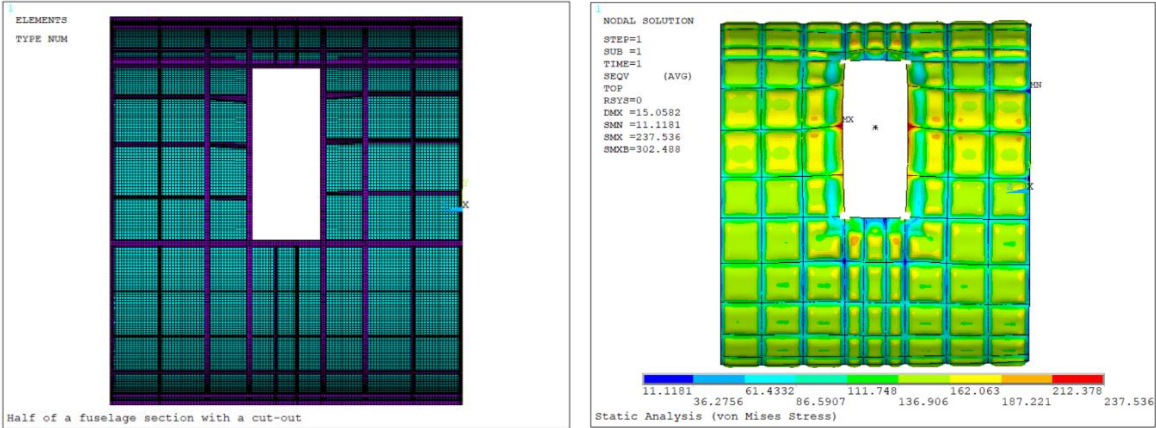


Figure 37 - Stress distribution in the chosen configuration (mv1o.mac).

For a width of B = 810 mm, the height was also varied to evaluate the behaviour due to the implemented changes. The plots are in Figure 38.

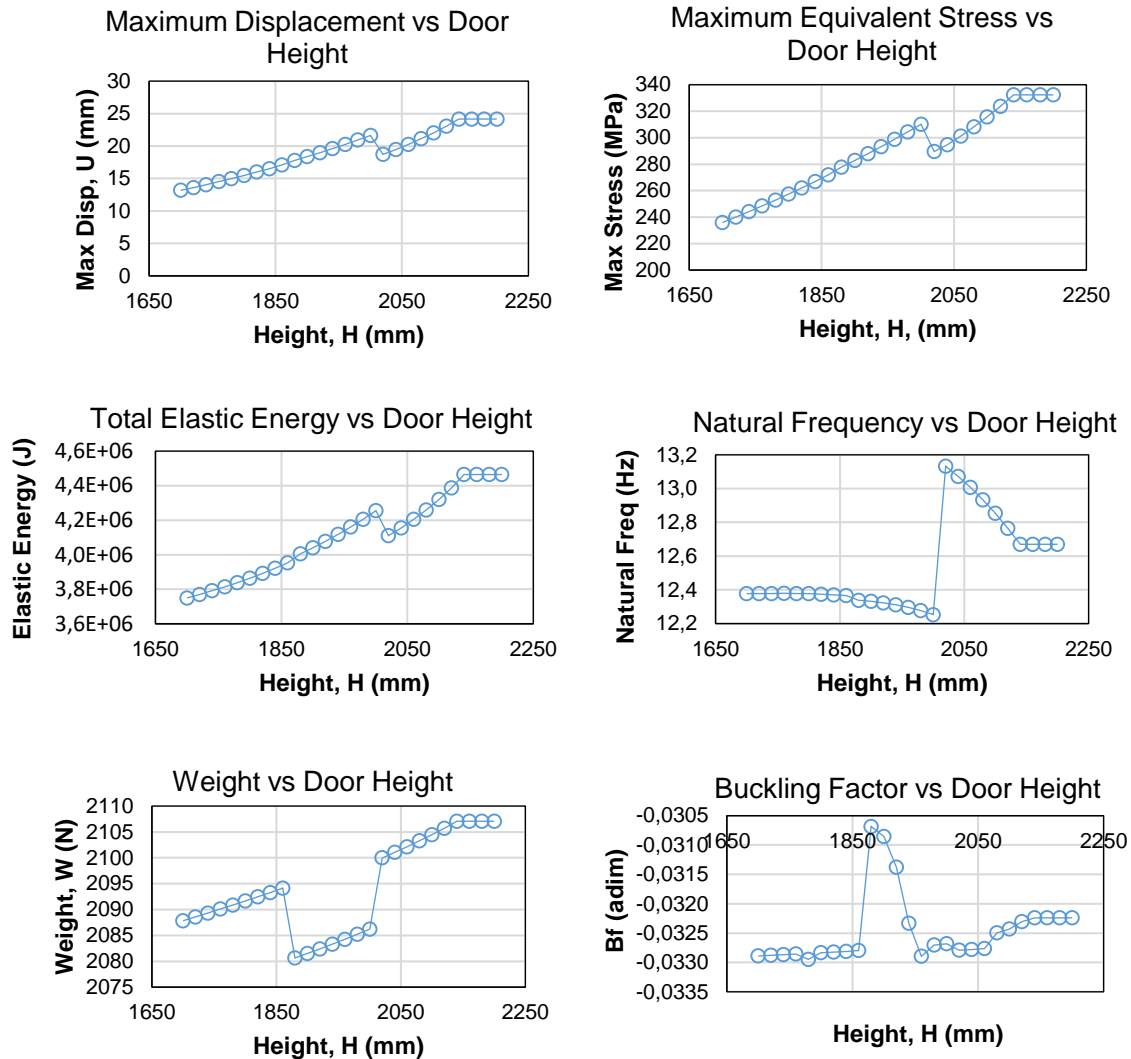


Figure 38 - Variation with height after changes are done in the geometry of Version 1 (mv1o.mac).

In general, the weight increases with the door height and also the stresses and displacements, though there is a decrease in the weight at $H = 1880$ mm, meaning that a stringer disappeared from the model as the height increased. However, a jump in the stress levels is not verified and is, in fact, below the strength of the material, so this is the chosen configuration.

Table 8 - Chosen configuration in terms of displacements for $B=810$ mm (mv1o.mac).

Variable	Value
Width, B	810 mm
Height, H	1880 mm
Weight, W	2080,64 N
Maximum Stress	277,73 MPa
Maximum displacement	17,78 mm
Total elastic energy	4005,51 KJ
Natural frequency	12,33 Hz

Relatively to the same point in the reference structure, there was a decrease in the Weight of 531,80 N (see Figure 34).

- **Version 2, load case 1: variation of cut-out's door width (height = 1850 mm)**

For the case of Version 2, where the number of stringers on each part is fixed, the ranges of variation of the width and the height were the same. In the case of buckling factor, the plots goes only until H = 1980 mm, because for higher cut-out heights ANSYS would hang and the results would not be written. It means two analyses were performed, each of them taking approximately 30 minutes.

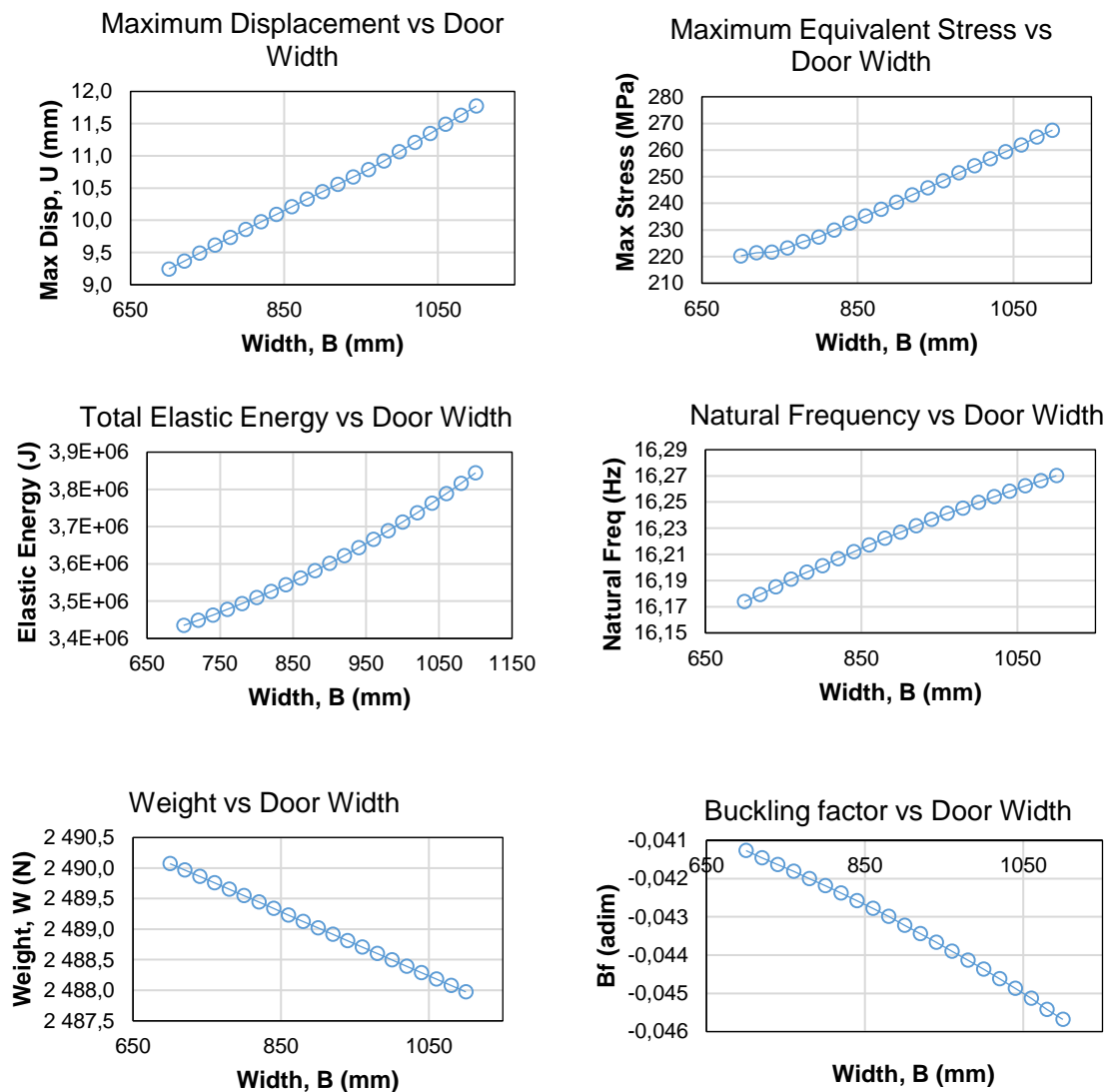


Figure 39 – Variation in model 2 with the cut-out's width (mv2s.mac).

- **Version 2, load case 1: variation of cut-out's door height (width=810 mm)**

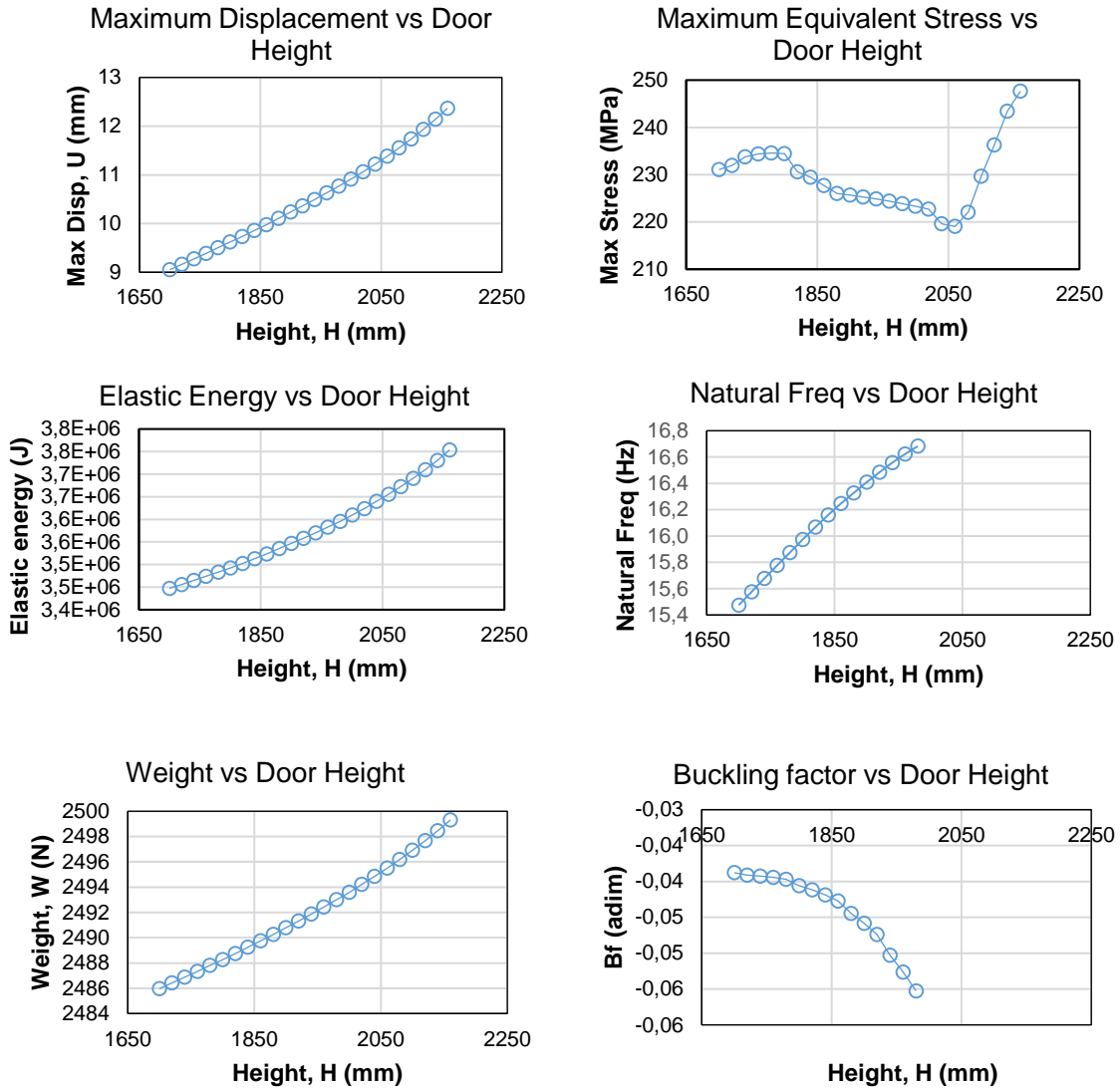


Figure 40 – Variation in model 2 with the cut-out's height (mv2s.mac).

The maximum stress is never surpassed, which gives space to a decrease in mass of the structure. There is a discontinuity in the stress plot, where the value starts unexpectedly decreasing, occurring another increase starting on $H = 2050$ mm. A possible reason for this could be a transition of the maximum value from the considered zone of highest stress to another place, due to increased rigidity in the new zone. After running the static analysis for the height's $H=1800$ mm, $H=1805$ mm and $H=1810$ mm, it is observed that the maximum value occurs in the same area – above the cut-out (Figure 41).

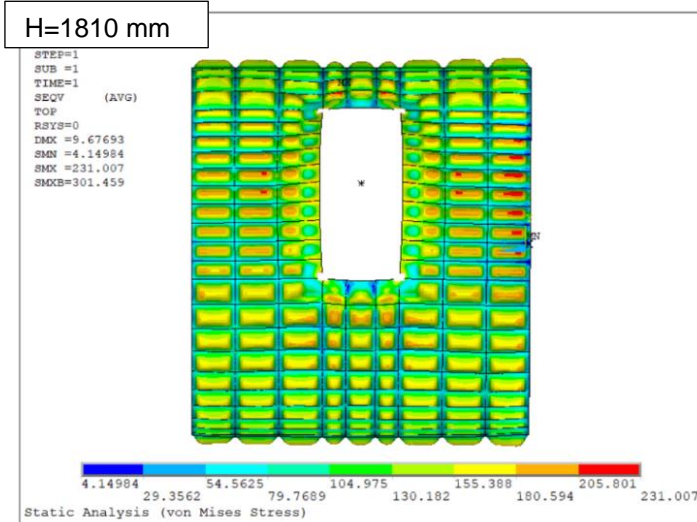
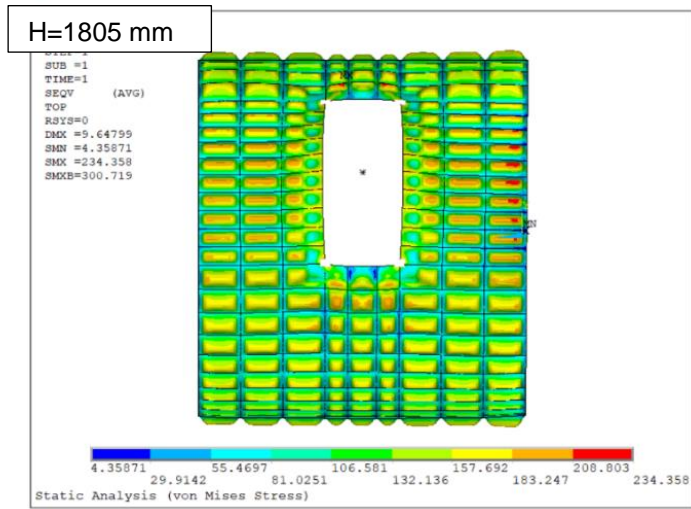
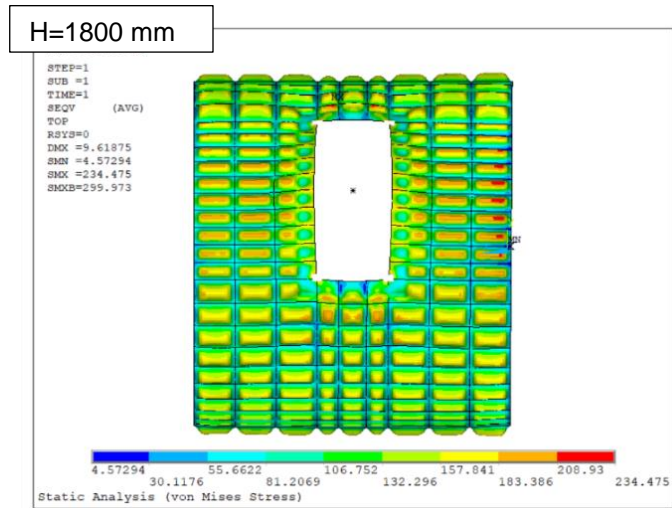


Figure 41 – Distribution of stress in configurations H=1800 mm, H=1805 mm and H=1810 mm (mv2s.mac)

Observing the other plots of stresses in defined zones (Figure 42), in all of them discontinuities occur, although for different configurations in each zone. The stress increases in zone 1 (above the cut-out)

for a height below 1,82 m, while in the other zones the slopes are negative. It is possible that the zones were wrongly defined.

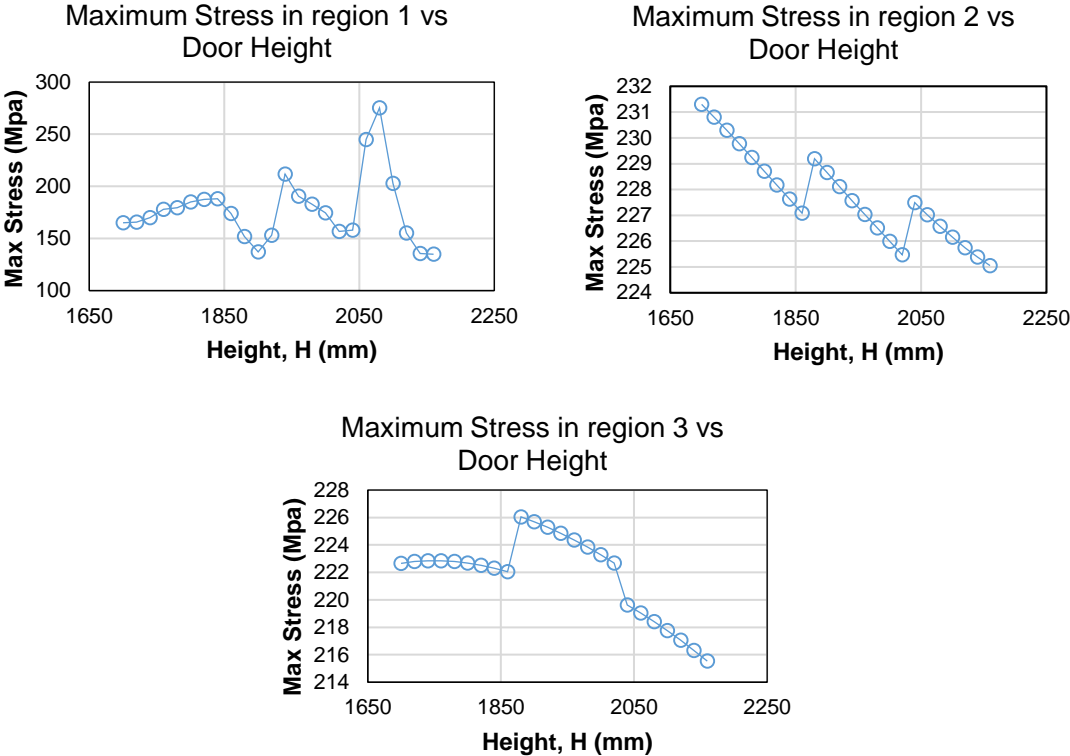


Figure 42 - Maximum stress in regions 1, 2 and 3 for version 2 for height variation (mv2s.mac).

As observed the buckling factor is always negative, which means there is no global instability of the structure for the internal pressure only. The absolute value of the buckling factor increases with both parameters. For version 2 with the full model, the buckling analysis was not performed because for some number of elements, ANSYS hung in the middle of analysis.

The weight changes linearly with the defined design variables, although more with the width than with the height. For higher values of the width the analysis could not be run for some reason.

- Parametric Study of Model 2 based on the Stress

The changes done were the following:

- the frame web height decreased to 50 mm;
- the same dimension of edge frame decreased to 100 mm;
- the flange width of the frame decreased to 20 mm;
- the thickness of each Sill decreased to 1,2 mm;
- the number of stringers below the cut-out, went from 10 to 8;

- the flange and web of the stringers were decreased to 10 and 20 mm respectively;
- the doubler thickness decreased to 2 mm.

The configuration of the altered version (for B = 810 mm and H = 1850 mm) is in Figure 43 and the new plots of the variation of the quantities to the variation in cut-out's width are in Figure 44.

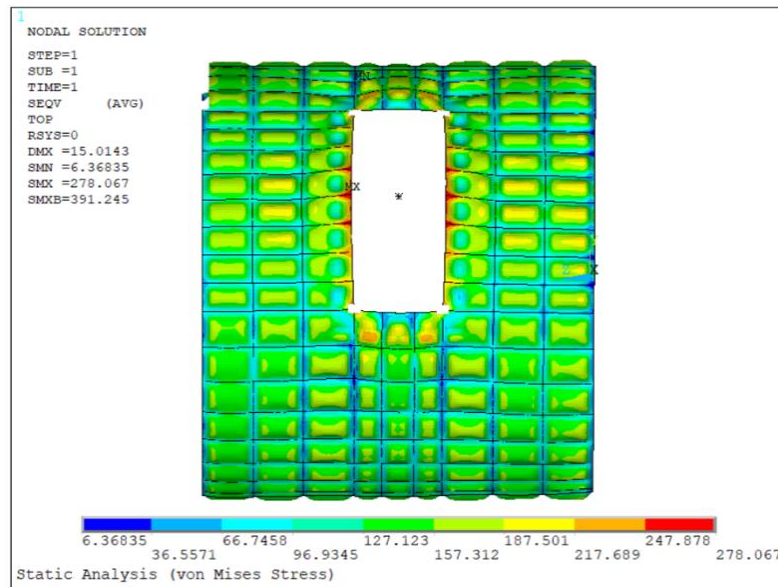


Figure 43 – Stress distribution in altered version 2 (mv2o.mac).

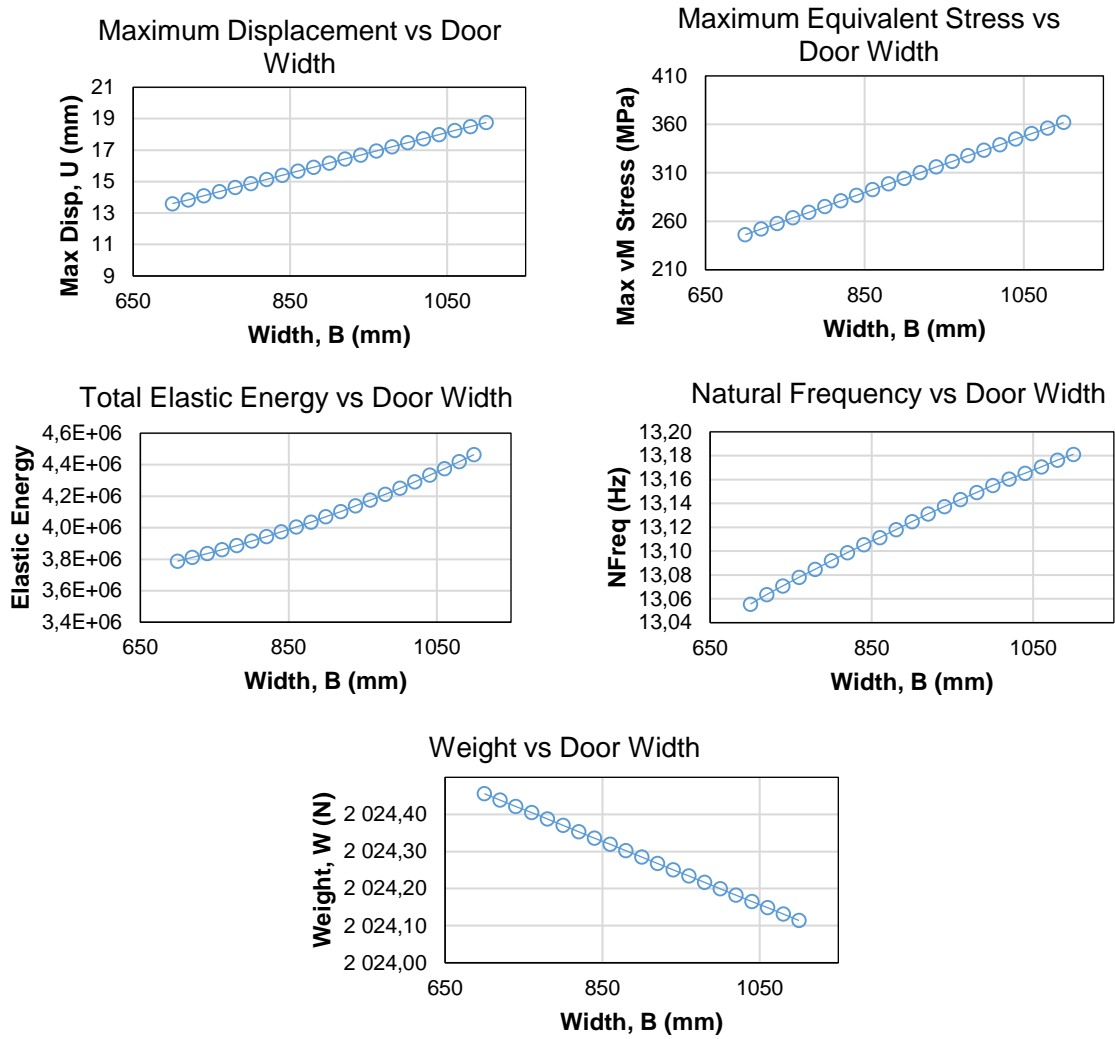


Figure 44 - Variation with width after changes are done in the geometry of Version 2 (mv2o.mac).

As the weight decreases with the door width, the configuration that is chosen is based on the maximum allowed stress (Table 9).

Table 9 - Chosen configuration for a structure subject to pressurisation for H=1850 mm (mv2o.mac).

Variable	Value
Width, B	840 mm
Height, H	1850 mm
Weight, W	2024,34 N
Maximum Stress	286,86 MPa
Maximum displacement	15,40 mm
Total elastic energy	3972,98 KJ
Natural frequency	13,11 Hz

For a door width of 810 mm in the altered model, the height was variated and the respective plots obtained (Figure 45). The chosen configuration was based on the weight, as it is still in the range of low

stresses (Table 10). There was a decrease in the Weight of 463,28 N relatively to the same point in the reference structure.

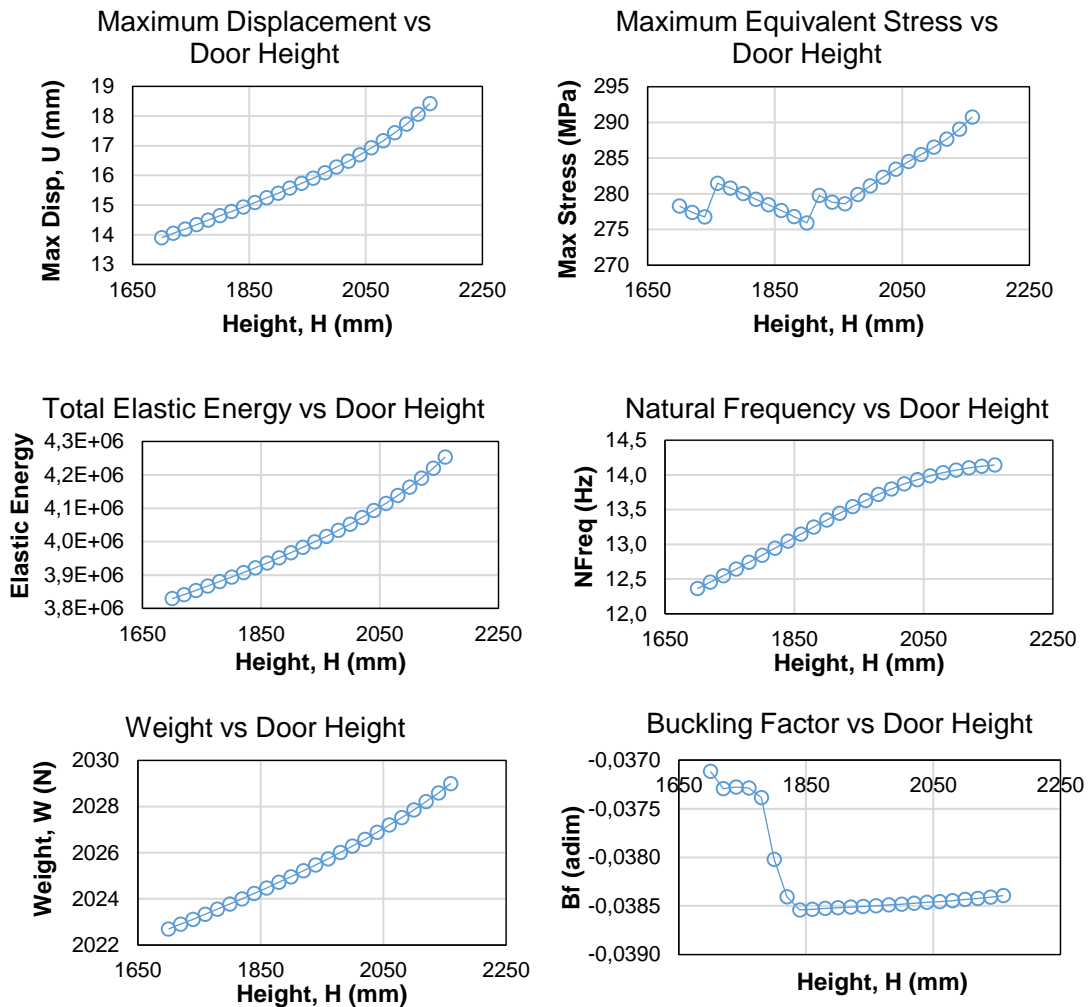


Figure 45 - Variation with height after changes are done in the geometry of Version 2 (mv2o.mac).

Table 10 - Chosen configuration for a structure subject to pressurisation for B=810 mm (mv2o.mac).

Variable	Value
Width, B	810 mm
Height, H	1700 mm
Weight, W	2022,70 N
Maximum Stress	278,30 MPa
Maximum displacement	13,90 mm
Total elastic energy	3829,16 KJ
Natural frequency	12,36 Hz

5.1.2 Case 2: Internal Pressure + Shear Load

For the case of the shear load, a force was applied at the free end using the MPC method. As already said in chapter 3, the used constraints influence the solution. The displacements in the case of group 1 are the same as the ones obtained if no shear load was there, so the analyses will be done for the 2nd group of constraints, whose distribution of displacements is depicted in Figure 46.

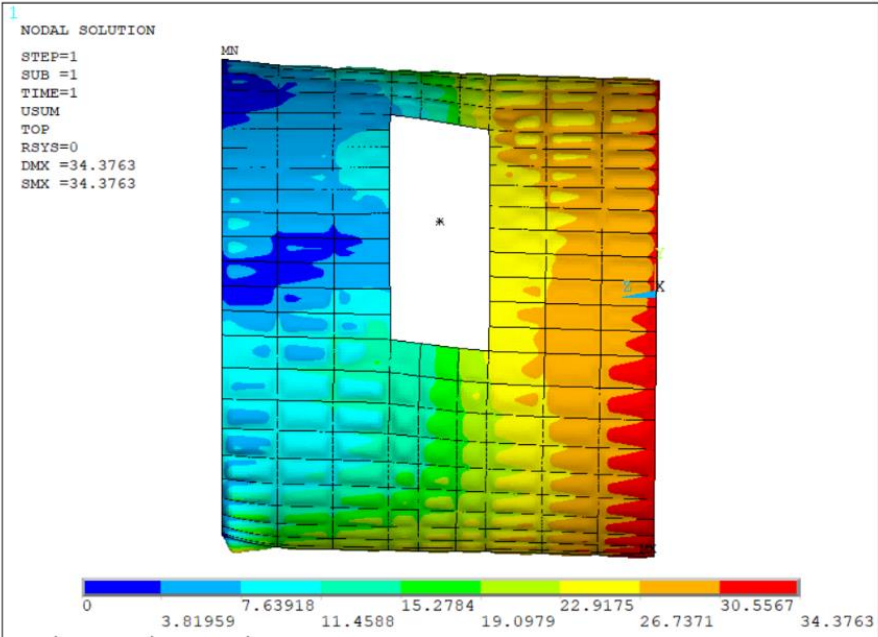


Figure 46 – Displacements caused by load case 2

After taking groups of nodes from the model, where singularities would occur, a convergence analysis was done, giving the variation in Figure 47. Then the parametric study was performed for both the design variables, and the plots with exception for the structural weight of the model were obtained (Figures 48 and 49).

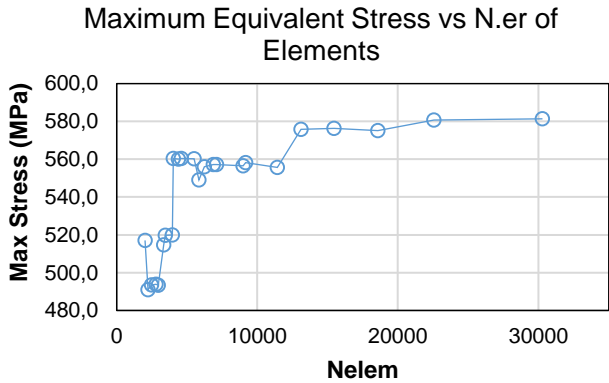


Figure 47 – convergence analysis for reference model with load case 2 (mv2sf.mac).

- **Version 2, load case 2: Variation of cut-out's width, B**

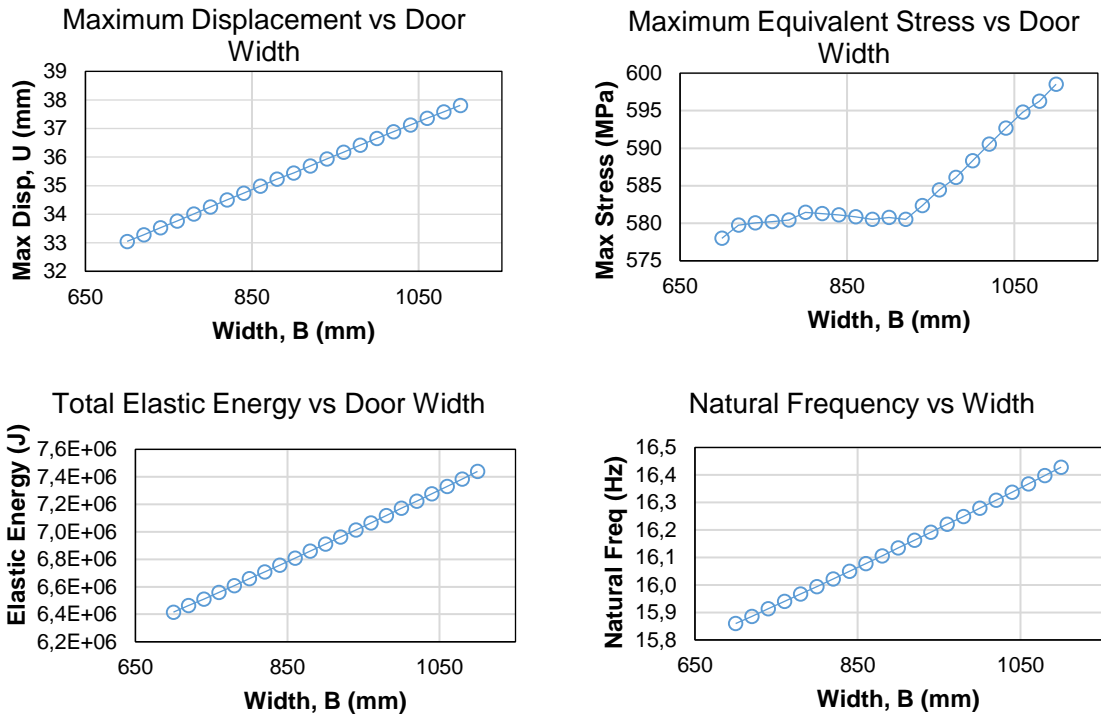


Figure 48 – Variation in Version 2 with the cut-out's width (mv2sf.mac).

- **Version 2, load case 2: Variation of cut-out's height, H**

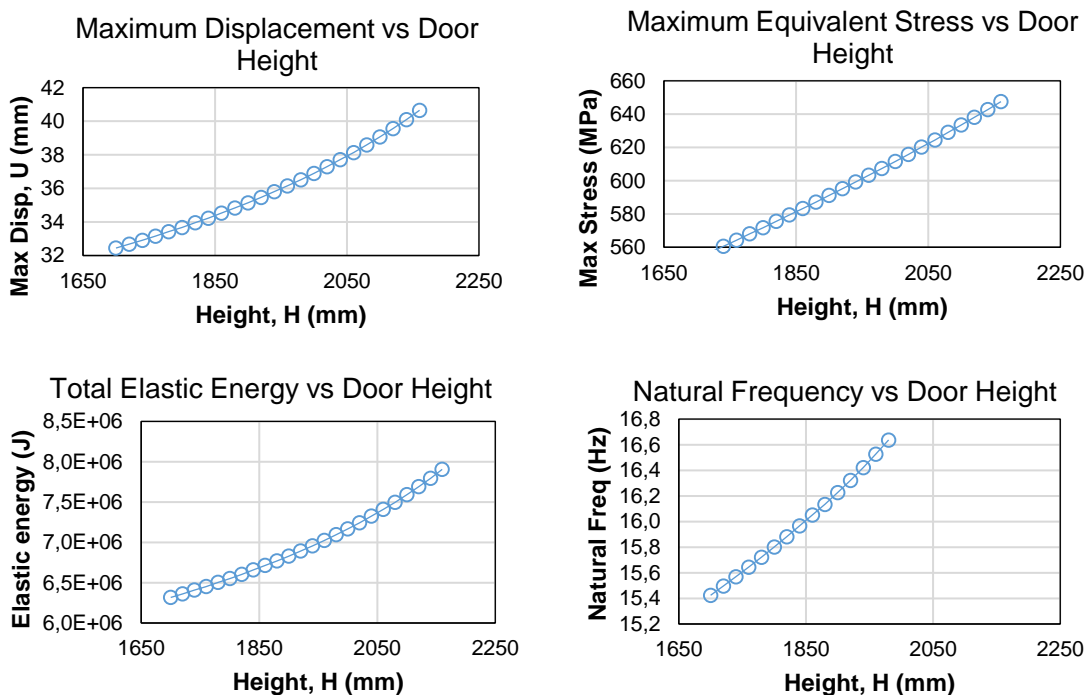


Figure 49 – Variation in model 2 with the cut-out's height (mv2sf.mac).

The stress levels are too high. A decrease of mass must be done to the model so that the values will decrease.

- Parametric Study of Model 2 with load case 2

This time there is a need for stiffening the model, so that the stress levels decrease to valid levels. Also the maximum displacement seems too high, so increased rigidity is needed, which can also be concluded by observing the plot of Elastic Energy of Deformation. Furthermore, the weight of the model will have to increase. The way of changing the model was:

- the skin thickness increased to 1,5 mm;
- the doubler thickness increased to 4 mm;
- the frame flange height increased to 100 mm;
- the same dimension of edge frame increased to 120 mm;
- the stringer flange height increased to 50 mm;
- the thickness of each frame increased to 1,5 mm.

Running an analysis with all of these changes, the plot of Stresses gives the Figure 50. One can observe that the highest stress is below the cut-out. This value is not considered a singularity, as, like already verified, it is a stabilized value (Figure 51). One possible way to improve the structure without putting up too much weight would have been to differentiate between two types of Sills: a Main Sill and an Auxiliary Sill, making one of three different configurations, a one-, two- or three-stringer bays below and above the cut-out (see Figure 1). Regardless of the high stress obtained with the reference door dimensions, for other configurations the stresses could eventually reach good values. However, by observing the variation of the maximum stress with the width, which increases, one can verify that in the range 700-810 the slope is greatly reduced, so it can be deduced that a stress of below 290 MPa would be unlikely to be reached with this model for this load case and this group of constraints. The same can be said regarding the high variation, whose improvements in stresses with the new model would be only approximately 50 MPa.

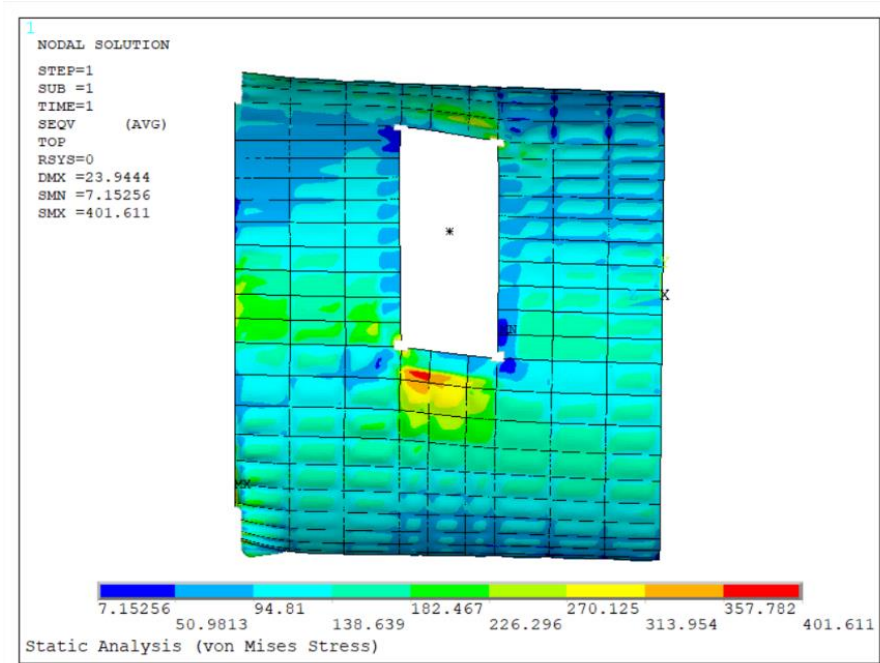


Figure 50 - Stress distribution in reference structure (version 2) subject to case load 2 (mv2sf.mac).

In terms of displacements, a configuration can be obtained if further changes are done:

- the shell thickness increased to 2 mm;
- the number of stringers below cut-out increased to 12.

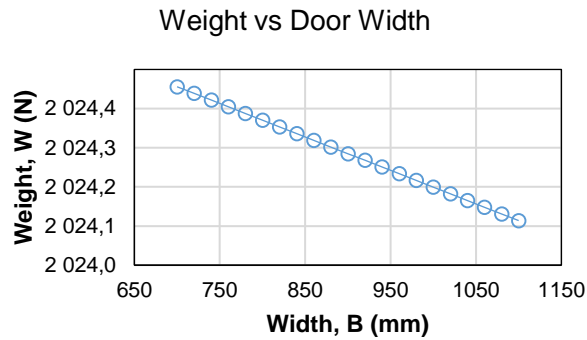


Figure 51 - Weight vs door width for comparison with improved model (mv2sf.mac).

For a door height of 1850 mm in the altered model, the height was variated and the respective plots obtained (Figure 52).

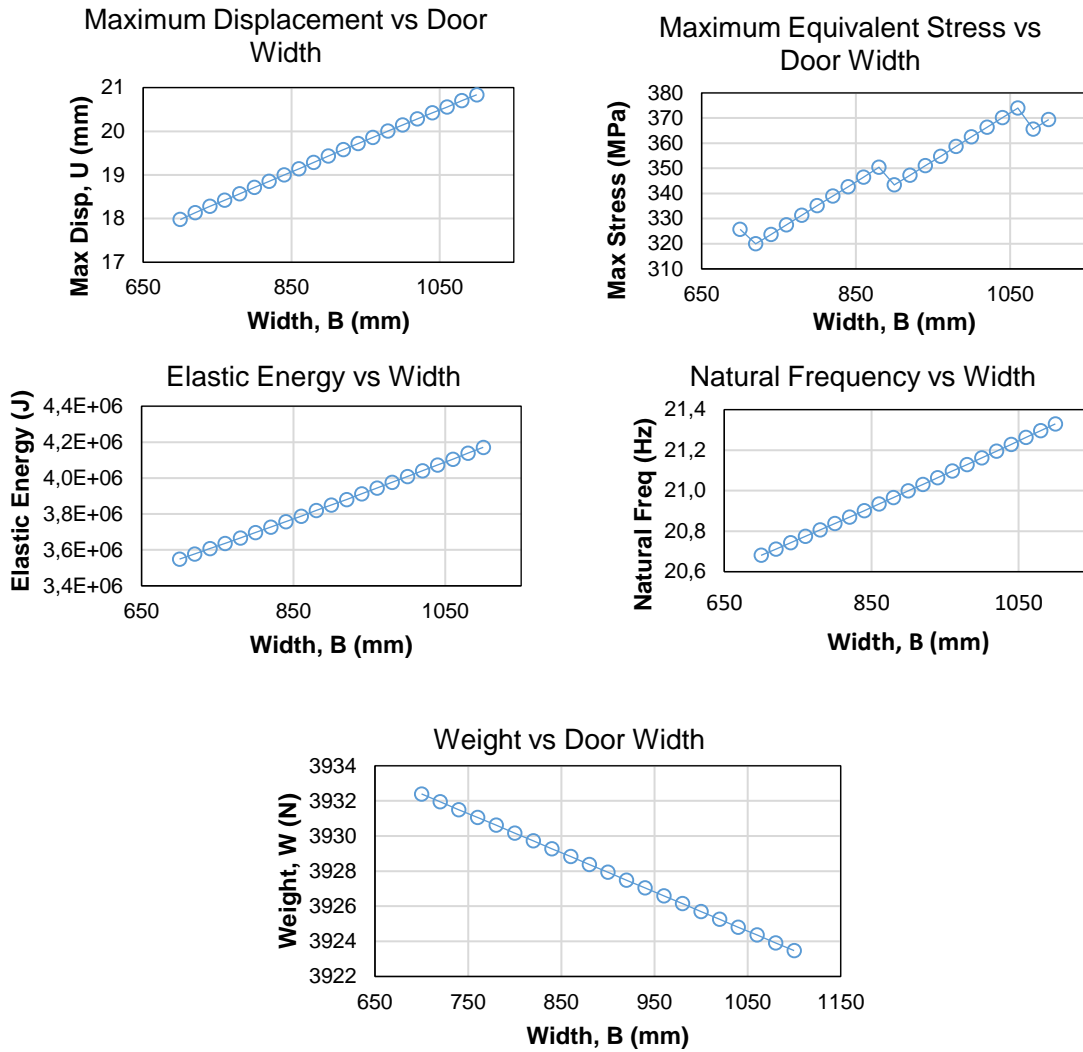


Figure 52 - Variation with width of altered model 2 (mv2of.mac).

The chosen configuration is based on the maximum displacement, as the levels of stress are still too high and further reinforcement is needed. The best configuration for a H = 1850 mm seems to be the one with $U_{max} = 17,97$ mm (Table 11).

Table 11 - Chosen configuration for a structure subject to pressurisation and shear load

Variable	Value
Width, B	700 mm
Height, H	1850 mm
Weight, W	3932,40 N
Maximum Stress	325,74 MPa
Maximum displacement	17,97 mm
Total elastic energy	3548,62 KJ
Natural frequency	20,68 Hz

5.1.3 Case 3: Internal Pressure + Bending Moment

A bending moment was added to the Internal Pressure applied to the structure, using again the MPC method. Regarding the constraints, comparing both groups, the results are not very different in terms of stresses (Figure 53), with the higher stresses occurring in upper line and at the constrained edge, as expected. Concerning the displacement vector sum plot (Figure 54), as the door deformation is higher when constraining the upper line in vertical direction, it may be more interesting to study its deformation using the first group of constraints.

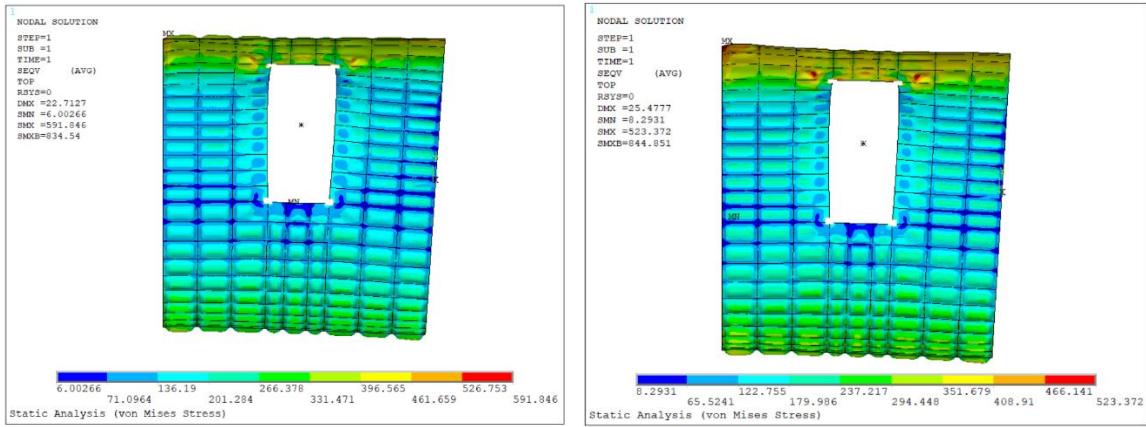


Figure 53 – Distribution of stresses in load case 3. Left: group 1 of constraints. Right: group 2.

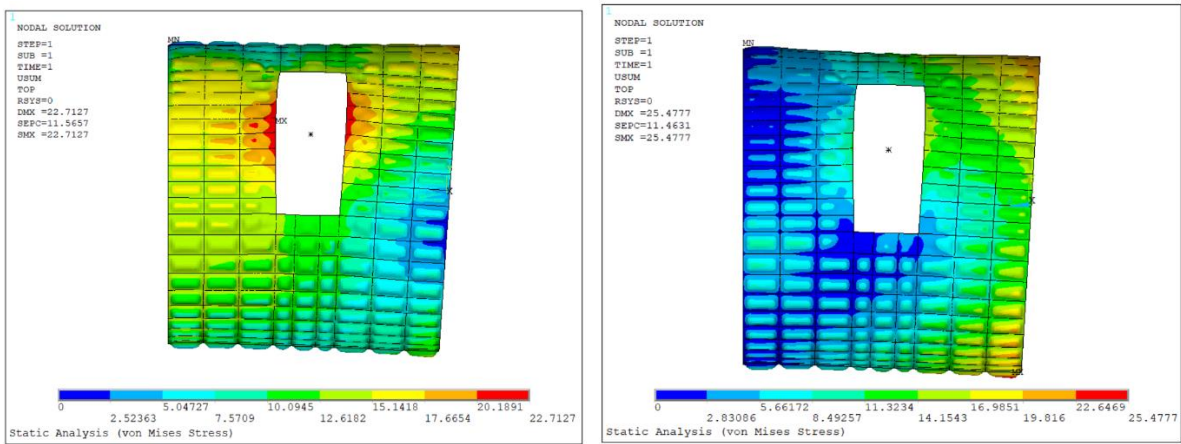


Figure 54 – Displacements caused by load case 3. Left: group 1 of constraints. Right: group 2.

After a convergence study, to see if the stress values converged, some more nodes had to be taken from the model in order to delete singularities. Observing the plot in Figure 55 it is difficult to say if there is a convergence in the stress. Further from changing the areas of nodes to be deleted, also new zones of high stresses were identified, based on the reference geometry (Figure 56). By observing the plots of

the stresses taken on those two zones, where there is a value to which the stress converges, it could be concluded that the model converges. Indeed, the value obtained for Smax with size = 30 mm is the same value obtained in zone 2 (left to the cut-out), $S_{max} = S_2 = 478,72 \text{ MPa}$.

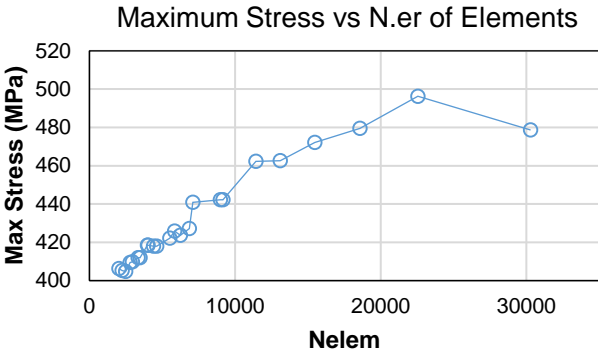


Figure 55 – Convergence of Stress in reference structure (Version 2) subject to case load 2.

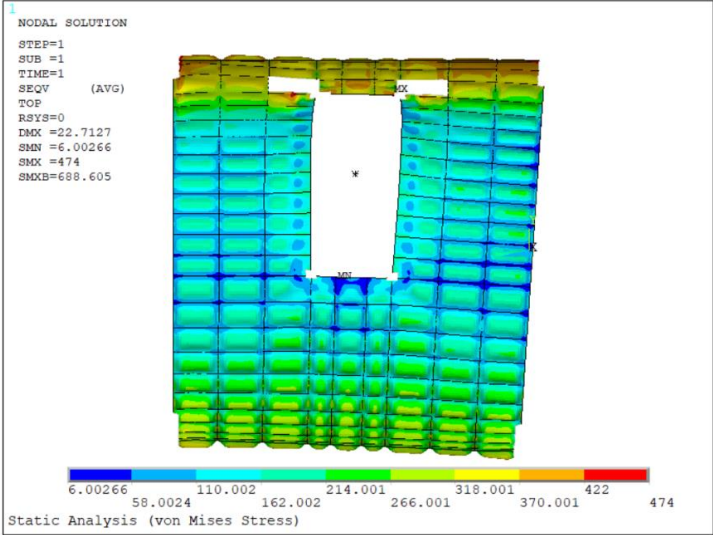


Figure 56 - Contour plot of the model subject to case load 2 showing the deleted nodes and also the regions where maximum stresses will be taken. Note: the image is previews to the change in internal pressure value (mv2sm.mac).

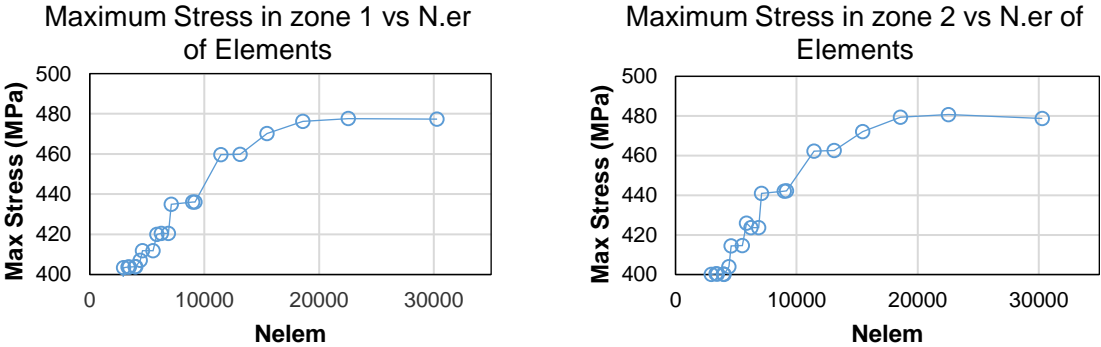


Figure 57 - Convergence of Stress in reference structure subject to case load 2 in defined zones.

- **Version 2, load case 3: Variation of cut-out's width, B**

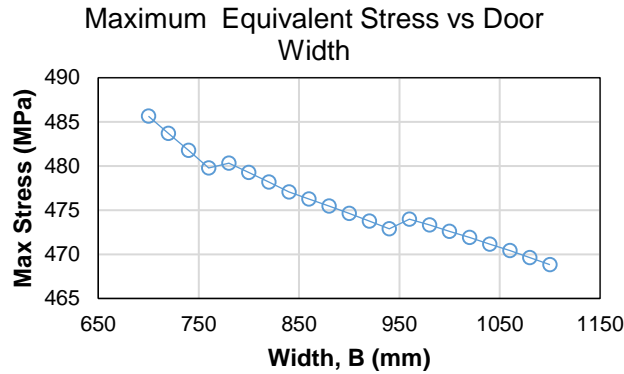


Figure 58 – Variation in model 2 with the cut-out's width (mv2sm.mac).

Observing the plot of stresses against the door width, there are two discontinuities in the plot, which could suggest a shift of the maximum stress to another point. By running manually the simulation, that is not the case (Figure 59), so it is difficult to explain why it happens. The same is encountered in the plots of the other defined zones (Figure 60).

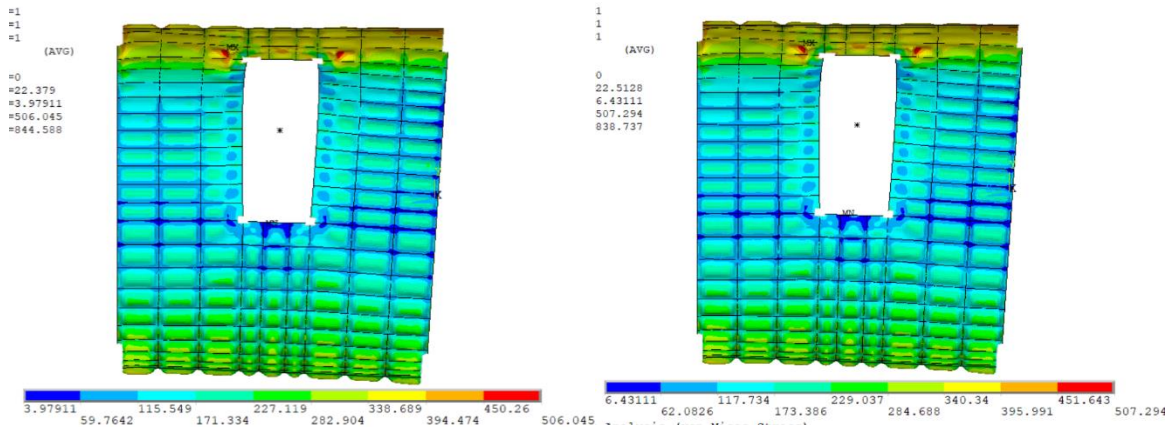


Figure 59 - Maximum stress (mv2sm.mac). Left: B=760mm (Smax= 479,79 MPa); Right: B=780mm (Smax= 480,34 MPa).

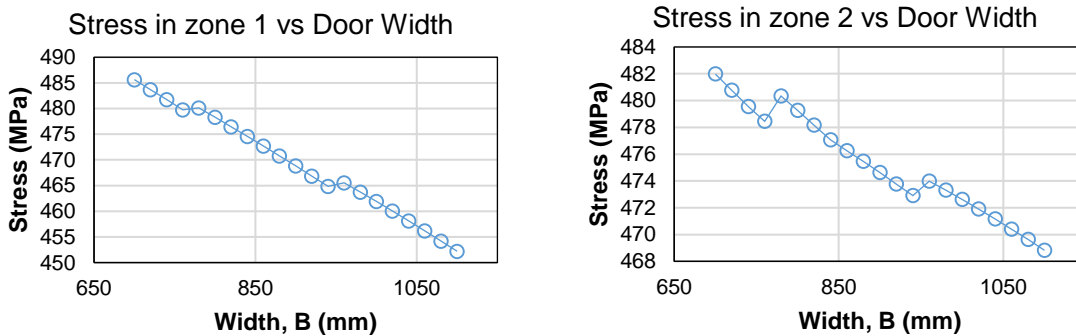


Figure 60 - Plots of Stresses in zones 1 and 2 vs door width (mv2sm.mac).

- **Version 2, load case 3: Variation of cut-out's height, H**

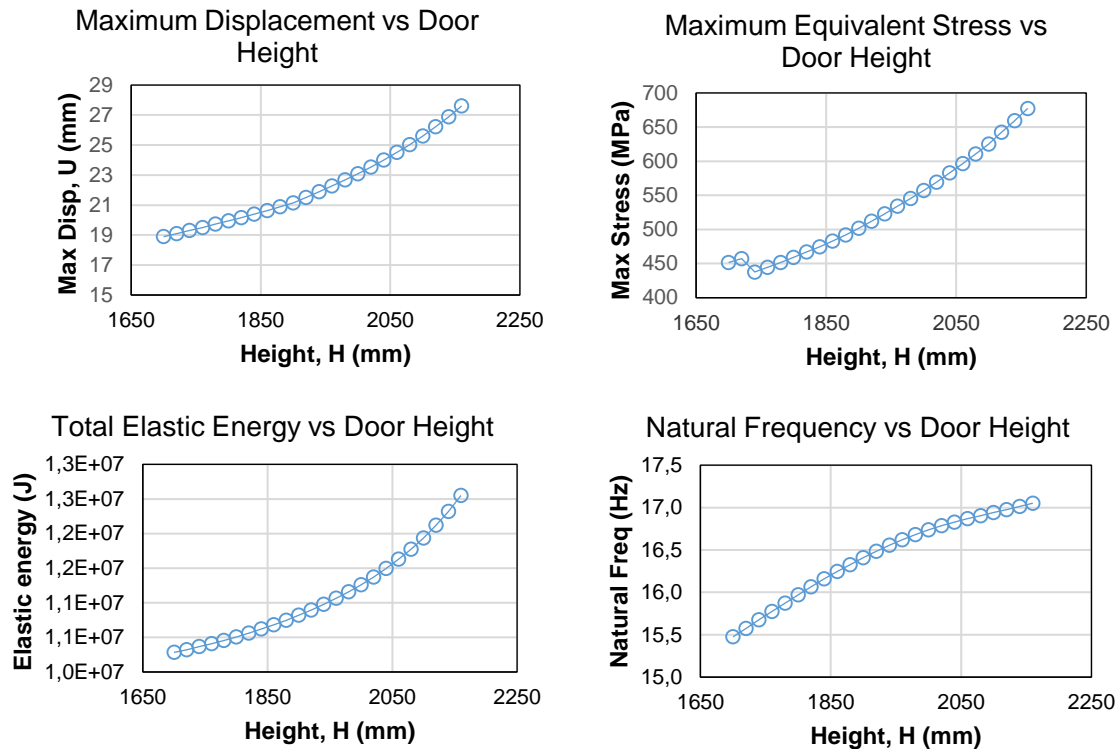


Figure 61 – Variation in model 2 with the cut-out's height (mv2sm.mac).

At a height of $H = 1980\text{mm}$, the analysis hangs and the file with the results is not written, possibly because of some error with the buckling analysis. As the stress levels are too high, a decrease of mass must be done to the model so that the values will decrease.

- **Parametric Study of Model 2 with load case 3**

This time there is a need for stiffening the model, so that the stress levels decrease to valid levels. Also the maximum displacement seems too high, so increased rigidity is needed, which can also be concluded by observing the plot of Elastic Energy of deformation. Furthermore, the weight of the model will have to increase. The way of changing the model was:

- the skin thickness increased to 1,5 mm;
- the doubler thickness increased to 4 mm;
- the number of stringer above cut-out increased to 5;
- the edge frame thickness to 1,5 mm;
- the stringer web height increased to 50 mm;
- the stringer flange width increased to 30 mm.

Having run an analysis with all of these changes, the obtained plots of the variation of the quantities to the variation in cut-out's width are in Figure 62 and with the door height in Figure 63.

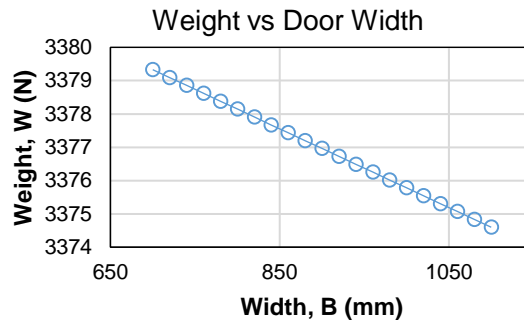
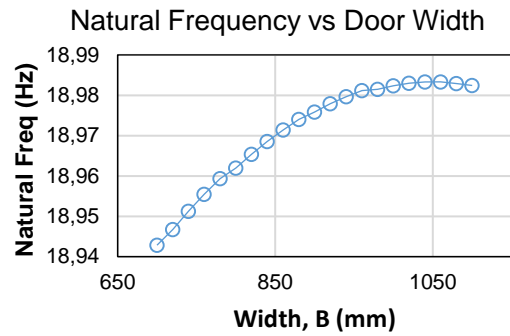
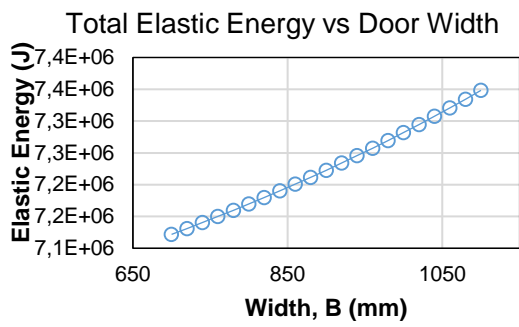
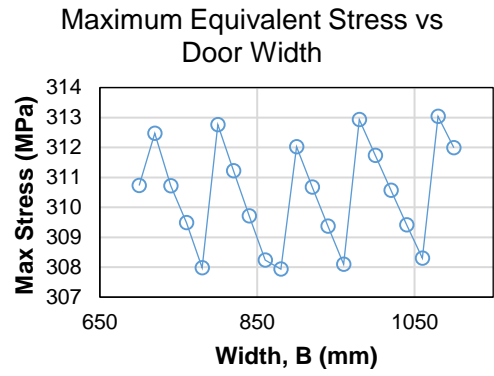
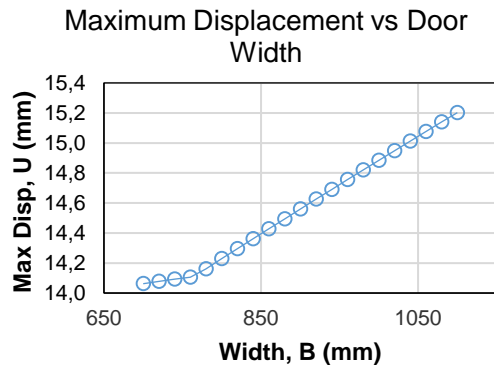


Figure 62 - Variation of B for version 2 (mv2om.mac).

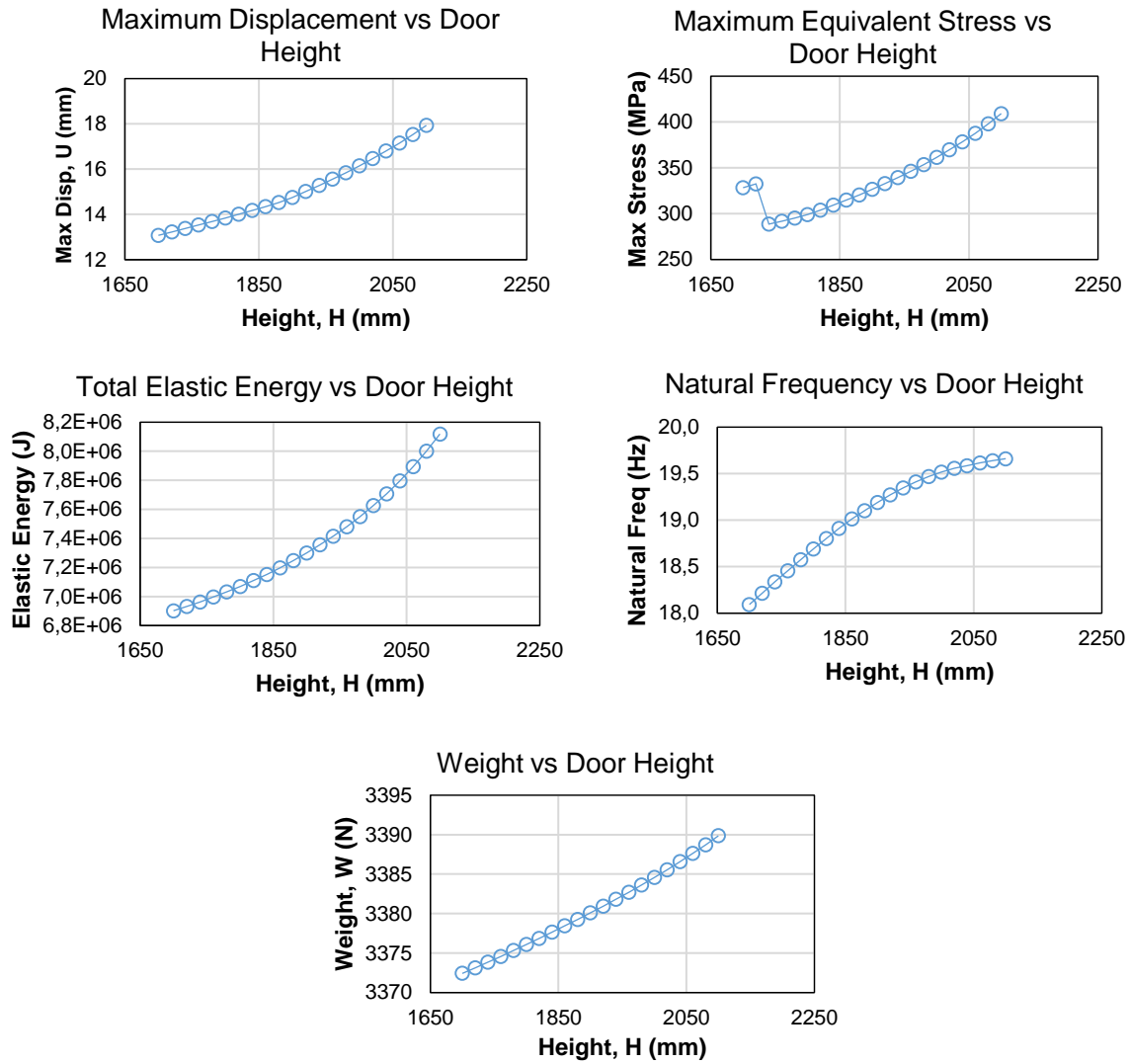


Figure 63 - Variation of H for version 2 (mv2om.mac).

It seems that for a configuration of ($B = 810$ mm, $H = 1740$ mm), the highest stress is below the materials strength ($S_{max} = 288,6$ MPa), being this the only configuration, from the choices made, that fulfils the strength constraint. Another variation of the width was done using this value, so one optimised configuration could be reached for the case of internal pressure and bending moment applied. The plot of the stress is in Figure 64.

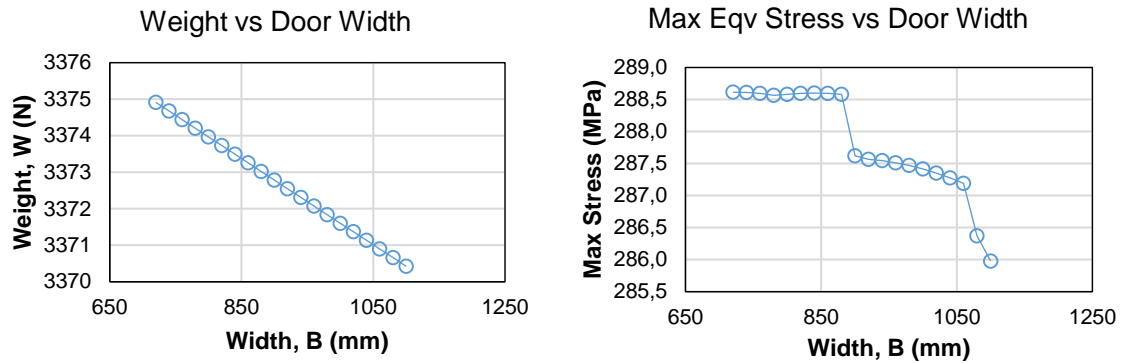


Figure 64 - Stress plot of the altered version of the model (version 2, mv2om.mac).

Choosing the best configuration based on the strength of the structure, the one with less weight will be chosen, because the stress decreases with the door width.

Table 12 - Chosen configuration for a structure subject to pressurisation and bending moment.

Variable	Value
Width, B	1100 mm
Height, H	1740 mm
Weight, W	3370,42 N
Maximum Stress	285,98 MPa
Maximum displacement	14,31 mm
Total elastic energy	7122,80 KJ
Natural frequency	18,52 Hz

A final discussion must be done concerning the obtained results. Even having optimized configurations, these are for each of the parameters, fixing one of the other. The advantage of a Sensitivity Analysis to the design comes from varying more than one parameter at the same time and changing the configuration for each of the points (B,H) to satisfy the design constraints. According to Sobieszczanski-Sobieski, “a parametric study determines a function character over the entire range of interest and tells whether extrema exist and where they are located, but it does that for one variable at a time at the price of solving the system at discrete points within that range (...). Sensitivity Analysis provides the function slope information at a single point but may do it for all n design variables at hand while solving the system only once.” ([10], pg. 1000). In the next section of this work an attempt to implement a Sensitivity Analysis of this type using the Finite Differences Method is made.

5.2 Finite Differences

A routine in MATLAB was created to calculate the derivatives of the function of interest, the weight, and the constraint function, the von Mises Stress, in order to the design variables, the width, B, and the Height, H. The calculation of derivatives is only possible if a smooth function exists, which does not happen with version 1, due to the discontinuities in the plots relative to the height. The design variables were varied in their own range, with increments of 50 mm. For each configuration, the derivative of the interest functions were evaluated, making a total of $m \times n = 9 \times 6 = 54$ points. Using Forward Differences, the number of analyses was then $m \times n \times 3$, because for each pair (B, H) two more points must be calculated. With Central Differences, the number of analyses would jump to $m \times n \times 3 \times 2$.

The analysis was performed with version 2 of the model and for the 1st load case (Internal pressure), using the Forward Difference Scheme. It took 2 hours and 30 minutes in total, using a PC Intel® Core™ i7-4700MQ CPU @ 2,40GHz and 8Gb RAM.

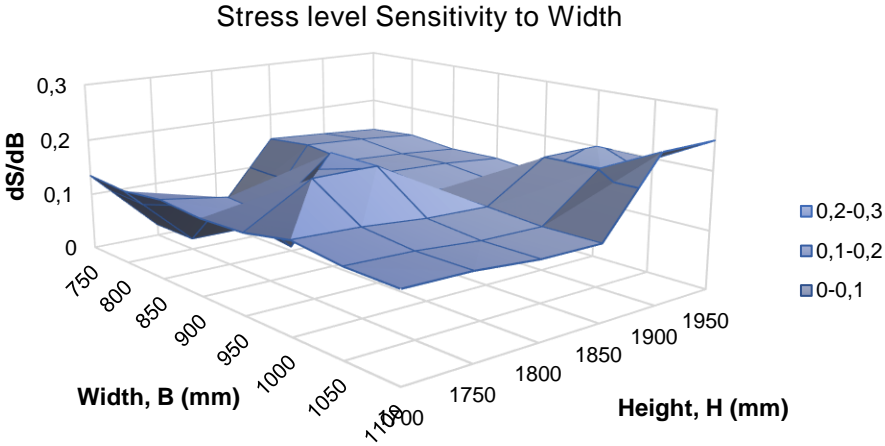


Figure 65 – Sensitivity of the maximum stress to the width, for each configuration

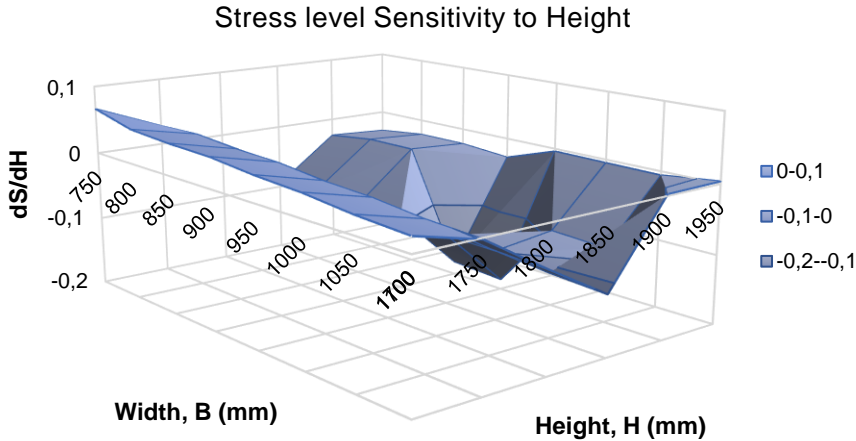


Figure 66 – Sensitivity of the maximum stress to the height, for each configuration

Observing the obtained sensitivity of the weight to changes in the studied parameters, the important conclusion to take is that for each increase of the width of the cut-out, the weight will always decrease.

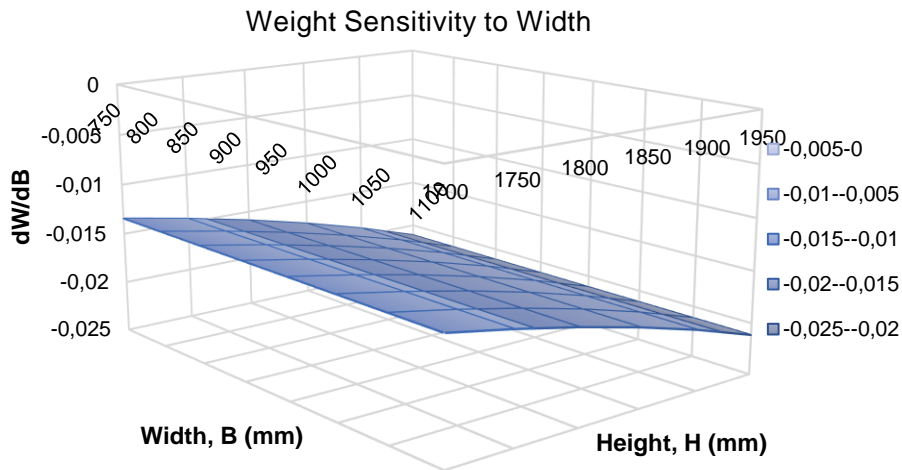


Figure 67 – Sensitivity of the weight to the width, for each configuration

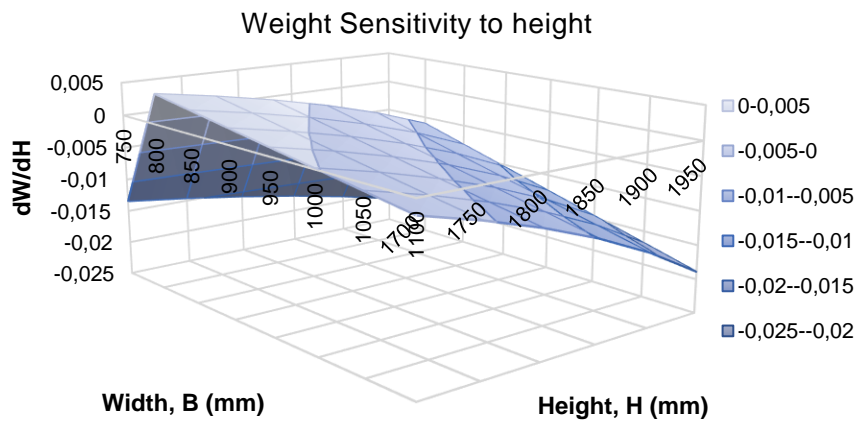


Figure 68 – Sensitivity of the weight to the height, for each configuration

Figures 67 and 68 are interpreted as the obtained derivatives $\frac{dW}{dB}$ and $\frac{dW}{dH}$ for each point (B,H). Observing the plots, one can conclude that the weight always decreases with an increasing variation in the width, but the same does not happen for the variation in height with the same sign. In the range approximately between 800 mm and 1000 mm, for H = 1100 mm, the variation is positive, meaning that the weight is increasing. The information contained in these plots created after calculating Finite Differences could be obtained also observing the overall change of the weight and the stress versus both parameters. These plots are shown in Figures 69 and 70.

The results from all of these plots are inconclusive relatively to the sensitivity of the weight, because they take into consideration the calculation of the door mass, which may not be right. Furthermore, for a comparison between the weight of structures that fulfil the design constraints for each dimension of the cut-out, a manual or automatic optimisation based on adding of removing material to the structure should be done, a task that is left to a further work.

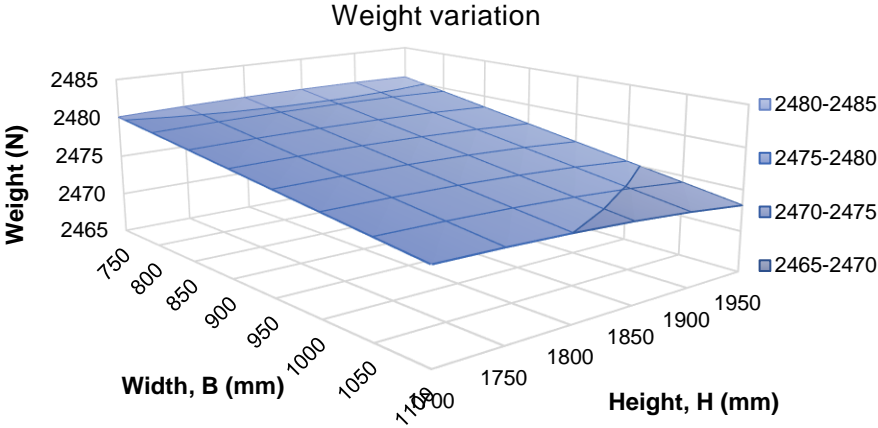


Figure 69 – variation of the weight with both variables (mv2s.mac).

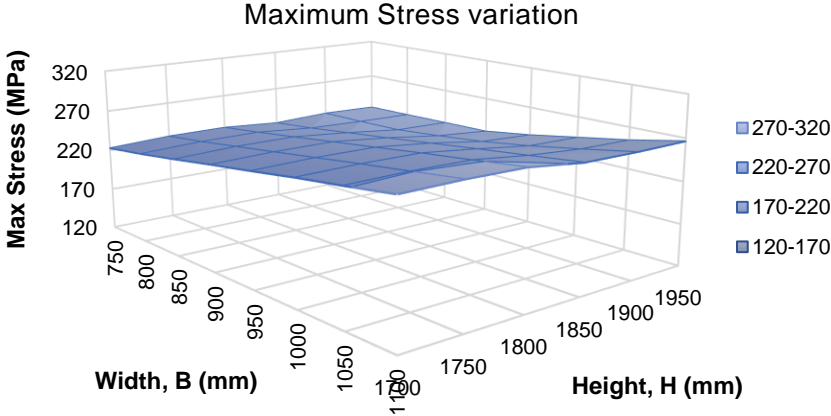


Figure 70 – variation of the maximum stress with both variables (mv2s.mac).

6. Conclusions and Further Work

A study was conducted using a fuselage section with a door cut-out with the goal of studying the sensitivity of the weight and other structural measures to the change in parameters of its surrounding structure. To accomplish this, two versions of a same structure were modelled. Both models were used to investigate the influence of door cut-out width and height on functions of interest. However, they offer possibilities to be changed for other parameters, which is the main reason why the model was constructed in Ansys APDL. To handle the data obtained in Ansys, all values of interest were written in *.txt* files and then read and saved in MATLAB.

For all the other variables fixed in their reference value, the structure was changed on these two parameters, first individually and then at the same time. For the first model, as the number of stringers is not fixed, the plots obtained when varying the door's height have discontinuities, though having the same monotony in each stretch. The second model did not present the same results for the same values of B and H because the spacing was chosen to be more uniform and dependent on the dimension of the cut-out. The fact that the number of elements is fixed makes all the functions more continuous and passive of being differentiated. The sensitivity of each parameter could then be obtained using Finite Differences.

The variation of the weight with the increase of the parameters is linear, making the task of calculating derivatives unworthy. However, this study could have been done for other quantities, whose variations are not linear. The behaviour of the material concerning its strength and stability is not straightforward and a more detailed study should be done in order to justify some of the results.

The studied model does of course not correspond to the reality, as the real geometries today are more complicated than the ones modelled. The door cut-out is not straight, having filleted corners, and each member has rivets and bolts along its length to be attached to other member. Also, a floor beam was not included, although it is an important part of this structure, as it provides support in X-direction. Nevertheless, in general the models capture some important features of the real structure.

Recommendations and Further Work

Being the present thesis incident in metallic fuselages, so the results only stand for these, it would be interesting to have the same study being implemented in a composite fuselage. Composite-made panels are used more and more in airplane structures, and a similar study will imply more design variables, e.g. in the case of laminates, the stacking sequence, the number, type and orientation of laminas.

Concerning the changes to the Finite Element model in APDL, what is suggested is:

- To model the cut-out with round corners, with the radius of the corner as a design variable: they normally have round corners to decrease the high stress concentrations in those zones; it would

be an advantage if the modelling took this feature into account, as also a fatigue analysis could be performed.

- To make the cross-section of the sills changeable along their length, like it is done in the intercostals;
- To add a floor to the model, below the door sill, so it would give more precise results;
- To allow for the choice for a double-bubble fuselage section;
- To include at least one window at one side of the door cut-out and investigate the influence of its presence and position in the behaviour of the structure;
- To include the door in the model.

As to the analyses, many possible studies can be implemented:

- The static and buckling analyses both were performed without non-linear effects (Hooke's law). A more general result would be obtained if these were included.
- Still on the Buckling analysis, a more detailed study is needed, as the results in this study were inconclusive;
- One of the main problems encountered in the door corners are fatigue cracks, which can occur for stress levels below the static loadings [4]. So it is also suggested a dynamic analysis that evaluates fatigue cracks and stress concentration factors;
- To have more accurate results in order to get realistic Sensitivity data for optimisation, a detailed load analysis of the fuselage is recommended.
- Finally, to account for other types of loads rather than only structural loads in an optimisation of the model – a multidisciplinary optimisation (MDO) – acoustic and thermal loads from other studies can also be included in the formulation of the problem.

The obtained results in each performed analysis represent trends in the studied quantities with the developed models. For some of the models and load cases, configurations were chosen based in “what-if” changes, followed by new parametric studies. The sensitivity of each function (the calculation of derivatives) would give information on the rate of change for each width or height alone, which can be used for a gradient-based optimisation, using for example the function *fmincon*, existent in MATLAB optimisation toolbox. A Sensitivity Analysis was attempted in the final section (5.2). These derivatives can be used to make a more complex optimisation, with two design variables, using only the material's strength as design constraint. An extension of this section can be for example calculating the sensitivities of the buckling factor and the maximum displacement, to changes in more than two design variables, and perform that work for the three load cases.

Regarding the methods, a comparison should be done between different methods for Sensitivity Analysis and for Optimisation. Using the developed models, other softwares rather than MATLAB can be used.

References

- [1] Niu, M. C. Y., "Airframe Structural Design", Jan 1999, Hong Kong : Hong Kong Conmilit Press Ltd., 2006. – ISBN 9627128090;
- [2] Niu, M., C. Y., "Airframe Stress Analysis and Sizing", 2nd edition, 1997, Hong Kong : Hong Kong Conmilit Press Ltd., 1999. – ISBN 9627128082;
- [3] Dream Airplanes: <https://engineering.purdue.edu/AAE450s/generaldesign/dream-airplane-systems-bias.pdf> (accessed 3/2/2018);
- [4] Heerschapp, M. E., "An Interactive Computer Aided Design for Cut-Outs in pressurized Aircraft Fuselages", TUDelft, Faculty of Aerospace Engineering, Delft, The Netherlands;
- [5] Van Tooren, M., Krakkers, L., "Multi-disciplinary Design of Aircraft Fuselage Structures", 45th AIAA Aerospace Sciences Meeting and Exhibit, 2007, Reno, Nevada;
- [6] Seeger, J., Wolfe, K., "Multi-objective design of complex aircraft structures using evolutionary algorithms", Proceedings of the Institution of Mechanical Engineers, Part G: Journal of Aerospace Engineering, Vol 225, Issue 10, pp. 1153 – 1164, First Published August 15, 2011;
- [7] Dexl, F., "Durchführung einer FEM-basierten Sensitivitätsanalyse wesentlicher Einflussgrößen auf Türumgebungsstrukturen von Flugzeugrümpfen", 2015, Institut für Luft- und Raumfahrttechnik, TUDresden, Germany;
- [8] Bruyneel *et al*, "Fuselage Structure Optimisation", Advances in Collaborative Civil Aeronautical Multidisciplinary Design Optimisation, Volume 233, Chapter 7, American Institute of Aeronautics and Astronautics;
- [9] Reinforcement of a Door-Cut-Out in a Pressurized Aircraft Fuselage: https://w3-mediapool.hm.edu/mediapool/media/fk03/fk03_lokal/temp/verschiedenes/rumpler_1/konws9900_1/konws9900.html;
- [10] Sobieszczanski-Sobieski, J., "Sensitivity Analysis and Multidisciplinary Optimisation for Aircraft Design: Recent Advances and Results", NASA Langley Research Center, Hampton, Virginia, Journal of Aircraft, vol 27, n°12, 1990;
- [11] Akgün, M. A. *et al*, "Efficient Structural Optimization for Multiple Load Cases Using Adjoint Sensitivities", AIAA Journal, vol 31, n°3, pp 511-516, March 2001;
- [12] DeHavilland Comet 1A: <http://www.c-and-e-museum.org/marville/photos/planes/comet-105b.jpg>;
- [13] Achternbosch, M., *et al*, "Stoffstromanalysen zum Einsatz von carbonfaserverstärkten Kunststoffen im Flugzeugbau", Technikfolgenabschätzung in Theorie und Praxis Nr 1, 11, pp 41-50, March 2002.
- [14] The Yak-152 trainer aircraft features monocoque fuselage. Courtesy of Eas4200c.f08.nine.o. Source: airforce-technology.com (accessed on 23-10-2018);

- [15] Megson, T. H. G., "Aircraft Structures for Engineering Students", 4th version, Elsevier Science and Technology, first published 2007 - ISBN-10: 0-750-667397
- [16] FAA Advisory Circular, Subject: fuselage doors and hatches, AC 25.783-1A, 25/04/2005;
- [17] FAA FAR Part 25 C - Airworthiness Standards: Transport Category Airplanes, Federal Aviation Administration.
- [18] EASA CS-25 Large airplanes, Sub-part C;
- [19] ANSYS 18.2 Student Documentation;
- [20] Roylance, D., "Pressure Vessels," Department of Materials Science and Engineering, Massachusetts Institute of Technology, MIT OpenCourseWare, August 23, 2001;
- [21] Teixeira-Dias, F., et al, "Método dos Elementos Finitos – Técnicas de Simulação Numérica em Engenharia", 2010, Lidel – Edições Técnicas, Lda., Mafra;
- [22] MSc Nastran 2017 – "Design Sensitivity and Optimisation User's Guide", MSc Software, 2016;
- [23] Arora, J. S., Haug, E. J., "Methods of Design Sensitivity Analysis in Structural Optimisation", AIAA Journal vol 17, nº 9, pp 970-974, Iowa, 1990;
- [24] Ansys coordinate systems: http://www.ansys.stuba.sk/html/guide_55/g-mod/gmod3.htm
- [25] Aluminium 2024-T3 Specifications (Matweb):
<http://www.matweb.com/search/DataSheet.aspx?MatGUID=57483b4d782940faaf12964a1821fb61>
- [26] "A320 - AIRCRAFT CHARACTERISTICS AIRPORT AND MAINTENANCE PLANNING", Airbus, Issue of 30/September/1986, Revised in 15/May/2017.
- [27] Şen, İlhan, "Aircraft Fuselage Design Study", Master Thesis, TuDelft, Netherlands, 10/12/2010;
- [28] Nelson, T., Wang, E., "Reliable FE-Modeling with ANSYS", CADFEM GmbH, Munich, Germany
- [29] Harris, T., "A New Connection: MPC184 Elements", The Focus, issue 19, PADT, Inc., 2002
- [30] https://www.sharcnet.ca/Software/Ansys/17.0/en-us/help/ans_elem/Hlp_E_MPC184link.html (accessed 1/11/2017)
- [31] Imaoka, S., "ANSYS.NET Tips and Tricks: CERIG vs RBE3, RIGID184", Ansys.net Tips and Tricks Newsletter, issue of July 7, 2002.

Appendix

A.1 mv2s.mac

```
! Parametric Fuselage Section v2 - stringer spacing prescribed by N.er of Stringers below cut
! * The pitch is different above, below the cut-out and in the lateral (cut-stringers)
! * spacing is regular inside each part
! * the n.er of stringers is fixed in every part

FINISH
/CLEAR,START
/batch
/PREP7

/UNITS,MPA                ! Units system (mm, ton, MPa, ...)
mm = 25.4                 ! 1 inch = 25,4 mm
*AFUN,DEG                ! change angular data from radians to degrees
PI = 3.14
g = 9.81                  ! m/s^2
size = 30                 ! size of elements (only goes until 30mm due to Student version)

! Input file
*ULIB,'param_file'.txt
PARRES,CHANGE,param_file.txt ! reads input from user (text parameter file in the same directory of this
macro)
tam = size

!-----
!                ** DIMENSIONS **

! Skin
b_s = 3600                ! Skin Width
r_s = 1975                ! Skin Radius (D=3950 m)
t_s = 1                   ! Skin Thickness (FIXED) (range: 1-2 mm)

! Cutout
b_c = 810                 ! (Type I)
h_c = 1850                ! Cutout Width (VARIABLE) (range: 0.700-1.100 m)
beta = acos((r_s-1660)/r_s) ! Cutout Height (VARIABLE) (range: 1.700-2.200 m)
beta2 = beta-10          ! Cutout Position counting with doublers from lowest line (FIXED VALUE)
delta = 90-beta          ! Cutout Position without doublers from lowest line (skin line)
h_c_l = sin(delta)*r_s   ! Cutout Position below the CSYS,0 line (counting with doublers)
h_c_u = h_c-h_c_l        ! (delta projected in YZ plane (mm) )
alpha = asin(h_c_u/r_s)  ! Cutout position counting with doublers from the CSYS,0 line (mm)
alpha2 = alpha+10        ! (h_c_u in the cylindrical coordinate system (°))
phi = 90-alpha           ! Cutout Position without doublers from CSYS,1 line (skin line)
gamma = alpha+delta      ! Cutout Height in °
cp = b_s/2-b_c/2         ! Cutout position in Z (edge-frame distance to origin of Z)
cen = b_s/2              ! Z-position of Center of cutout
cen_yy = 180-(gama/2-delta) ! Y-position of Center of cutout in °
cen_y = sin(gama/2-delta)*r_s ! (in mm)
ATurX = b_c*h_c
x_u = -cos(alpha)*r_s
x_l = -cos(delta)*r_s
ATurY = b_c*abs(x_u-x_l)
ATur = (gama/180)*PI*r_s*b_c ! (mm^2)

! stringers
n_str = 10                ! N.er of Stringers below cut (FIXED)
n_stru = 4                ! N.er of Stringers above and lateral to cut (FIXED) (total: 24 on each side)
b_str = 20                ! Stringer base width
h_str = 35                ! Stringer web height
```

```

t_str = 1                ! Stringer web and flange thickness
s_str = beta/n_str      ! Stringer spacing/pitch below cut-out
s_strc = gama/n_str    ! Stringer spacing/pitch in cut-stringers
s_stru = phi/n_stru    ! Stringer spacing above cut-out

! frames
n_fra = 3                ! N.er of main frames (on each side) (FIXED)
b_fra = 35               ! Frame base width
h_fra = 100              ! Frame web height
t_fra = 1.2              ! Frame web and flange thickness
s_fra = (cp-2*t_fra)/n_fra ! Frame spacing/pitch (now: 415 mm) (dist do cutout - 2*espesura)/n_fra
s_fra2 = (b_c-2*b_fra)/3 ! Frame spacing above and below cut

! Edge Frames
b_ef = 50                ! Edge Frame Width
h_ef = 120               ! Edge Frame Height
t_ef = 1.2               ! Edge Frame Thickness

! doubler
b_d_deg = 5              ! Doublers Width
b_d = abs(sin(b_d_deg))*r_s ! (in mm)
h_d_deg = 5              ! Doublers Height
h_d = abs(sin(h_d_deg))*r_s ! (in mm)
t_d = 3                  ! Doublers thickness

! sills
b_si = 50                ! Sill Width (mm)
h_si = 100               ! Sill Height (mm)
t_si = 1.5               ! Sill Thickness (mm)

! intercostals
b_l = b_str              ! Intercostal base width (now with dimensions of stringers)
t_l = t_str              ! Intercostal thickness (now with dimensions of stringers)

! Loads
IntPres = 1.33*61500e-6 ! cabin pressure p=61500 N/m^2 = 61500e-6 MPa
Fz = (1/2)*IntPres*r_s*r_s*PI ! normal force due to bulkheads
FdsX = IntPres*ATurX    ! force exerted on door-stops (X-component)
FdsY = IntPres*ATurY    ! force exerted on door-stops (Y-component)
! (from van Tooren)
Fy = (1/2)*600000        ! Vertical Shear Force, FY=600.000 N
Mx = (1/2)*4400000000    ! Bending Moment, MX=4.400.000 N

```

```

=====
! ** MATERIAL **           ! from MatWeb !MPLIST,ALL,,,EVL

```

```

!Aluminum 2024-T3 Properties
E = 73.1e3                ! MPa
rho = 2780*1e-12         ! ton/mm^3
niu = 0.33

MPTEMP,1,0
MPDATA,EX,1,,E           ! Youngs Modulus, E (73.1 GPa)
MPDATA,PRXY,1,,niu      ! Poisson Coeficient (0.33)
MPDATA,DENS,1,,rho      ! Density (2.78 g/cm3)

```

```

=====
! ** MESH ATTRIBUTES **

```

```

! Definition of elements -----

```

```

ET,1,SHELL181            ! Skin
ET,2,BEAM188             ! Stiffeners
/NERR,,,,,0              ! tells ANSYS not to terminate a batch job on an error
ET,3,MASS21              ! Structural mass for use of Coupling Equations (CERIG or RBE3)

```

! Shell and Beam Section properties-----

CSYS,0
 strl=3
 stru=4
 frame=5
 ef=6
 fm=7
 efm=8
 sillu=9
 silll=10
 int=13
 intrm=16
 du=2
 dl=17

! Skin
 SECT, 1, SHELL,, skin ! SHELL (number, type, , name)
 SECOFFSET,USER,t_s/2 ! Offset defined by user (mid - midplane of the section)
 SECDATA,t_s,1,0,3 ! thickness + n^o layers + integration points
 seccontrol,,,, , , ,

! Doubler location (skin+doubler)
 SECT, du, SHELL,, doub
 SECOFFSET,USER,t_d/2 ! (t_d-t_s = 5-1.5 = 3.5)
 SECDATA,t_d,1,0,3
 seccontrol,,,, , , ,

! Doubler for lower part
 SECT, dl, SHELL,, doub
 SECOFFSET,USER,t_d/2!-t_s ! (t_d-t_s = 5-1.5 = 3.5)
 SECDATA,t_d,1,0,3
 seccontrol,,,, , , ,

! Lower Stringers
 SECTYPE, strl, BEAM, Z, Str,0 ! BEAM (number, type, profile, name)
 SECOFFSET,USER,-(b_str+t_str/2),-t_s-t_str/2 ! Offset: Y,Z coord of the section CSys to tell where to start
 section from the meshed line
 SECDATA,b_str,b_str,h_str,t_str,t_str ! (widths, height, thicknesses)

! Upper Stringers
 SECTYPE, stru, BEAM, Z, Str,0
 SECOFFSET,USER,b_str+t_str/2,-t_s-t_str/2
 SECDATA,b_str,b_str,h_str,t_str,t_str

! Frame
 SECTYPE, frame, BEAM, Z, Fra,0
 SECOFFSET,USER,b_fra+t_fra/2,-t_s-t_fra/2
 SECDATA,b_fra-t_fra/2,b_fra-t_fra/2,h_fra,t_fra,t_fra,t_fra

! Edge Frame
 SECTYPE, ef, BEAM, CHAN, EFra,0
 SECOFFSET,USER,-(t_ef/2),-t_s-t_ef/2
 SECDATA,b_ef,b_ef,h_ef,t_ef,t_ef,t_ef

! Edge Frame after mirror
 SECTYPE, efm, BEAM, CHAN, EFra,0
 SECOFFSET,USER,(t_ef/2),-t_s-t_ef/2
 SECDATA,b_ef,b_ef,h_ef,t_ef,t_ef,t_ef

! Frame after mirror
 SECTYPE, fm, BEAM, Z, Fra,0
 SECOFFSET,USER,-(b_fra+t_fra/2),-t_s-t_fra/2
 SECDATA,b_fra-t_fra/2,b_fra-t_fra/2,h_fra,t_fra,t_fra,t_fra

! Upper Sill

```

SECTYPE, sillu, BEAM, CHAN, Sill,0
SECOFFSET,USER,0,-t_s-t_si/2
SECDATA,b_si,b_si,h_si,t_si,t_si,t_si

! Lower Sill
SECTYPE, silll, BEAM, CHAN, Sill,0
SECOFFSET,USER,0,-t_s-t_si/2
SECDATA,b_si,b_si,h_si,t_si,t_si,t_si

! Intercostal init                                     ! bigger height (Tapered beams)
SECTYPE, 11, BEAM, Z,Int, 0
SECOFFSET, USER,-(b_str+t_str/2),-t_s-t_str/2
SECDATA,b_l,b_l,h_str,t_l,t_l,t_l
! Intercostal end                                     ! lower height (Tapered beams)
SECTYPE, 12, BEAM, Z,Int, 0
SECOFFSET, USER,-(b_str+t_str/2),-t_s-t_str/2
SECDATA,b_l,b_l,h_ef,t_l,t_l,t_l
SECTYPE, int, TAPER,
SECDATA, 11,0,0,2*s_fra,
SECDATA, 12,0,0,cp,
! initial section position (Sec_IDn, XLOC, YLOC, ZLOC)
! end section position

! Intercostal after mirror init                       ! bigger height (Tapered beams)
SECTYPE, 14, BEAM, Z,Int, 0
SECOFFSET, USER,b_str+t_str/2,-t_s-t_str/2
SECDATA,b_l,b_l,h_str,t_l,t_l,t_l
! Intercostal after mirror end                       ! lower height (Tapered beams)
SECTYPE, 15, BEAM, Z,Int, 0
SECOFFSET, USER,b_str+t_str/2,-t_s-t_str/2
SECDATA,b_l,b_l,h_ef,t_l,t_l,t_l
SECTYPE, intm, TAPER,
SECDATA, 14,0,0,b_s-2*s_fra,
SECDATA, 15,0,0,b_s-cp,
! initial section position (frame)
! end section position (edge frame)

! Visualization -----

/PNUM,KP,1
/PNUM,LINE,1
/PNUM,AREA,1
/PNUM,NODE,1
! NUMERACAO Keypoints
! Lines
! Areas
! Nodes

!/VIEW,1,1,1,1
!/VIEW,1,,,1
/VIEW,1,1
! isometric
! taleral (front)
! front (lateral)
/ANG,1
/REP,FAST

! Elements
/SHRINK,0
/ESHAPE,1
/EFACET,1
/RATIO,1,1,1
/CFORMAT,32,0
! No shrinkage (não encolhe os elementos)
! Beam elements with cross section visible
! Element facets
! No distortion of the model's geometry

=====
! ** MODELLING **

CSYS,1

K,1,0,0,0,
K,2,0,0,b_s
! axis right extremity
! axis left extremity

! Orientation KPs
K,,0,0,s_fra
K,,0,0,2*s_fra
K,,0,0,cp

```

```

K,,0,0,cp+s_fra2          ! for cut-frames, s_fra2 = (b_c-2*b_fra)/3 (2 frames above and below the cut)
*GET,ori_f,KP,0,NUM,MAXD

! Orientation KPs for mirrored part
K,,0,0,b_s-s_fra
K,,0,0,b_s-2*s_fra
K,,0,0,b_s-cp
K,,0,0,b_s-cp-s_fra2
*GET,ori_fm,KP,0,NUM,MAXD

!UPPER PART

K,11,r_s,90,0             ! 7 KP
K,12,r_s,90,s_fra
K,13,r_s,90,2*s_fra
K,14,r_s,90,cp-b_d       ! doubler
K,15,r_s,90,cp           ! cutout
K,16,r_s,90,cp+s_fra2    ! cut frame
K,17,r_s,90,b_s/2        ! middle
*GET,Ks,KP,0,NUM,MAXD
L,11,12                   ! 6 lines
*GET,first_u,LINE,0,NUM,MAXD
L,12,13
L,13,14
L,14,15
L,15,16
L,16,Ks

! Stringer mesh attributes
LSEL,S,LOC,Y,90           ! select lines at ang=90 deg (1st stringer)
LREVERSE,all             ! Change the lines' axis orientation
LATT,1,,2,,1,,stru       ! STRINGER: mat=5(stringer), element type=2(beam188), orientation KP=1,
sectype=

! loop to create all upper areas
auxu=0
*DO,i,1,n_stru-1         ! until stringer number n_str
  ! Areas
  LSEL,S,LOC,Y,90+auxu*s_stru ! only the five horizontal lines created
  AROTAT,ALL,,,,,1,2,s_stru ! create areas with stringer spacing dimension
  ! Mesh attributes
  *GET,lin,LINE,0,NUM,MAXD
  LSEL,,,,lin-12,lin-7    ! select only the horizontal lines              7 lines
  LATT,1,,2,,1,,stru      ! STRINGER: mat=1, element type=2(beam188) sectype=9(Z)
  auxu=auxu+1
*ENDDO
*GET,kp1,KP,0,NUM,MAXD    ! last created KP (of last lines)
*GET,y_1,KP,kp1,LOC,Y     ! y-location in csys,1
*GET,last_u,LINE,0,NUM,MAXD ! last created line number
last_u=last_u-12          ! 1st line of last stringer
! Skin mesh attributes
ASEL,all                  ! select the areas just created
AATT,1,,1,0,1            ! SKIN: mat=1, element type=1(shell181) sectype=1
allsel

! Doubler
allsel
LSEL,,,,last_u,last_u+5   ! picks last upper stringer
AROTAT,all,,,,,1,2,s_stru-h_d_deg ! distancia do stringer ao doubler (supostamente = ao dist1 no mv1)
*GET,d_u,LINE,0,NUM,MAXD
*GET,d_k_u,KP,0,NUM,MAXD
*GET,y_au,KP,d_k_u,LOC,Y  ! coord cilindricas
dist1=y_au-y_1           ! distancia do stringer ao doubler (N DEVO PRECISAR DISTO)
d_u=d_u-7
*GET,area1,AREA,0,NUM,MAXD
ASEL,,,,area1-5,area1    ! SKIN

```

```

AATT,1,,1,0,1

! Sill
LSEL,,,,d_u-5,d_u
LATT,1,,1,0,du           ! Doubler element
AROTAT,all,,,,,1,2,h_d_deg   ! part of this will have doubler attributes and part with skin attributes (at
end creates sill line)
! Sill, doubler and skin mesh attributes
sill_u=d_u+13             ! SILL (upper)
*GET,area2,AREA,0,NUM,MAXD
ASEL,,,,area2-5,area2-3     ! SKIN
AATT,1,,1,0,1
ASEL,,,,area2-2,area2       ! DOUBLER
!AREVERSE,all
AATT,1,,1,0,du
LSEL,,,,sill_u-5,sill_u     ! Com isto o conjunto de linhas que eram um stringer (mat=5) passou a
ser o upper sill
LATT,1,,2,,1,,sillu        ! UPPER SILL
*GET,si_k,KP,0,NUM,MAXD
*GET,y_su,KP,si_k,LOC,Y     ! (in °)
allsel

!LOWER PART

K,,r_s,-90,0
K,,r_s,-90,s_fra
K,,r_s,-90,2*s_fra
K,,r_s,-90,cp-b_d           ! doubler
K,,r_s,-90,cp               ! cut-out edge
K,,r_s,-90,cp+s_fra2       ! cut-frame
K,,r_s,-90,b_s/2           ! centre
*GET,Ks,KP,0,NUM,MAXD
L,Ks-6,Ks-5
*GET,first_l,LINE,0,NUM,MAXD
L,Ks-5,Ks-4
L,Ks-4,Ks-3
L,Ks-3,Ks-2
L,Ks-2,Ks-1
L,Ks-1,Ks

! Stringer mesh attributes
LSEL,S,LOC,Y,-90,         ! lines at ang=-90 deg (1st stringer)
LREVERSE,all              ! Change the lines' axis orientation
LATT,1,,2,,1,,strl       ! mat=1, element type=2(beam188), orientation_KP=1, sectype=3(Z)

! loop to create all lower areas
auxl=0
*DO,i,1,n_str-1           ! until stringer number n_str
  ! Areas
  LSEL,S,LOC,Y,-90-auxl*s_str ! only the five horizontal lines created
  AROTAT,ALL,,,,,2,1,s_str   ! create areas with stringer spacing dimension
  ! Mesh attributes
  *GET,lin,LINE,0,NUM,MAXD
  LSEL,,,,lin-12,lin-7       ! select only the horizontal lines           7 lines
  LATT,1,,2,,1,,strl        ! STRINGER: mat=1, element type=2(beam188) sectype=9(Z)
  LSEL,,,,lin-6,lin         ! select only the vertical lines
  LREVERSE,all
  auxl=auxl+1
*ENDDO
*GET,kp2,KP,0,NUM,MAXD     ! last created KP (of last lines)
*GET,y_2,KP,kp2,LOC,Y     ! y-location in csys,1
*GET,last_l,LINE,0,NUM,MAXD ! last created line number
last_l=last_l-12          ! 1st line of last stringer
ASEL,all                  ! select the areas just created
AATT,1,,1,0,1             ! SKIN: mat=1, element type=1(shell181) sectype=1

```

```

! Doubler
allsel
LSEL,,,last_l,last_l+5           ! picks last lower stringer
AROTAT,all,,,,,2,1,s_str-h_d_deg ! distancia do stringer ao doubler (supostamente = ao dist1 no mv1)
*GET,d_l,LINE,0,NUM,MAXD
*GET,d_k_l,KP,0,NUM,MAXD
*GET,y_al,KP,d_k_u,LOC,Y         ! coord cilindricas
dist3=y_al-y_2                   ! distancia do stringer ao doubler
d_l=d_l-7
*GET,area3,AREA,0,NUM,MAXD
ASEL,,,area3-5,area3            ! SKIN
AATT,1,,1,0,1

! Sill
LSEL,,,d_l-5,d_l                ! pega na ultima linha criada no pattern - um stringer - e faz a área que
                                ! ainda é casca acima do doubler
LATT,1,,1,0,2                   ! Doubler element
AROTAT,all,,,,,2,1,h_d_deg
sill_l=d_l+13
*GET,area4,AREA,0,NUM,MAXD
ASEL,,,area4-5,area4-3          ! SKIN
AATT,1,,1,0,1
ASEL,,,area4-2,area4            ! DOUBLER
AREVERSE,all
AATT,1,,1,0,d_l
LSEL,,,sill_l-5,sill_l          ! SILL
LREVERSE,all
LATT,1,,2,,1,,sill_l
LSEL,,,sill_l-12,sill_l-6       ! pick the frames to change their orientation
LSEL,A,,sill_l+1,sill_l+7
LREVERSE,all
!*
*GET,sill_k,KP,0,NUM,MAXD
*GET,y_sl,KP,sill_k,LOC,Y
CSYS,0
*GET,y_sl_mm,KP,sill_k,LOC,Y     ! cota do lower sill em mm
CSYS,1
!dist2=y_2-y_al
dist2=y_sl-y_al

! CUT STRINGERS-----
CSYS,1

LSEL,,,sill_u-5,sill_u
lin=sill_u-2
*DO,i,1,n_str
  LSEL,,,lin-3,lin
  AROTAT,ALL,,,,,1,2,s_strc      ! create areas with stringer spacing dimension
  ! Mesh attributes
  *GET,lin,LINE,0,NUM,MAXD
  lin=lin-5
  LSEL,,,lin-3,lin-2            ! stringer
  !LREVERSE,all
  LATT,1,,2,,1,,str_l
  LSEL,,,lin-1,lin              ! intercostal
  !LREVERSE,all
  LATT,1,,2,,ori_f,,int
  *GET,area5,AREA,0,NUM,MAXD
  ASEL,,,area5-3,area5-1        ! skin
  AATT,1,,1,0,1
  ASEL,,,area5                  ! doubler
  !AREVERSE,all
  AATT,1,,1,0,2
*ENDDO
allsel

```

! MESH OF THE ELEMENTS OF THE RIGHT

! Left Frames mesh attributes

LSEL,S,LOC,Z,cp+s_fra2
LATT,1,,2,,ori_f,,frame ! CUT-FRAME: mat=1, element type=2(beam188) sectype=frame
LSEL,S,LOC,Z,cp
LATT,1,,2,,ori_f-1,,ef ! EDGE FRAME: mat=1, element type=2(beam188) sectype=edge frame
LSEL,S,LOC,Z,2*s_fra ! ADJACENT FRAME
LREVERSE,all
LATT,1,,2,,ori_f-2,,ef
LSEL,S,LOC,Z,s_fra ! 2nd FRAME
LATT,1,,2,,ori_f-3,,frame
LSEL,S,LOC,Z,0 ! 3rd FRAME
LATT,1,,2,,1,,frame

! Upper doubler

ASEL,,,,area2-2,area2 ! DOUBLER
AATT,1,,1,0,du

! Mirror -----

CSYS,1

! Cartesian Coord. Sist. n.er 11

numcmp,all
K,,0,0,b_s/2 ! center
K,,5,0,b_s/2 ! axis y
K,,r_s,90,b_s/2 ! axis z
*GET,k_sym,KP,0,NUM,MAXD
CSKP,11,0,k_sym-2,k_sym-1,k_sym,1,1
CSYS,11 ! cartesian coordinates

! Mirror

allsel
ARSYM,Z,all,, , ,0,0 ! only copies lines that are attached to areas
LSEL,,,,sill_u-5,sill_u
LSEL,A,,,,sill_l-5,sill_l
LSYMM,Z,all,,,,0,0 ! copia as linhas

! MESH OF THE ELEMENTS OF THE LEFT

CSYS,1

! Left Frames new mesh

LSEL,S,LOC,Z,b_s-cp-s_fra2 ! CUT-FRAME after mirror
LATT,1,,2,,ori_fm,,fm ! mat=1, element type=2(beam188) sectype=left frame
LSEL,S,LOC,Z,b_s-cp ! EDGE FRAME after mirror
LREVERSE,all
LATT,1,,2,,ori_fm-1,,efm ! mat=1, element type=2(beam188) sectype=left edge frame
LSEL,S,LOC,Z,b_s-2*s_fra ! adjacent Frame
LREVERSE,all
LATT,1,,2,,ori_fm-2,,efm
LSEL,S,LOC,Z,b_s-s_fra ! 2nd Frame
LATT,1,,2,,ori_fm-3,,fm
LSEL,S,LOC,Z,b_s ! 3rd Frame
LATT,1,,2,,2,,fm

! Stringers and Intercostals new mesh ! STRINGERS

LSEL,S,SEC,,strl ! (lower)
LSEL,A,SEC,,stru ! (upper)
LSEL,R,LOC,Z,b_s/2,b_s ! Stringers after mirror
LREVERSE,all
LATT,1,,2,,1,,stru ! mat=1, element type=2(beam188), orientation KP=1, sectype=upper stringer

```

LSEL,R,LOC,Y,-90,-180      ! Down
LATT,1,,2,,1,,strl        ! mat=1, element type=2(beam188), orientation KP=1, sectype=lower
                             ! stringer
LSEL,S,SEC,,int           ! pick the INTERCOSTALS (new current set)
LSEL,R,LOC,Z,b_s/2,b_s    ! Intercostals after mirror
LSEL,R,LOC,Y,90,180       ! Intercostals (upper)
LREVERSE,all
LATT,1,,2,,1,,intm        ! tapered beam
LSEL,S,SEC,,int           ! pick the INTERCOSTALS (new current set)
LSEL,R,LOC,Z,b_s/2,b_s    ! Intercostals after mirror
LSEL,R,LOC,Y,-90,-180     ! Intercostals (lower)
LATT,1,,2,,1,,intm

! Sills new mesh
LSEL,,SEC,,sillu          ! SILLS (upper)
LSEL,R,LOC,Z,b_s/2,b_s    ! sills after mirror
LREVERSE,all
LATT,1,,2,,1,,sillu
LSEL,,SEC,,silll          ! SILLS (lower)
LSEL,R,LOC,Z,b_s/2,b_s    ! sills after mirror
LREVERSE,all
LATT,1,,2,,1,,silll      ! mat=1, element type=2(beam188), orientation KP=1, sectype=lower sill

```

```

!-----
!                               ** MESHING **

```

```

allsel
nummrg,KP
LSEL,S,type,,2           ! only the lines with element type 2 (beams...)
LESIZE,all,tam,,,,,1
MSHKEY,1
LMESH,all

ASEL,all
AMESH,all
/title,Half of a fuselage section with a cut-out
allsel
/PNUM,NODE,0
EPLOT
*GET,eNum,ELEM,,COUNT   ! Counts number of elements, eNum

/VIEW,1,1,1,1           ! isometric view
/ANG,1
/REP,FAST

!/eshape,0
!/NORMAL,1,1            ! to visualize shell normals (and check the pressure distribution)
/REPLOT

csys,1
asel,,LOC,Y,-90,-180+delta
asel,R,SEC,,1
areverse,all

```

```

!-----
!                               ** BOUNDARY CONDITIONS AND LOADS **

```

```

Lcase = L
AType = A

! boundary conditions -----
! Displacements: UX, UY, UZ
CSYS,1                   ! Rotations: ROTX, ROTY, ROTZ
allsel                   ! 3D model - 6 dofs constrained

! BC at y=90 (upper line)
LSEL,,LOC,Y,90

```

```

DL,all,,UY,0          ! horizontal and vertical constraints
DL,all,,SYMM          ! symmetry in lowest line

! BC at y=-90 (lower line)
LSEL,,LOC,Y,-90
DL,all,,SYMM          ! symmetry in lowest line

! BC at z=b_s (left edge)
LSEL,,LOC,Z,b_s
DL,all,,UZ,0          ! axial constraint
IDL,all,,UY,0         ! clamped end

! loads -----

CSYS,1

! LOAD CASE 1: Cabin Pressurisation

!internal pressure on skin
asel,all              ! select all areas (skin+doubler)
SFA,all,1,PRES,IntPres

!force due to pressure on door
! Masternode
numcmp,all
K,,r_s,cen_yy,b_s/2
*GET,ks2,KP,0,NUM,MAXD
KSEL,,,ks2            ! (K,,r_s,cen_yy,b_s/2)
R,1,1,1,1,0.5,0.5,0.5, ! Real constant set (=1), to be used by masternode
TYPE,3
REAL,1
KMESH,ks2
masternode = NODE(r_s,cen_yy,b_s/2) ! node n.er 4124, element n.er 4103
! create the RBE3 elements          ! RBE3: Force-distributed constraint
LSEL,,sec,,int          ! select intercostals
LSEL,A,sec,,intm
KSL,S                  ! select keypoints of intercostals
KSEL,R,loc,Z,cp,cp+b_c ! select only keypoints at the edge of the cut-out
NSLK,S                 ! slave nodes
NSEL,A,NODE,,masternode ! masternode
RBE3,masternode,ALL,ALL,,
allsel
! apply the loads to the masternode
F,masternode,Fx,-FdsX  ! (Fds = IntPress*ATur)
F,masternode,Fy,FdsY

!longitudinal force due to pressure on bulkheads
! Creation of rigid region through MPC
CSYS,1
allsel
*GET,Nnodes,NODE,0,Count,
N,Nnodes+1,0,0,0       ! creation of node at centre of right edge
!N,Nnodes+1,0,0,-500  ! creation of node at a distance from the edge
masternode = Nnodes+1  ! updates the value of the masternode
NSEL,,LOC,Z,0
NSEL,R,LOC,X,r_s
*GET,n_edge,NODE,0,Count,
NSEL,A,,,masternode
nmast_ = masternode
*USE,mpc_gen.mac       ! Creates rigid beams (CHECK FILE mpc_gen.mac)
INSEL,A,LOC,Z,0

F,masternode,Fz,-Fz    ! Axial force applied in the 'master' node
!F,masternode,Fy,-Fy  ! Vertical force

```

!F,masternode,Mx,Mx

! Bending moment in x

!-----
! ** ANALYSIS **

FINISH
CSYS,0
/SOLU

/RGB,INDEX,100,100,100,0 ! white background
/RGB,INDEX,80,80,80,13
/RGB,INDEX,60,60,60,14
/RGB,INDEX,0,0,0,15
/REPLOT

! Static Analysis-----

ALLSEL
ANTYPE,0
PSTRES,ON
SOLVE
FINISH

! POST-PROCESSING

/POST1
SAVE
/ESHAPE,0
/PNUM,NODE,0
/EFACET,1
/title,Static Analysis (von Mises Stress)
allsel
/GRAPHICS,FULL

! Nodal displacements
PLNSOL,U,SUM

*GET,Umax,PLNSOL,0,MAX,,
nset,all
nsort,U,SUM,1,0,,1
*GET,U_max,sort,0,MAX
*GET,U_max_n,sort,0,IMAX
/OUTPUT,Displacements.txt,'C:\Users\Ana Macedo\Dropbox\Tese\Interface' ,
PRNSOL,U,COMP
/OUT

! Para ver a tensão máxima no modelo todo

CSYS,0
nset,,loc,Y,h_c_u-30,h_c_u+5 ! canto superior esq
nset,r,loc,Z,cp+b_c-30,cp+b_c+30
CM,sing3,node
nset,,loc,Y,h_c_u-30,h_c_u+5 ! canto superior drt
nset,r,loc,Z,cp+30,cp-30
CM,sing4,node
nset,,loc,Y,-h_c_l+40,-h_c_l-5 ! canto inferior drt
nset,r,loc,Z,cp+30,cp-30
CM,sing5,node
nset,,loc,Y,-h_c_l+40,-h_c_l-5 ! canto inferior esq
nset,r,loc,Z,cp+b_c-30,cp+b_c+30
CM,sing6,node
nset,,loc,Y,h_c_u+30,h_c_u+100
nset,r,loc,Z,b_s-30,b_s
CM,sing7,node

```

CSYS,1
nsele,loc,Y,90,90+30          ! clamped top
nsele,r,loc,Z,b_s-30,b_s
CM,sing8,node

cmsele,all
nsele,inve
CSYS,0

! Nodal principal stresses in model
!/show,png
PLNSOL,S,EQV,0,1
!/show,close
!/sys,copy *.png C:\Users\Ana Macedo\Dropbox\Tese\Interface\images
*GET,Smax,PLNSOL,0,MAX,,,
nsele,S,EQV,1,0,,1          ! ETABLE,Smax,S,EQV
*GET,S_max,sele,0,MAX       ! tira o valor da tensão máx
*GET,S_max_n,sele,0,IMAX
*GET,IX,NODE,S_max_n,LOC,X  ! registrar a localização do nó de Smax
*GET,IY,NODE,S_max_n,LOC,Y
*GET,IZ,NODE,S_max_n,LOC,Z
!*GET,IX,ELEM,S_max_n,CENT,X ! No caso de querer ver a solução por elemento
/OUTPUT,Stresses.txt,'C:\Users\Ana Macedo\Dropbox\Tese\Interface',
PRNSOL,S,PRIN
/OUT

! Maximum stress in different regions:
nsele,loc,Y,1739,1761
CSYS,1
Insele,loc,Y,y_1,y_1+s_str   ! ZONE 1 - above cutout
nsele,r,loc,Z,cp,cp+b_c
CM,stress1,node
nsele,S,EQV,1,0,,1
*GET,S1,sele,0,MAX

nsele,loc,Y,y_2-s_str,y_2-s_str/2 ! ZONE 2 - below cutout
nsele,r,loc,Z,cp,cp+b_c
CM,stress2,node
nsele,S,EQV,1,0,,1
*GET,S2,sele,0,MAX

nsele,loc,Y,cen_yy-s_str,cen_yy+s_str ! ZONE 3 - right to cutout
nsele,r,loc,Z,0,cp-s_fra
CM,stress3,node
nsele,S,EQV,1,0,,1
*GET,S3,sele,0,MAX

! Displacements of cut-out:
CSYS,1
nsele,loc,Y,cen_yy-s_str,cen_yy+s_str ! left to cutout
nsele,r,loc,Z,cp
nsele,U,Z,1,0,,1
*GET,U1,sele,0,Min

nsele,loc,Y,cen_yy-s_str,cen_yy+s_str ! right to cutout
nsele,r,loc,Z,b_s-cp
nsele,U,Z,1,0,,1
*GET,U2,sele,0,Max

allsele

! Elastic Strain Energy
PLNSOL,SEND,ELASTIC,0,1
PRESOL,SENE
ETABLE,Energy,SENE

```

```
SSUM
*GET,TotalE,SSUM,,ITEM,Energy
```

```
! Calculus of the Mass-----
```

```
allsel
! Volume
ESEL,,type,,1
ESEL,A,type,,2
ETABLE,VOLUME,VOLU
SSUM
*GET,VOL,SSUM,,ITEM,VOLUME      ! vol (mm^3)
FINISH

mass1=2*vol*rho*10**3           ! calculates overall mass (1 ton = 1000 kg), rho=2780*1e-12 ton/mm^3
mass2=2*ATur*t_s*rho*10**3     ! door mass contribution
mass=mass1 + mass2
Weight=mass*g                   ! calcules weight of the model          g=9.81
```

```
! Buckling Analysis-----
```

```
/SOLU
ANTYPE,1
BUCOPT,SUBS,1                   ! BUCOPT,LANB,1
allsel
SOLVE
FINISH
```

```
! POST-PROCESSING
```

```
/POST1
SET,LIST                        ! List eigenvalue solution - Time/Freq listing is the force required for
                                ! buckling (in N for this case).
SET,LAST                        ! Read in data for the desired mode
!/show,png
PLDISP                          ! Plots the deflected shape (animation: ANMODE,30,0.1, ,0)
!/show,close
*GET,Bf,ACTIVE,0,SET,FREQ      ! load factor (Buckling factor)
FINISH
```

```
! Modal Analysis-----
```

```
/SOLU
ANTYPE,2
MODEOPT,LANB,1
EQSLV,SPAR
MXPAND,0, , ,0
LUMPM,0
PSTRES,0
allsel
SOLVE
FINISH
```

```
! POST-PROCESSING
```

```
/POST1
SET,FIRST
SET,LIST
/show,png
PLDISP                          ! mode shape (animation: ANMODE,10,0.5, ,0)
/show,close
```

```
*GET,NF,ACTIVE,0,SET,FREQ      ! Natural Frequency
```

```
! Writing of the values in Output file Results.txt -----
```

```
En = 'Nel='  
W = 'Weight='  
U = 'MaxDisp='  
S = 'MaxEqvStress='  
N = 'on node'  
P = 'Bf='  
E = 'Energy'  
D = '1*Freq='  
L = 'Loc='  
t1 = 'S1='  
t2 = 'S2='  
t3 = 'S3='  
d1 = 'U1='  
d2 = 'U2='
```

```
! results always in this order (for reading in MATLAB)  
/OUTPUT,'Results','txt','C:\Users\Ana Macedo\Dropbox\Tese\Interface',
```

```
*VWRITE,'B=',b_c  
(A2,F4.0)  
*VWRITE,'H=',h_c  
(A2,F5.0)  
*VWRITE,W,Weight  
(A7,E21.15,x)  
*VWRITE,U,U_max  
(A8,E21.15)  
*VWRITE,S,S_max  
(A8,E22.15)  
*VWRITE,E,TotalE  
(A6,E22.15)  
*VWRITE,P,Bf  
(A3,E22.15)  
*VWRITE,D,NF  
(A3,E22.15)  
!*VWRITE,En,eNum  
!(A6,F6.0)  
!*VWRITE,tam  
!(F4.0)  
*VWRITE,L,IX,IY,IZ  
(A5,/,F6.0,/,F6.0,/,F6.0)  
*VWRITE,N,S_max_n  
(A7,F6.0)  
*VWRITE,t1,S1  
(A3,E22.15)  
*VWRITE,t2,S2  
(A3,E22.15)  
*VWRITE,t3,S3  
(A3,E22.15)  
*VWRITE,d1,U1  
(A3,E22.15)  
*VWRITE,d2,U2  
(A3,E22.15)  
/OUT  
FINISH
```

```
!                ** END **
```

```
=====
```

A.2 B_variation.m

```
% Parametric Study varying the width, B
% case 1

clear all;
clc;

% GEOMETRY
%x=input('Choose one option: \n\n 1-Reference values \n\n 2-User inputs
\n\n 3-Sensitivity Analysis \n\n');
d=3;
switch d
    case 1
        B=810;
        H=1850;
        disp('analysis done with reference geometry');
    case 2
        B=input('door width? (mm)');
        H=input('door height? (mm)');
    case 3
        B=700:20:1100;           % vector of door widths
        B=B';
        m=length(B);
        H=1850;                 % door height
    otherwise
        disp('no analysis is done');
end

L=1;
A=0;

% Column vectors
W=zeros(m,1);
Umax=zeros(m,1);
Smax=zeros(m,1);
Ener=zeros(m,1);
Bf=zeros(m,1);
Nf=zeros(m,1);
%Nelem=zeros(n,1);
locX=zeros(m,1);
locY=zeros(m,1);
locZ=zeros(m,1);
node=zeros(m,1);
S1=zeros(m,1);
S2=zeros(m,1);
S3=zeros(m,1);
D1=zeros(m,1);
D2=zeros(m,1);
min=zeros(m,1);
g=0;           %number of unsuccessful Ansys analyses

t0=clock
% Corre o(a) vector/matriz e faz análise ponto a ponto
for i=1:m      % size(B) % corre o vector de configurações (largura da porta
                variável)
    %for j=1:n  % size(H)
    % file for the design variables and the user inputs:
    fid=fopen('C:\Users\Ana Macedo\Dropbox\Tese\Interface\param_file.txt','w');
    % creates new file for writing (discards existing contents, if any)
```

```

fprintf(fid, 'B=%d\n H=%d\n L=%d\n A=%d\n', B(i), H, L, A);
fclose(fid);

% calling of ANSYS and running of the solution (dos=disk operating system,
runs a command from the Command Line)

% dos(' "ANSYS path" -b -j results file name -dir "results file path
(working directory) " -i "input file (.txt)" -o "output files (.out)" ')

% -b activates the ANSYS program in batch mode
% -j ANSYS jobname (report) -> files: .err, doc de texto,
% -dir replaces ANSYS working directory by a especificed one
% -i input file -> file .mac
% -o output file that has info of the activity window (results) ->
file .out
if exist("report.lock", 'file')
    delete report.lock
    g=g+1;
end
t1 = clock;
[str,errmsg] = system(['SET KMP_STACKSIZE=2048k & "C:\Program files\ANSYS
Student\v182\ansys\bin\winx64\ansys182.exe"...
    ' -dir "C:/Users\Ana Macedo\Dropbox\Tese\Interface" ' ...
    ' -b ' ...
    ' -j report ' ...
    ' -i "C:\Users\Ana Macedo\Dropbox\Tese\Interface\mv2s.mac"
'...
    ' -o "C:\Users\Ana
Macedo\Dropbox\Tese\Interface\results.out" ' ...
]);

% (ANSYS ANALYSIS)

% reads the values from Results.txt file
fid2=fopen('C:\Users\Ana Macedo\Dropbox\Tese\Interface\Results.txt','r');

% Weight
text=fscanf(fid2,'%c',24);
W1=fscanf(fid2,'%c',23);
W(i) = str2num(W1); % Weight
% Displacement
text2=fscanf(fid2,'%c',8);
Umax1=fscanf(fid2,'%c',23);
Umax(i) = str2num(Umax1) % Maximum Displacement
% Stress
text3=fscanf(fid2,'%c',9);
Smax1=fscanf(fid2,'%c',23);
Smax(i) = str2num(Smax1) % Maximum von Mises Stress
% Elastic energy
text4=fscanf(fid2,'%c',6);
Ener1=fscanf(fid2,'%c',23);
Ener(i) = str2num(Ener1); % Elastic Energy
% Bf
text5=fscanf(fid2,'%c',4);
Bf1=fscanf(fid2,'%c',23);
Bf(i) = str2num(Bf1); % Buckling Factor
% freq natural
text6=fscanf(fid2,'%c',4);
Nf1=fscanf(fid2,'%c',23);
Nf(i) = str2num(Nf1); % Natural Frequency

```

```

% location of node of max Stress
text8=fscanf(fid2,'%c',6);
locX1=fscanf(fid2,'%c',8); % X-location of node of max Stress
locX(i) = str2num(locX1);
locY1=fscanf(fid2,'%c',8); % Y-location of node of max Stress
locY(i) = str2num(locY1);
locZ1=fscanf(fid2,'%c',8); % Z-location of node of max Stress
locZ(i) = str2num(locZ1);
% number of node of max Stress
text9=fscanf(fid2,'%c',9); % "on node"
nodel=fscanf(fid2,'%c',7);
node(i) = str2num(nodel);
% Stress on region 1
text10=fscanf(fid2,'%c',4); % "S1="
tensao1=fscanf(fid2,'%c',23); % stress on region above cut-out
S1(i) = str2num(tensao1);
% Stress on region 2
text11=fscanf(fid2,'%c',4); % "S2="
tensao2=fscanf(fid2,'%c',23); % stress on region right to cut-out
S2(i) = str2num(tensao2);
% Stress on region 3
%text12=fscanf(fid2,'%c',4); % "S3="
%tensao3=fscanf(fid2,'%c',23); % stress on region below to cut-out
%S3(i) = str2num(tensao3);
% Displ
text13=fscanf(fid2,'%c',4);
deslocamento1=fscanf(fid2,'%c',23);
D1(i) = str2num(deslocamento1);
% disp2
text14=fscanf(fid2,'%c',4);
deslocamento2=fscanf(fid2,'%c',23);
D2(i) = str2num(deslocamento2);

fclose('all');

t2=clock;
seg = etime(t2,t1);
min(i)=seg/60;
end

t3=clock;
e2=etime(t3,t0)/60;

% Plots:
figure
ax1=subplot(3,2,1);
scatter(ax1,B,W,'xb')
title(ax1,'Weight vs Door Width')
xlabel(ax1,'Width, B (mm)')
ylabel(ax1,'Weight (N)')
ax2=subplot(3,2,2);
scatter(ax2,B,Umax,'xb')
title(ax2,'Max Displacement vs Door Width')
xlabel(ax2,'Width, B (mm)')
ylabel(ax2,'Umax (mm)')
ax3=subplot(3,2,3);
scatter(ax3,B,Smax,'xb')
title(ax3,'Max Stress vs Door Width')
xlabel(ax3,'Width, B (mm)')
ylabel(ax3,'Smax (MPa)')
ax4=subplot(3,2,4);
scatter(ax4,B,Ener,'xb')

```

```
title(ax4, 'Elastic Energy vs Door Width')
xlabel(ax4, 'Width, B (mm)')
ylabel(ax4, 'Energy (J)')
ax5=subplot(3,2,5);
scatter(ax5,B,Nf, 'xb')
title(ax5, 'Natural Frequency vs Door Width')
xlabel(ax5, 'Width, B (mm)')
ylabel(ax5, 'NF (Hz)')
ax6=subplot(3,2,6);
scatter(ax6,B,Bf, 'xb')
title(ax6, 'Buckling Factor vs Door Width')
xlabel(ax6, 'Width, B (mm)')
ylabel(ax6, 'Bf')
```